Electrospun Fibrous Architectures for Drug Delivery, Tissue Engineering and Cancer Therapy

Ding, Yaping

2019-01

Ding , Y , Li , W , Zhang , F , Liu , Z , Ezazi , N Z , Liu , D & Santos , H A 2019 , ' Electrospun Fibrous Architectures for Drug Delivery, Tissue Engineering and Cancer Therapy ' , Advanced Functional Materials , vol. 29 , no. 2 , 1802852 . https://doi.org/10.1002/adfm.201802852

http://hdl.handle.net/10138/327321
https://doi.org/10.1002/adfm.201802852

acceptedVersion

Advanced Functional Materials

Electrospun Fibrous Architectures for Drug Delivery, Tissue Engineering and Cancer Therapy

--Manuscript Draft--

Manuscript Number:	adfm.201802852R3
Full Title:	Electrospun Fibrous Architectures for Drug Delivery, Tissue Engineering and Cancer Therapy
Article Type:	Invited Review
Section/Category:	
Keywords:	Electrospinning; drug delivery system; tissue engineering; cancer therapy; Biomedical applications
Corresponding Author:	Helder Santos, D.Sc. (Chem. Eng.) University of Helsinki Helsinki, Helsinki FINLAND
Additional Information:	
Question	**Response**
Please submit a plain text version of your cover letter here.	Dr. Jos Lenders Editor Advanced Functional Materials Dear Dr. Jos Lenders, Thank you very much for the second consideration on our manuscript and thank you for sending us the new referee's comments on our review. The comments from the three new reviewers are very valuable and highly helpful in improving our manuscript. A revised version of our manuscript addressing all the comments of the referees is provided. All the changes are clearly marked and highlighted in the text in yellow in the supplementary revised file. Another copy of the revised manuscript without marks is also provided as the main yrct. All the permissions for figures adapted from the literature have been uploaded as separated files. In the response letter, we have replied point-by-point to all of the reviewer's comments. I look forward to your positive response soon. Thank you very much in advanced for your kind consideration! Yours Sincerely, Hélder Santos _____ Dr. Hélder A. Santos, D.Sc. (Chem. Eng.), Associate Professor, Head of Division Head of the Division of Pharmaceutical Chemistry and Technology Head of the Nanomedicines and Biomedical Engineering Group Head of Preclinical Drug Formulation and Analysis Group

	Drug Research Program, Faculty of Pharmacy, University of Helsinki, Finland; & Helsinki Institute of Life Science (HiLIFE), University of Helsinki, Finland @: helder.santos@helsinki.fi, http://www.helsinki.fi/~hsantos/ https://scholar.google.com/citations?hl=en-EN&user=K3Pj_gwAAAAJ
Do you or any of your co-authors have a conflict of interest to declare?	No. The authors declare no conflict of interest.
Corresponding Author Secondary Information:	
Corresponding Author's Institution:	University of Helsinki
Corresponding Author's Secondary Institution:	
First Author:	Yapin Ding
First Author Secondary Information:	
Order of Authors:	Yapin Ding
	Wei Li
	Feng Zhang
	Zehua Liu
	Nazanin Zanjanizadeh Ezazi
	Dongfei Liu
	Helder Santos, D.Sc. (Chem. Eng.)
Order of Authors Secondary Information:	
Abstract:	The versatile electrospinning technique has been recognized as an efficient strategy to deliver active pharmaceutical ingredients and gained tremendous progress in drug delivery, tissue engineering, cancer therapy, and disease diagnosis. The current review presents numerous drug delivery systems fabricated through electrospinning regarding the carrier compositions, drug incorporation techniques, release kinetics and the subsequent therapeutic efficacy. Targeting for distinct applications, the composition of drug carriers vary from natural/synthetic polymers/blends, inorganic materials and even hybrids. Various drug incorporation approaches through electrospinning are thoroughly discussed with respect to the principles, benefits and limitations. To meet the various requirements in actual sophisticated in vivo environments and to overcome the limitations of single carrier system, feasible combination of multiple drug-inclusion processes via electrospinning could be employed to achieve programmed, multi-staged or stimuli-triggered release of multiple drugs. The therapeutic efficacy of the designed electrospun drug-eluting systems is further verified in multiple biomedical applications and is comprehensively overviewed here, demonstrating promising potential to address a variety of clinical challenges.

WILEY-VCH

DOI: 10.1002/adfm.201802852
Article type: Review

Electrospun Fibrous Architectures for Drug Delivery, Tissue Engineering and Cancer Therapy

Yaping Ding*, Wei Li, Feng Zhang, Zehua Liu, Nazanin Zanjanizadeh Ezazi, Dongfei Liu, Hélder A. Santos*

Drug Research Program, Division of Pharmaceutical Chemistry and Technology

Faculty of Pharmacy

University of Helsinki

FI-00014 Helsinki, Finland

*E-mail: yaping.ding@helsinki.fi; helder.santos@helsinki.fi

Keywords: electrospinning; drug delivery; tissue engineering; cancer therapy

Abstract

The versatile electrospinning technique has been recognized as an efficient strategy to deliver active pharmaceutical ingredients and gained tremendous progress in drug delivery, tissue engineering, cancer therapy, and disease diagnosis. The current review presents numerous drug delivery systems fabricated through electrospinning regarding the carrier compositions, drug incorporation techniques, release kinetics and the subsequent therapeutic efficacy. Targeting for distinct applications, the composition of drug carriers vary from natural/synthetic polymers/blends, inorganic materials and even hybrids. Various drug incorporation approaches through electrospinning are thoroughly discussed with respect to the principles, benefits and limitations. To meet the various requirements in actual sophisticated *in vivo* environments and to overcome the limitations of single carrier system, feasible combination of multiple drug-inclusion processes *via* electrospinning could be employed to achieve programmed, multi-staged or stimuli-triggered release of multiple drugs. The therapeutic efficacy of the designed electrospun drug-eluting systems is further verified in multiple biomedical applications and is comprehensively overviewed here, demonstrating promising potential to address a variety of clinical challenges.

1. Introduction

Since the first patent relating to the process and apparatus for artificial fibers using electric charges was approved in 1934,[1] electrospun architectures have been intensively investigated for many decades regarding the working principles, apparatus modifications, and diverse applications extending to texture industry, energy applications, and biomedical applications.[2] Ascribing to the various benefits associated with electrospun fibrous structures, such as fine fiber diameter down to nanometer, highly interconnected porous architecture, extreme high surface area and porosity, high loading capacity, high encapsulation efficiency, and feasibility for multifunctionlization, drug-loaded electrospun structures as novel drug delivery systems (DDS) are gaining increasing attentions in multiple biomedical applications (e.g., drug delivery, tissue engineering and cancer therapy).[3]

In principle, micro/nanofibers can be continuously produced when polymeric jets are ejected from viscoelastic solutions and further stretched and elongated by electrostatic repulsion forces between surface charges.[4] By carefully manipulating on the apparatus and parameters, fiber diameter distribution, pore size, porosity and spatial arrangement can be controlled and adjusted; moreover, fibrous meshes with secondary structures such as porous fiber surfaces, core-shell or hollow tubular structures can be further designed and generated.[2c, 4b] Such exceptional control on morphological and dimensional variations provides numerous possibilities to carry and entrap a variety of drug molecules within the electrospun fibers. In case of materials and compositions, either single or multiple drugs can be incorporated into polymeric matrix or organic/inorganic composite matrix. Through technical management, drugs can be either evenly distributed within the fibers or locally concentrated in the outer or inner layer of fibers.[5] In view of release behavior, drugs could be released in a rapid, sustained, bi-phasic or zero-order manner, to meet specific therapeutic needs.[6] Regarding the superiority to conventional

DDS, electrospinning has its intrinsic advantages to overcome the challenges existing in contemporary pharmaceutical research, such as difficulty for location-specific targeting delivery, poor aqueous solubility of hydrophobic drugs (which amounted to nearly 40% of marketed drugs), and chemical and physical degradation of complex and bioactive molecules.[7] Obviously, implantable therapeutic drugs-loaded electrospun scaffolds can be feasibly operated for targeted delivery at specific tissues or organs; this top-down technique is able to molecularly disperse hydrophobic drugs in the nanofibers or to stabilize the drugs in the amorphous form, yielding a significant increase in the aqueous dissolution rate.[8] In case of sustained release of sensitive species, electrospun fibermats as stable formulations could act as a storage matrix and protect them from the light, heat or degradation medium, and thus, ameliorate the possible degradation.[7a]

In general, the electrospinning technique demonstrates its great potential to create implantable drug carriers, which could be further utilized for various biomedical applications requiring drug delivery function. Its history, fundamental principle, governing of parameters have been thoroughly reviewed and discussed in numerous literatures.[2a, 2c, 3a, 4b] However, the reported reviews related to electrospun DDS are either out-of-date or within limited application fields. A timely and comprehensive review focusing on the electrospun DDS for various biomedical applications is necessary. The current article will highlight the advances of electrospun DDS achieved in the past few years to meet clinical needs, mainly in simple drug delivery, tissue engineering and cancer therapy. The major purposes are: 1) to briefly discuss the fabrication of DDS through electrospinning, in terms of materials, drugs, techniques and drug release kinetics; 2) to overview the tremendous progress and summarize perspectives for the future studies.

2. Fabrication of Electrospun Drug Delivery Systems and the Release Kinetics

Two key elements, matrix materials and therapeutic drugs, build up the DDS for the intended applications. Both components, and the adopted strategies to combine them, have decisive influence on the release behavior, including drug release duration and the trend of profiles. The most studied materials and drugs used in electrospun DDS are overviewed in this section, and their influences on the drug release behavior are also discussed.

2.1 Materials and Drugs

Although the versatile electrospinning technique enables the nanofiber formation from more than 200 polymers,[2a] more specific requirements in different DDS could further narrow down the choosing pool of polymer matrix. Angelova and Hunkeler[9] thoroughly categorized the polymeric biomaterials and proposed a flowchart as guidelines for rationalized polymer selection regarding the structure-property-application relationships. In this review, only the materials and drugs frequently studied in recent electrospun DDS will be briefly summarized.

2.1.1 Structural materials for electrospun DDS

Biocompatible polymers with diverse hydrophilicity/hydrophobicity, permeability, and mechanical properties are considered as promising candidates to load specific drugs aiming for distinct therapeutic efficacy. Target application is the primary consideration to determine the compositions of DDS.

In fast dissolving drug delivery systems (FDDDS), drug dosage forms are supposed to rapidly disintegrate in the oral cavity, therefore hydrophilic biopolymers are considered as optimal candidates to carry the drugs, such as poly (vinyl alcohol) (PVA)[10] , polyvinylpyrrolidone (PVP)[11] and gelatin[12]. For a local drug delivery to the oral mucosa, cross-linked gelatin was

electrospun to form patches containing antifungal agents due to its biocompatibility and mucoadhesive property.[13] The varying cross-linking degrees of gelatin allow the adjustable and sustained release of antifungal agents in the oral cavity to maintain the therapeutic level.[14] To fabricate an oral formulation for drug releasing *via* the sublingual route, PVA/sodium alginate blend was chosen as the patch matrix to enable sustained drug release over 10 h.[15] Due to the pH sensitive feature, some smart materials, such as shellac and Eudragit S100, can prevent the drug release in low pH and allow rapid drug release in neutral pH condition, making them highly applicable for oral colon-targeted drug delivery.[16] Biodegradable and biocompatible fibrous patches, such as poly(lactic-co-glycolic acid) (PLGA),[17] cellulose derivatives,[18] polyurethane (PU),[19] chitosan,[20] PVP,[21] PVA,[22] polycaprolactone (PCL),[23] and polylactic acid (PLA) family,[24] can be produced from electrospinning to administrate drugs *via* transdermal drug delivery, since the high porosity and surface area of electrospun fibers could greatly enhance the drug diffusion and thus drug accumulation efficiency in comparison to the cast films.[17a]

A wide range of polymers were reported to act as the matrix in drug carriers for tissue engineering, which required controlled drug release and simultaneous physical support for tissue regeneration.[25] The polymeric matrix is supposed to degrade gradually as the neotissue growth and therapeutic agents will be subsequently released from the matrix *via* both diffusion paths and matrix degradation.[26] Natural polymers, such as collagen, chitosan, gelatin and hyaluronic acid attracted great attentions due to their unique cellular affinity. However, their applications were mainly limited by the inadequate mechanical strength and low stability in physiological conditions.[25] Synthetic biopolymers represent the majority materials applied in both tissue engineering and drug delivery applications, due to the feasible tunability in physiochemical and mechanical performances and scaffolds configurations for specific

requirements.[27] Polymers, such as PLA/PLLA,[28] PLGA,[29] polyhydroxyalkanoates (PHAs),[30] and PCL,[31] were the representatives and extensively studied in recent years. Nevertheless, single polymer usually cannot fulfill the requirements in the complex *in vivo* environments, therefore polymer blending is a simply approach to adjust the physicochemical features and degradation rates of the fabricated scaffolds. For example, the blending of stiff and flexible polymers in the scaffolds could combine and balance the stiffness and elasticity;[32] the blending of natural polymers with synthetic polymers endowed the scaffolds with both cell-affinity feature and high mechanical properties;[31a, 33] the blending of varying ratios of water-soluble materials with hydrophobic polymers can adjust the medium penetration rate and subsequent drug diffusion rate and release profiles.[34] For instance, in the study of Zhu *et al.*[34a], up to 50 wt.% of PEG was blended with PLLA fibers to adjust the release behavior of papaverine. *In vitro* drug release studies showed that blended fibers with PEG ratios of 20%, 30%, 40% and 50% exhibited complete drug release on days 13, 11, 8 and 4, respectively.

Most electrospun drug carriers are fabricated from polymers due to their flexibility and feasible processability. However, in some fields, e.g., disease diagnosis, inorganic nanofibers exhibited better performances owing to their unique physiological performances. For instance, ZnO nanofibers were reported to provide an excellent electrical conduction path between biomarkers and electrodes, and enabled the creation of a biodevice with hypersensitivity.[35] Ali *et al.*[36] reported the fabrication of mesoporous ZnO nanofibers through electrospinning of the precursor solution and created a highly efficient and reproducible immunosensor by conjugating the ZnO nanofibers with a biomarker (anti-ErbB2; epidermal growth factor receptor 2) to diagnose the early breast cancer. This platform should also apply for other cancer detection through conjugation with corresponding biomarkers, making it a superior immunosensor with higher stability, rapid response, selectivity and simplicity.[36] In a study of Jang *et al.*[37], SnO_2

nanotubes with bimodal meso- and micro-pores were synthesized through modified electrospinning and then loaded with Pt catalyst to directly monitor simulated diabetic breath. Unlike polymer nanofibers, inorganic nanofibers or tubes were usually fabricated through electrospinning in combination with a sacrificial templating route. Therefore, the precise control on post-treatments after electrospinning, including drying and calcination, was able to customize the fiber morphology and therefore modulate the resultant functions.[38] Furthermore, drug delivery systems based on polymeric/inorganic composite materials were fabricated to combine the advantageous merits of both organic and inorganic materials. [39]

2.1.2 Smart materials for electrospun DDS

Stimuli-responsive polymers play important roles in DDS due to their rapid changes in conformation, solubility, morphological or mechanical performances when exposed to the external stimuli, such as pH, temperature, light, ultrasound, electric or magnetic field.[40] The high surface-to-volume ratio and porosity of electrospun scaffolds allow fast diffusion of stimulus and rapid contact with fibers resulting hypersensitive responses. Electrospinning of these stimuli-responsive polymers thus opened-up new horizons for on-demand DDS in many applications, e.g. oral drug delivery, tropical cancer drug administration or sequential drug release in tissue engineering.[40-41]

Eudragit polymers represent a type of pH-sensitive polymers that were developed based on the functionalization of methacrylic acids. By varying the composition ratios, Eudragit polymers soluble in fluids of distinct organs at different physiological pH were synthesized and widely applied in oral drug formulations.[42] For instance, Eudragit E 100 can only be dissolved in gastric fluid up to pH 5, Eudragit L 100 (EL100) was designed to be dissolved in intestinal fluid above pH 6 and Eudragit S 100 (ES100) above pH 7.[43] Yang *et al.* [16b] and Jin *et al.*[44]

prepared ES100 (shell)/lecithin-diclofenac sodium(core) and ES100(shell)/indomethacin (core) fibrous scaffolds to protect the drug from acid gastric fluid and achieve colon-targeted release. Han *et al.*[43] comparatively studied the pH-responsive release of two model drugs from EL100 (core)/ES100 (shell) and ES 100 (core)/EL100 (shell) core-shell fibers and demonstrated multi-pH responsive and selective pH-responsive performances of the different Eudragit polymer combinations (**Figure 1**a). Additionally, new class of pH sensitive copolymers, such as poly(4-vinylbenzoic acid-co-(ar-vinylbenzyl)trimethylammonium chloride) [poly(VBA-co-VBTAC)], was synthesized and electrospun into nanofibers to deliver ciprofloxacin in response to acid, neutral or basic conditions.[45]

Poly (N-isopropylacrylamide) (PNIPAM) is widely applied in thermos-responsive systems since it is able to reversibly switch its swelling state below lower critical solution temperature (LCST, at 32°C) and the deswelling state above LCST.[46] Li *et al.*[47] embedded P(IPAAm- co-AAc) nanogels within the PCL shell of drug-loaded electrospun fibers. The deswelling of embedded nanogels above 40°C created cavities and diffusion paths around the gels and allowed rapid drug release, whereas the re-swelling of nanogels then closed the cavities resulting delayed drug release (**Figure 1**b). Similarly, electrospun PNIPAAm/ethyl cellulose fibers loaded with ketoprofen were applied to achieve on-demand drug release in responsive to temperature.[48] A copolymer of poly(N-isopropylacrylamide-co-methacrylic acid) (PNIPAM-co-MAA), which combined the stimuli-responsive features of both PNIPAM and methacrylic acids, is responsive to both temperature and pH simultaneously.[49] In a study of Yuan *et al.* [50], electrospun chitosan-graft-poly(N-isopropylacrylamide) (CTS-g-PNIPAAm) fibrous scaffolds showed responsive feature to both pH and temperature, since chitosan was reported to be pH-sensitive owing to the ionization of the amino groups. Li *et al.*[51] incorporated gold nanorods with photothermal effect into doxorubicin (DOX)-loaded PNIPAM cross-linked

fibers through electrospinning, thereby fabricating hybrid scaffolds with near-infrared (NIR) light-driven and subsequent temperature-triggered drug release. In their study, the heat-up of gold nanoparticles upon exposure to NIR light could initiate the shrinkage of PNIPAM and then speed up the drug release.

In a study of Song *et al*.,[52] the authors proposed that the ultrasound irradiation could trigger the on-demand drug release from a dual-drug-loaded PLGA composite fibers containing both fluorescein (FLU) and rhodamine B-loaded mesoporous silica nanoparticles (RHB loaded MSNs) (**Figure 1**c). The enhanced drug release both from PLGA fibers and MSNs was attributed to the elevated temperature, which can be controlled through ultrasonic stimulation. By selectively manipulating the ultrasonic powers and pulsed cycles, on-demand drug release can be easily achieved.

Han *et al.*[53] synthesized a self-immolative polymer (SIP) and then fabricated SIP/ polyacrylonitrile (PAN) fibers with PVP/dye in core section through co-axial electrospinning (**Figure 1**d). Due to the extremely high surface area, nano-sized diameter and high porosity, SIP in the fiber shell could display very fast and responsive depolymerization upon external stimuli, resulting in on-demand drug release.

The magnetic-filed responsive feature was normally introduced by magnetic nanoparticles, i.e., iron oxide nanoparticles (IONPs). Wang *et al*.[54] created drug-loaded magnetic fibers by loading IONPs into PCL shell and confining ketoconazole within PCL hollow core through co-axial electrospinning. The release study showed that the introduction of an auxiliary magnetic field could accelerate the ketoconazole release due to the intensified motion of molecules activated by IONPs.

Additionally, the promising applications of other electrospun systems for tumor-triggered drug release[55], and inflammation-sensitive release[56] were also explored. These systems are further discussed later in this review.

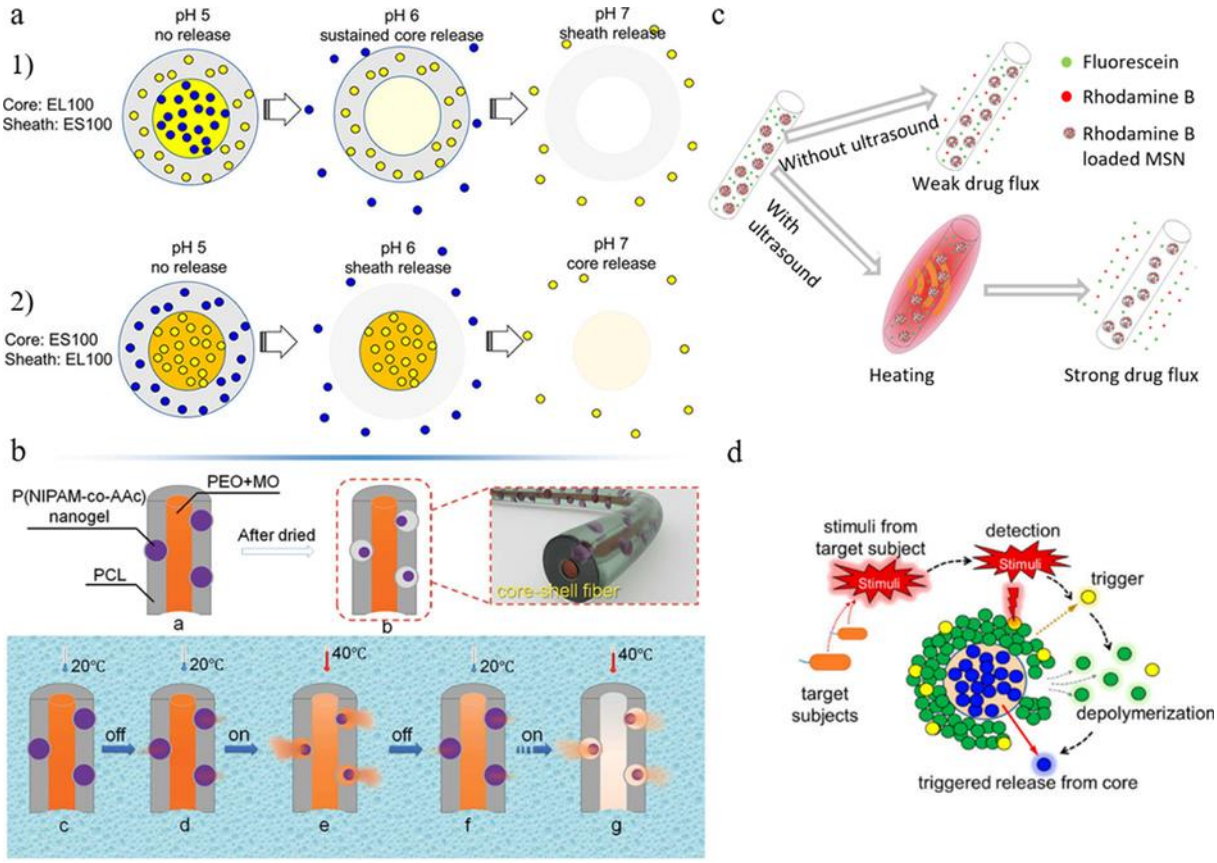

Figure 1. Several representative studies of stimuli-responsive drug release systems *via* electrospinning. (a) Electrospun core-shell fibers from pH-responsive polymers: (1) ES 100(shell)/EL100 (core) and (2) ES100 (core)/EL100 (shell). Reproduced with permission;[43] Copyright 2017, American Chemical Society. (b) Electrospun core-shell fibers using temperature-sensitive P(NIPAM-co-AAc) nanogels as valve to achieve temperature-responsive drug release. Reproduced with permission;[47] Copyright 2015, John Wiley and Sons. (c) Ultrasound-triggered drug release from PLGA composite fibers. Reproduced with permission;[52] Copyright 2015, Oxford University Press. (d) Electrospun self-immolative

polymer/PAN core-shell fibers for stimuli-responsive drug release. Reproduced with permission;[53] Copyright 2017, American Chemical Society.

2.1.3 Multiple drugs involved in electrospun DDS

As the key component in DDS, drugs are also known as active pharmaceutical ingredients (APIs), which have the responsibility to achieve satisfactory therapeutic efficacy. In current biomedical applications, APIs not only indicate the traditional small-molecule drugs, but also refer to all the ingredients that have desired therapeutic functions.

To achieve antibacterial function, a large range of antibiotics were encapsulated into fibers through electrospinning, such as tetracycline, cefoxitin, amoxicillin, gentamycin or ciprofloxacin.[57] The simple process of electrospinning usually allows the feasible addition of large amount of antibiotics; and the drug inclusion could also affect the solution properties, such as viscosity, conductivity and thereby influence the fiber structures. However, a higher risk of burst release often associated with the antibiotics/polymer systems due to the incompatibility between hydrophilic drugs and hydrophobic polymers.[31a] Moreover, the incorporation and release of silver, titanium dioxide, and zinc oxide nanoparticles from electrospun fibers have also been investigated to prevent the inflammation and infections.[57-58] In addition to the antibacterial function, some other biological enhancements could also be achieved, such as the improved osteoconductivity introduced by zinc oxide for an application in periodontal membrane.[58b]

Anti-cancer drugs are another group of APIs which were intensively investigated in drug carrier systems for cancer therapy. Electrospun fibers containing paclitaxel, doxorubicin, camptothecin, hydroxycamptothecin, bortezomib, temozolomide, titanocene dichloride, daunorubicin, cisplatin were widely explored for chemotherapy to treat glioma, breast cancer, lung cancer,

skin cancer, leukemia, and avoid tumor recurrence.[34b, 55, 59] Additionally, IONPs were co-incorporated with bortezomib by Sasikala *et al.* [55b] to achieve combined hyperthermia therapy and chemotherapy. In a study of Zhang *et al.*[60], multi-walled carbon nanotubes were co-blended with doxorubicin in PLLA fibers to combine photothermal therapy and chemotherapy.

Growth factors, peptides and genes representing the biologically active molecules could also be encapsulated and delivered through electrospun fibers to regulate and modulate the biological signals between cells and the extracellular matrix (ECM) for tissue regeneration.[61] For instance, basic fibroblast growth factor (bFGF) and endothelial growth factor (EGF) were embedded in collagen and hyaluronic acid fiber to accelerate epithelialization and vasculature sprouting, whereas vascular endothelial growth factor (VEGF) and platelet-derived growth factor (PDGF) were expected to induce blood vessels maturation.[62] Recombinant human transforming growth factor-b1 (rhTGF-b1) was confined within PCL fibers to stimulate chondrogenic differentiation of bone marrow-derived stem cells (BMSCs).[63] Nerve Growth Factor (NGF)-loaded PCL fibers were proved to sustainably induce the neuronal differentiation.[64] In a study of Li *et al.*[65] to repair critical-sized rat calvarial defect, bone morphogenetic protein-2 (BMP-2) was loaded to obtain osteoinductivity. For gene delivery, nonviral vehicles such as plasmid DNA or small nucleic acids and viral vehicles such as recombinant adeno-associated viral (AAV), have been promisingly applied in gene therapy. Aiming for vascular tissue regeneration, Zhou *et al.*[66] loaded microRNA-126 complexes within the inner layer of a bilayer tubular scaffold through dual-power electrospinning since microRNA-126 could essentially manipulate the vascular integrity and angiogenesis *via* regulating the angiogenic growth factors. James *et al.*[67] included microRNA-29a into cross-linked gelatin fibers to increase the synthesis and deposition of ECM for bone tissue regeneration. Attributed to the low pathogenicity and persistent transgene expression of AAV,

Gu *et al.*[68] incorporated AAV encoding green fluorescent protein (GFP) into polyester urethane urea fibers as elastic epicardial patch to restore cardiac function. The biomacromolecules usually are chemically unstable and have short half-life *in vivo*. Additionally, the harsh conditions in conventional electrospinning may harm their bioactivity and cause denaturation. Thus, modified electrospinning technique, such as co-axial electrospinning was considered as a superior option to avoid the denaturation.

Living cells have also been successfully encapsulated into biomedical polymer fibers through co-axial electrospinning to form cell-bearing fibers or scaffolds.[69] The cell suspensions within inner needle were safely shielded and protected by the outer polymer solutions and *in vitro* and *in vivo* studies certified well-maintained functions of the viable cells during and after the electrospinning.[69c]

2.2 Drug Incorporation Techniques

As one of the major factors for determining release kinetics, the location of drugs within fiber matrix can be simply arranged through different loading techniques. The drugs can be included onto the surface, within surface vicinity, throughout the whole fiber, exclusively within shell layer or core layer *via* surface immobilization, blend electrospinning, co-axial electrospinning or emulsion electrospinning. A secondary barrier could also be added to the system to further prolong the drug release and provide the possibility for simultaneous release of multiple drugs. The current section will focus on a comprehensive elaboration on these different drug encapsulation approaches and resultant release profiles.

2.2.1 Surface immobilization

Surface immobilization, also referring to surface coating or surface functionalization, is regarded as one of the easy approach to absorb the drug molecules onto the fiber surfaces through chemical (covalent bonding) or physical interactions (electrostatic interaction, van der Waals interaction or hydrogen bonding, etc.).[70] As a result of the high surface-to-volume ratio of electrospun fibers, numerous adhesion sites exist for drug molecules to attach and modify the resultant performances, such as wettability, cellular adhesion and genes expression.[71] Multiple methods were developed to achieve the functionalization *via* various bonding. **Table 1** lists several recent electrospun drug-loaded scaffolds *via* surface immobilization and the associated highlights and applications are also described.

The common method for feasible coating is to immerse fibers in target solutions for passive adsorption of biomolecules. Yao *et al.* [33a] dip-coated the PCL/chitosan scaffolds with heparin *via* ionic bonding between heparin and chitosan for vascular grafts application, resulting in sustained release of heparin over 37 days. Moreover, increasing the chitosan ratio could further efficiently prolong the drug release. Qiu *et al.*[72] functionalized PCU fibers with plasma treatment and subsequent conjugation of heparin *via* end-point immobilization. Polydopamine (pDA) chemistry is one of the popular approaches to immobilize proteins, peptides and antibodies onto hydrophobic fiber mats to enhance the cell affinity, cell-matrix interactions and introduce specific bio-signals (**Figure 2**a).[28b, 29c, 55b, 73] Oxidative self-polymerization of dopamine into pDA on fiber surface could provide abundant hydroxyl and amine groups to covalently bond with biomolecules under weak alkaline conditions. In the works of Lee *et al.* and Cho *et al.* [28b, 29c], bone-forming peptide 1 (BFP1) and bone morphogenetic protein-2(BMP-2) were subsequently immobilized onto PLGA and PLLA fibrous fibers, respectively, after initial self-polymerization of pDA coating. Stable retention of BMP-2 on the fiber surface can

be lasted up to 28 days with minimum burst release.[28b] PDA coating itself was also reported to be biocompatible and to enhance cell proliferation. Taskin *et al.*[31c] collected the electrospun PCL fibers in dopamine solution bath to form 3D coiled PCL fiber scaffolds with in-situ polymerized pDA coatings. In addition to pDA, a di-amino-poly (ethylene glycol) linker (di-amino-PEG), was also employed to act as an intermediate cross-linker to covalently bond mucin onto the fibrous scaffolds.[74] This conjugated mucin was more stable than simply absorbed mucin under static and flow conditions.

In addition to biomolecules, organically modified glass (ormoglass) layer containing bioactive ions was also covalently immobilized onto fiber surface through four functionalization steps: NaOH hydrolysis, ethyl(dimethyl-aminopropyl)carbodiimide/N-hydroxysuccinimide (EDC/NHS)treatment, immersion in 3-aminopropyltriethoxysilane (APTES) solution and subsequent ormoglass coating (**Figure 2**b).[71c] The hybrid organic/inorganic glass coating remarkably enhanced the mechanical performances, wettability and roughness. Moreover, calcium ions were sustained released for 14 days despite the burst release in the first day.

Jia *et al.*[75] employed an inkjet printing to precisely deposit the growth factors onto fiber surfaces (**Figure 2**c). Through optimization of printing parameters, the biomolecules and subsequent cellular distribution were spatially organized in designed patterns. Although no strong interactions occurred, the deposited growth factors were still remained on the fibrous scaffold for more than 1 week, enabling the successful regulation function of TGF-β1 on the fibroblast differentiation. In addition, the precisely controlled deposition of biomolecules enforces the formation of biomolecular fibrous network, which could essentially mimic the biofunctions *in vivo* conditions.

Since the immobilizations usually only occurred on the surface or near surface vicinity, the incorporation of drugs or biomolecules would not alter the overall physical performances and the degradation properties of the original electrospun fibers. Additionally, post-immobilization of biomacromolecules could feasibly avoid the denaturation caused by the harsh condition of organic solutions.

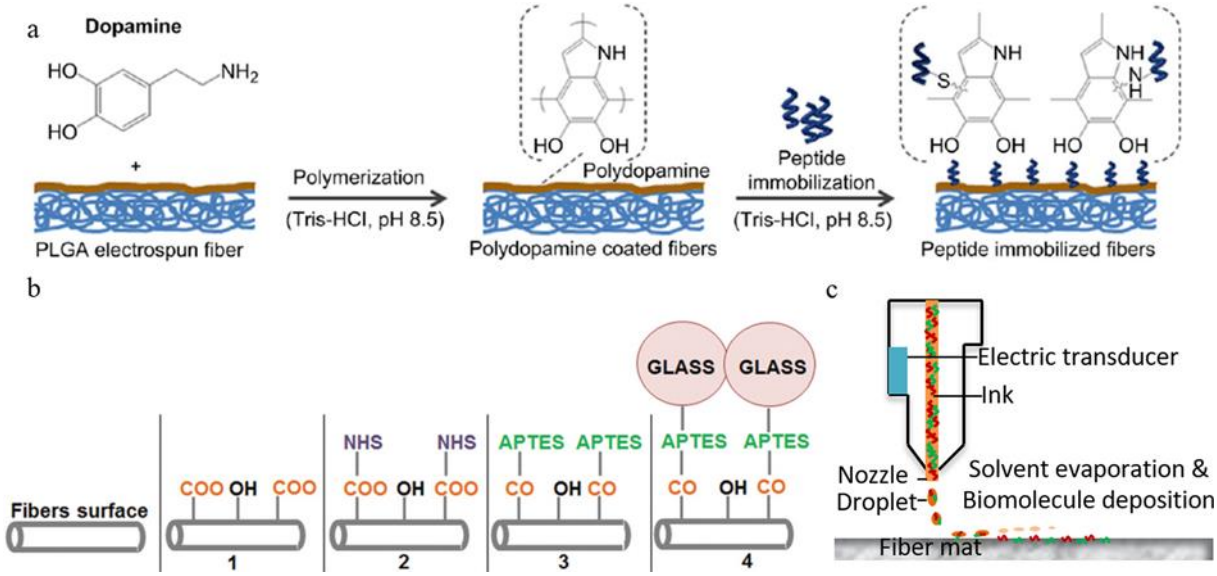

Figure 2. (a) Peptides immobilization onto PLGA fibers surface through pDA chemistry. Reproduced with permission;[29c] Copyright 2013, Elsevier B.V. (b) Bioactive glass phase was coated onto the electrospun fibers through a four-step process. Reproduced with permission;[71c] Copyright 2015, Royal Society of Chemistry. (c) Patterned biomolecule deposition onto electrospun fibermats *via* inkjet printing. Reproduced with permission;[75] Copyright 2017, John Wiley and Sons.

Table 1. Representative electrospun DDS *via* surface immobilization and the associated highlights and applications.

Materials	Drugs	Highlights	Applications	Ref.
PCL/ Chitosan	Heparin	Drug immobilization *via* strong ionic bonding between heparin and chitosan; Burst release in 1 d followed by sustained release until 37 d.	Vascular grafts	[33a]
PCL/ Collagen	SDF1α	Growth factors were embedded in radically aligned fibers through collagen-binding domain; Gradual release for 7 d without burst release.	Guiding nerve regeneration	[33b]
PCL /Gelatin	APA-coated AuNPs	20.4% of AuNPs were rapidly released in 1 d and then sustained released for 14 d, exhibiting striking ability to remedy multidrug-resistant bacteria wound infections.	Wound healing	[33c]
PLGA	Polydopamine Bortezomib	Bortezomib conjugation onto the fiber surface through dopamine coating; 70% vs 20% of drug was released in the first 12 h at pH 5.5 vs 7.4.	Cancer therapy	[55b]
PLA	Si–Ca–P_2 ormoglass *via* covalent bonding	Sustained release of Ca^{2+} ions for over 16 d; The lower the Si^{4+} content, the higher the Ca^{2+} release.	Regenerative medicine	[71c]
PCU	Heparin	PCU fibers were treated by plasma and then conjugated with heparin *via* end-point immobilization; Conjugated heparin dramatically improved the patency of vascular grafts, the early stages of endothelialization and graft integration *in vivo.*	Vascular graft	[72]
PLGA	Polydopamine, BFP1	Significant increase of newly formed bone volume after implantation of pDA-BFP1-coated scaffolds after 8 weeks.	Guided bone regeneration	[29c]
PLLA	Polydopamine, BMP-2	90% of BMP-2 remained on the fiber surface for 28 d.	Bone regeneration	[28b]
PLLA	Polydopamine, Osteogenic peptide (OP)	After 8 h of polydopamine coating, 80% of immobilized OP can be retained on the fiber surface for 28 d.	Guide bone regeneration	[73]
PCL	Polydopamine	3D-coiled fibrous scaffolds with polydopamine coating were collected in dopamine solution.	Tissue engineering	[31c]

PLLA PLCG/ PCL	BSM conjugation *via* EDC and NHS coating and di-amino-PEG as linker	In comparison to absorbed BSM, conjugated BSM on the fiber surface significantly improved the patency of vascular grafts, prevented thrombosis and graft occlusion.	Vascular graft	[74]
PCL/ Collagen	BSA	A biomolecule network with designed biomimetic patterns, formed on the fiber substrates by inkjet printing.	Cancer therapy	[75]
PLLA	Fibronectin	Fibronectin coating on fibers effectively improved astrocytic adhesion and survival.	Nerve Regeneration	[28a]
PCL	RGD YIGSR	Self-assembled RGD/YIGSR coating on fiber surface highly improved the cell adhesion and survival of Schwann cells, promoted axonal regeneration and enhanced vascularization.	Nerve Regeneration	[76]
PCL	Azithromycin	Drugs immobilization through solvent evaporation technique; All drugs were rapidly released in the first 24 h and sustained released until 14 d.	Bone Regeneration	[77]
Silk fibroin	Antimicrobial peptide motif Cys-KR12	Immobilization of Cys-KR12 on to electrospun silk fibers through EDC/NHS and thiol-maleimide click chemistry; Antibacterial effect maintained for 3 wk.	Wound healing	[78]

PCL, polycaprolactone; SDF1α, stromal-cell-derived factor-1α; APA-coated AuNPs, (6-aminopenicillanic acid, APA)-coated gold nanoparticles; PCU, polycarbonate-urethane; PLGA, poly(lactic-co-glycolic acid); BFP1, bone-forming peptide 1; PLLA, poly(L-lactide); BMP-2, bone morphogenetic protein-2; OP, osteogenic peptide derived from BMP-2; PLCG, poly(L-lactide-co-caprolactone-co-glycolide); BSM, bovine submaxillary mucin; EDC, 1-ethyl-3-(3 dimethylaminopropyl) carbodiimide hydrochloride; NHS, N-hydroxysulfosuccinimide; PEG, poly(ethylene glycol); BSA, bovine serum albumin; RGD, arginine-glycine-aspartic; YIGSR, tyrosine-isoleucine-glycine-serine-arginine.

2.2.2 Blend electrospinning

Blend electrospinning is a one-step method to embed or encapsulate drug molecules into fiber matrix by electrospinning of miscible and stable mixture solution containing both drugs and

polymers. Blend electrospinning was the earliest attempt to form drug formulations through electrospinning, reported by Kenawy *et al.*[79] in 2002. They claimed that the drug release in electrospun fibers was much faster than the cast films due to the high surface-volume ratio of electrospun membranes and the drug release kinetics can be modulated through adjusting the polymer compositions. Soon after, Zeng *et al.*[80] investigated the decisive factors determining the release kinetics of blending fibers. Their study firstly revealed that the drug solubility and drug-polymer compatibility practically influenced the drug distribution throughout the fibers and thus the release profiles. In blending systems, a constant and stable drug release can only be achieved in lipophilic drug/lipophilic polymer or hydrophilic drug/hydrophilic polymers systems. Thereafter, numerous drug/polymer systems were fabricated by blending and their drug delivery functions were widely explored.[31a, 34a, 81] **Table 2** summarizes the recent drug-laden fibers through blend electrospinning. Fast drug release for such as 2 h or sustained release for such as 91 days can be accomplished *via* blend electrospinning when the appropriate drug/polymer were chosen.[81-82] By doping an enzyme-sensitive prodrug (poly(ibuprofen)) into polymer poly(hydroxyethyl methacrylate) (PHEMA) fibers *via* blend electrospinning (**Figure 3**a), Pan *et al.*[83] successfully managed a polymer degradation-synchronized drug release for 14 weeks (accelerated drug release when polymer underwent self-catalyzed degradation). Apart from the drug molecules, (6-aminopenicillanic acid, APA)-coated gold nanoparticles (AuNPs) were also doped into PCL/gelatin fibers to resist multidrug-resistant bacteria and promote wound healing (**Figure 3**b).[33c]

Obviously, blending is the simplest strategy to achieve drug delivery through electrospinning. The limitation of blend electrospinning is that biomolecules may denature in case of harsh organic solvents and incompatible drug/polymer systems may generate uncontrolled release behaviors.[84]

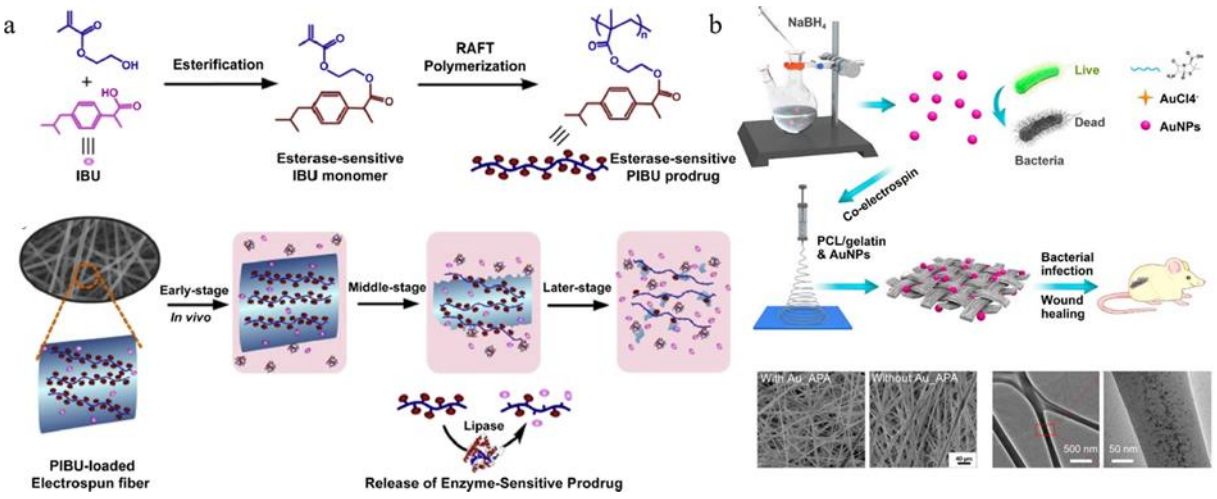

Figure 3. (a) Prodrugs were encapsulated in polymer fibers through blend electrospinning. Reproduced with permission;[83] Copyright 2015, Elsevier B.V. (b) PCL/gelatin fibers containing modified gold nanoparticles were fabricated through blend electrospinning. Reproduced with permission;[33c] Copyright 2017, American Chemical Society.

Table 2. Representative electrospun DDS *via* blend electrospinning and the associated highlights and applications.

Materials	Drugs	Highlights	Applications	Ref.
PCL/ gelatin	MNA	An initial burst release in 3 d (60%) and sustained release for 21 d.	Guided tissue regeneration	[31a]
PLLA/ PEG blend	Papaverine	Papaverine can be rapidly released in the first 2~7 d and then sustainably released until 14 d by varying the polymer blend ratios.	Preventing vasospasm	[34a]
PEO/PCL blend	Niclosamide	Gradual release of 40% of niclosamide over 21 d, following the Korsmeyer–Peppas model.	Cancer therapy	[34c]
PCL/ PGC-C_{18} blend	Cisplatin	Linear drug release over 90 d due to the blend superhydrophobic fiber meshes.	Anti-lung cancer recurrence	[59a]
BPU	Dipyridamole	Sustained Drug release over 91d due to the good compatibility; The higher the drug ratio, the slower the drug release.	Vascular grafts	[81]

PCL	PIBU	Incorporation of enzyme sensitive prodrug PIBU through blend electrospinning; Combination of initial enzyme-triggered release - moderate release of anti-inflammatory drugs and degradation-synchronized drug release in the later-stage over 14 wk.	To prevent biodegradation -induced inflammation	[83]
PCL, PNIPAAm	Nattokinase	Core-shell structure with thermal-responsive shell was self-assembled during the electrospinning; The thermal-responsive shell allowed faster drug release above the phase transition temperature (32°C), therefore resisted the platelet adhesion and facilitated red blood cells capture.	To capture red blood cells for diagnosis	[85]
PLGA	Poly-L-lysine covalently conjugated with YIGSR and RGD	Two adhesive peptides were uniformly distributed on the surface and inside of fibers, significantly enhancing the adhesion of cardiomyocytes.	Cardiac tissue engineering	[29b]
PLLA	Oxaliplatin Dichloroacetate	Fabrication of multilayer scaffolds with dual-drug-loaded layers through co-electrospinning; Time-programmed dual-release behaviors over 30 d.	Anti-cancer recurrence	[86]
PELCL (inner) PCL/ gelatin (outer)	MiR-126	Fabrication of multilayer tubular electrospun scaffolds through dual-power electrospinning; Sustained release of 60% of miR-126 over 56 d.	Blood vessel regeneration	[66]
Gelatin	MiR-29a	Burst release of miR-29a in 2 h and then sustained release over 72 h.	Tissue engineering	[67]
PLCL/ PEOz blend	VEGF and bFGF	Dual-growth factors release; Burst release of both growth factors in 7 h and then sustained release over 240 h.	Cardiac tissue regeneration	[87]
PCL	Methylcobalamin	Sustained release of less than 15% of drug over 8 weeks.	Nerve regeneration	[88]
PVA	Antifungal Cm-p1	Burst release in 2 h and following sustained release up to 3 d.	Anti-fungal infection	[89]
Gelatin	Polyhydroxy antibiotics (pDA)	Fiber fabrication through in-situ cross-linking of gelatin, pDA and antibiotics *via* strong interfacial interactions, resulting in extended antibacterial activity up to 20 d.	Antimicrobial-wound dressings	[90]

PLA	Paclitaxel	Drug release in concentration-dependent manner; Scaffolds with drug ratios from 0.02% to 3.26% all can gradually release the drugs over 84 d.	Nerve regeneration in spinal cord	[91]
PLLA PEO	TSA	Sustained release of less than 35% of TSA from aligned fibers over 90 h, following the Higuchi equation; Aligned fiber orientation delayed the drug release rate in comparison to random fiber meshes.	Tendon tissue engineering	[92]

PEO, polyethylene oxide; PGC-C18, poly(caprolactone-co-glycerol-monostearate); BPU, biodegradable elastic polyurethane urea; PIBU, poly (ibuprofen); PNIPAAm, poly(N-isopropylacrylamide); PELCL, poly(ethylene glycol)-b-poly(L-lactide-co-e-caprolactone); mir-126, microRNA-126 complexes; miR-29a, microRNA-29a complexes; PLCL, poly(L-lactide-co-caprolactone); PEOz, poly (2-ethyl-2-oxazoline); VEGF, vascular endothelial growth factor; bFGF, basic fibroblast growth factor; Cm-p1, cencritchis muricatus peptide 1; TSA, Trichostatin A.

2.2.3 Co-axial/ tri-axial electrospinning

High initial burst drug release often occurred in the fibers fabricated through direct blend electrospinning. The locally elevated drug concentration could cause cellular toxicity, and the short release period could not ensure the healing efficacy in many cases. Therefore, there is a demand for innovative modifications and alternatives to alleviate the burst release. Co-axial electrospinning, which was firstly reported by Sun *et al.*[93] in 2003, utilized a spinneret consisting of two concentrically aligned capillaries to push immiscible inner and outer solutions simultaneously for generating core-shell fibers. The second separate core nozzle enables the encapsulation of sensitive, water-soluble and bioactive molecules possible, and the deleterious effects from organic solvents can be avoided. Even unspinnable drug solution can be utilized in co-axial electrospinning, thus ultra-high drug loading into the central section could be realized independent of the solubility and viscosity of the drug solute.[94]

Table 3 summarizes the recent drug-laden fibers through co/tri-axial electrospinning. Various chemicals and bioactive agents for drug delivery and tissue engineering, such as growth factors, nucleic acids and living organisms, can be incorporated into the core section without losing their functions.[95] When shielded from the shell polymer, central-located bioactive agents can only be released through nano-path diffusion and/or shell polymer degradation. Therefore, by varying the composition of shell polymers, sustained release or sequential release of multiple drugs can be feasibly achieved.[96] For instance, rapid drug release prolife was shown in case of hydrophilic polymeric shell and slow and sustained release profile can be obtained in case of hydrophobic polymeric shell.[44, 68, 94]. Additionally, the release time-scale can be adjusted simply through altering the fiber surface texture and shell thickness (relevant to feeding rate of outer and inner solution).[97] Moreover, the interactions between inner and outer solutions were also reported to affect the release kinetics. Angkawinitwong *et al*.[98] discovered that the pH of core solutions could greatly influence the core-sheath structure and thus the release kinetics when they incorporated bevacizumab into PCL fibers through co-axial electrospinning. As shown in **Figure 4**a, the positively charged bevacizumab could uncontrollably migrate from the core solution to the PCL sheath solution, resulting in the inhomogeneous distribution of drug in both shell and core section, and thus a first order release up to 18 days. However, the neutral charged bevacizumab could be finely confined in the core section, forming a well-defined core-shell structure, and thus a zero-order release of drug up to 60 days.

To meet the demand of body temperature-stimuli responsive drug release, Li *et al*.[47] created a thermally switched drug release device through co-axial electrospinning. Thermally responsive nanogels, which were embedded into the PCL shell to act as valves, generated cavities as paths for the diffusion of encapsulated drugs during the shrinking and swelling at above or under LCST (**Figure 4**b). As an extension of co-axial electrospinning, tri-axial electrospinning

provides more possibilities to modify the materials, fiber structures and release kinetics. Yu *et al*.[99] used tri-axial electrospinning to synthesize a tri-layer composite fiber with drug gradient distribution (**Figure 4**c1). The drug content of the fibers was gradually increased from outer layer to middle and inner layer, which comprised a system to stably release the drug in a zero-order manner (**Figure 4**c2 and c3).

In summary, co-axial/tri-axial electrospinning could provide feasibility for sustained and multistage drug release. More importantly, co-axial/tri-axial electrospinning widen the drug solution range to unspinnable fluids.[99-100] The limitations of co-axial/tri-axial electrospinning are mainly the complexity of the set-up configuration, and various working parameters need to be well controlled and the interfacial tension of inner and outer solutions need to be well adjusted.

Table 3. Representative electrospun drug-loaded scaffolds *via* co-/tri-axial electrospinning and the associated highlights and applications.

Materials	Drugs	Highlights	Applications	Ref.
Shell	Core			
ES100	Diclofenac sodium phospholipids	Drug release in two stages *via* pH-responsive manner; The ES100 shell dissolved in acid condition firstly (pH 1.0, 2.1% of drug release in 2 h); Released drug phospholipids further gradually released the drug at pH 7.0, which reached 79% over 22 h.	Oral colon-targeted drug delivery	[16b]
ES100	Gd(DTPA)-loaded PEO and indomethacin	Therapeutic and imaging agents were delivered simultaneously to the colon. Indomethacin had less than 10% of release at pH 1 and sustained release over 29 h at pH 7.4.	Oral drug delivery	[44]

PCL/ nanogels	Methyl orange loaded PEO / DOX-loaded PEO	The swelling and shrinking of thermal responsive nanogels (LCST 32 °C) located in the shell could create cavities as drug diffusion paths to control the drug release in response to temperature.	Drug delivery system	[47]
Chitosan/ PVA blend	Curcumin	Delayed drug release; Rapid release of 40% of curcumin in 8 h and sustained release of 73% of drug over 10 d.	Wound healing	[94]
PEUU and PEEUU	AAV-loaded PEO	Sustained transgene expression over 2 months.	Cardiac tissue engineering	[68]
SF/CS/ nHAP	BMP-2	Sustained release of BMP-2 over 22 d; Fibers with thin shell thickness could release drugs in faster rate.	Bone tissue engineering	[97]
PCL	Bevacizumab	pH of core protein solution had influences on the resultant core-shell structure; With varying the pH, drugs can be released following a first-order kinetic ($t_{1/2}$ of 11.4 d) or a zero-order kinetic ($t_{1/2}$ of 52.9 d).	Age related macular degeneration	[98]
Ethyl cellulose	Ethyl cellulose /ketoprofen	Fibers with gradient distribution of drugs were prepared through tri-axial electrospinning; Linear drug release over 20 h.	Drug Delivery Systems	[99]
P(LLA-CL)/silk fibroin/ PANi	NGF/BSA	Sustained release of NGF from conductive core-shell fibers over 5 d, increased the percentage of neurite-bearing cells and median neurite length; NGF release was increased by electrical stimulation.	Neural tissue engineering	[101]
PCL CA	PVP/Nisin	Fabrication of fibers with three layers through tri-axial electrospinning; Biocidal activities were retained over 5 d.	Wound healing	[102]
PLGA /EGCG	Hyaluronic acid	Uniform distributed EGCG in PLGA shell was released in a stepwise manner for 28 d; Central-located hyaluronic acid was sustained released for 28 d.	Diabetic wound healing	[103]
PCL/Ag	Hyaluronic acid/ PEO	Complete release of Ag within 4 d; Initial rapid release of hyaluronic acid in 10 d and following sustained release over 21 d.	Anti-peritendinous adhesion	[104]

ES100, Eudragit S100; Gd(DTPA), Gd(III) diethylenetriaminepentaacetate hydrate; LCST, lower critical solution temperature; DOX, doxorubicin; PVA, polyvinyl alcohol; PEUU, polyester urethane

urea; PEEUU, polyester ether urethane urea; AAV, recombinant adeno-associated viral; SF, silk fibroin; CS, chitosan; nHAP, nanohydroxyapatite; P(LLA-CL), poly(L-lactic acid-co-3-caprolactone); PANi, polyaniline; CA, cellulose acetate; PVP, polyvinylpyrrolidone; EGCG, epigallocatechin-3-O-gallate.

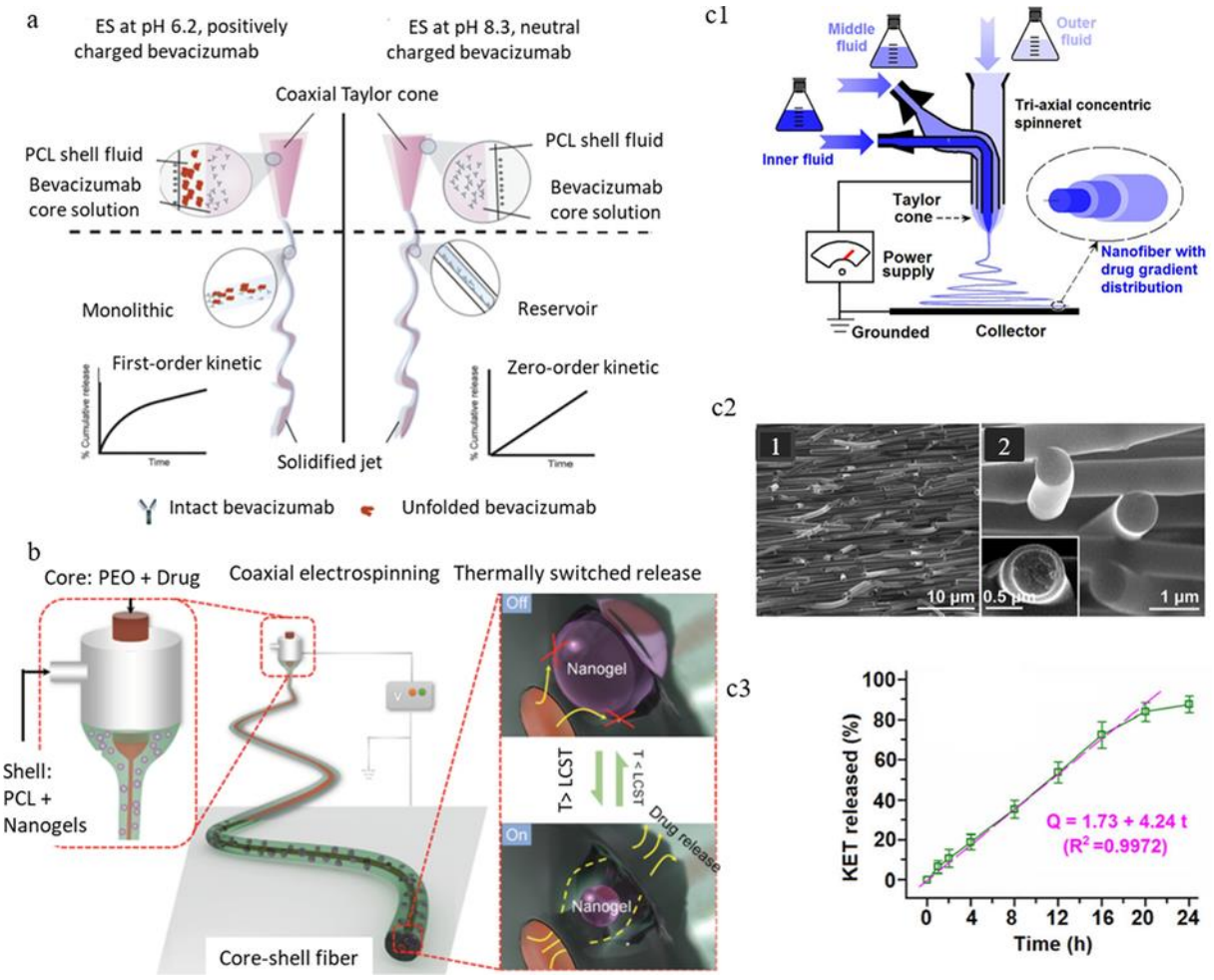

Figure 4. (a) A diagram illustrating the influence of pH of drug solution on the fiber structure, drug distribution, and release kinetics when produced through co-axial electrospinning. Reproduced with permission;[98] Copyright 2017, Elsevier B.V. (b) Thermal responsive fibers using shell-located nanogels as valve were fabricated through co-axial electrospinning. Reproduced with permission;[47] Copyright 2015, John Wiley and Sons. (c) A study of tri-layer drug-loaded fibers through tri-axial electrospinning process. (1) Schematic illustration of the tri-axial electrospinning. (2) SEM images of the fabricated tri-layer fibers. (3) The linear release

profile was achieved by the tri-layer drug-loaded fibers. Reproduced with permission;[99] Copyright, 2015, American Chemical Society.

2.2.4 Emulsion electrospinning

Sanders *et al.*[105] reported the first emulsion-electrospun fibrous structure in 2003. A two-phase W/O emulsion of BSA-water/poly (ethylene-covinyl acetate)-dichloromethane was used to enforce fiber formation through a single nozzle, generating a core-shell structure when the water droplets were stretched and solidified. Usually three phases comprise the spinnable emulsion: aqueous phase, oil phase and sometime surfactants, which enhance the stability of the W/O emulsion and influence the release behaviors (**Figure 5**a).[30a, 106] The emulsion stability, which is the essential factor determining the successful entrapment of biomolecules, can be maintained by choosing the appropriate surfactant, emulsification parameters and electrospinning parameters.[107] These factors synergically affect the successful spinning and the distribution of the bioactive molecules (either a core-shell structure or drug randomly embedded in matrix). Moreover, Yazgan *et al.*[108] found that relative humidity (RH%) and surfactant concentration had remarkable influences on the fiber structure, surface morphology, surface chemical composition and consequently the drug release kinetics in emulsion electrospinning. They proposed that optimized surfactant concentration with high RH% can render porous fiber surface, leading to rapid drug release. With increasing the concentration of surfactant Span 80, dense fiber surface can be formed, resulting in delayed drug release. In addition to the usually reported W/O emulsion, Basar *et al.*[109] synthesized PCL/ketoprofen(core)/gelatin(shell) fibers *via* electrospinning from an O/W emulsified suspension. The cross-linked gelatin was considered as a coating outside of the ketoprofen-loaded PCL fibers, and thus extended the drug release period from 20 h to 100 h. Moreover, the physical performance of PCL and the cellular

affinity of natural gelation were combined for wound healing applications. **Table 4** further summarizes the recent drug-loaded electrospun structures from emulsion electrospinning and describes the highlights.

Compared to co-axial/tri-axial electrospinning, emulsion electrospinning is a simpler one-step process to form core-shell fibers without complicated spinneret configuration. Water-soluble and fragile biomolecules can also be well confined in the core section of fibers *via* emulsion electrospinning (**Figure 5**b). Their release kinetics were mainly determined by the diffusion and degradation of polymer shell as well. However, the addition of water phase into polymer solution could greatly affect the viscosity, surface tension and conductivity of original polymer solutions, therefore influence the fiber topography and the mechanical performances of the final drug-loaded fibrous scaffolds.[110]

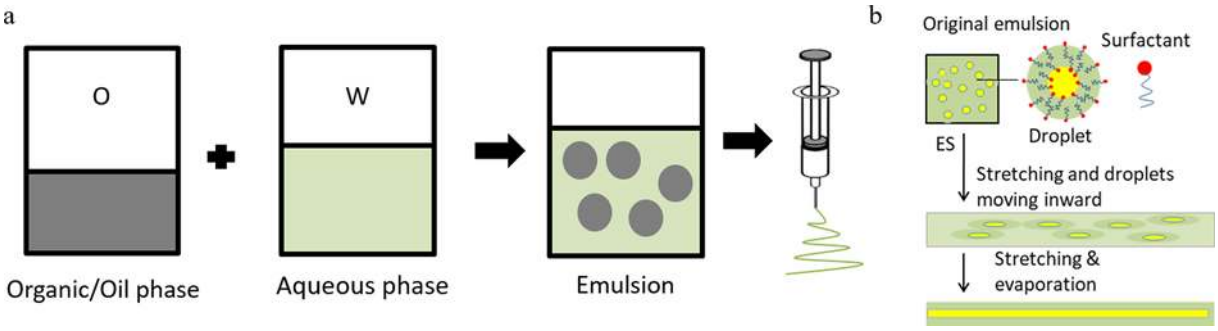

Figure 5. (a) An example of emulsion electrospinning process from W/O emulsions. Reproduced with permission;[111] Copyright 2014, Elsevier B.V. (b) Schematic illustration on the mechanism of the core-shell structure formation during the emulsion electrospinning process. Reproduced with permission;[112] Copyright 2006, John Wiley and Sons.

Table 4. Representative electrospun DDS *via* emulsion electrospinning (core-shell structure) and the associated highlights and applications.

Materials	Drugs	Highlights	Applications	Ref.
PCL PHBV (Oil phase)	Metformin hydrochloride or Metoprolol tartrate (Water phase)	The influences of polymer compositions, surfactants and drug characteristics on the release profiles were investigated; Slower and sustained drug release can be achieved over 21 d in comparison to blend electrospinning.	Drug delivery System	[30a]
PS PVP (Oil phase)	Fluorescein sodium salt (Water phase)	The higher the humidity, the more porous of the fiber surface leading faster drug release. With increasing the surfactant concentration, dense fiber surfaces could form, resulting in delayed drug release.	Drug delivery System	[108]
Gelatin (Water phase)	Ketoprofen in PCL (Oil phase)	PCL/drug fibers were coated with a cross-linked gelatin through emulsion electrospinning of an unusual O/W system, resulting in sustained drug release for 100 h.	Wound dressing	[109]
PLLA (Oil phase)	VEGF (Water phase)	10% of release in 1 d, and then sustained release over 4 wk.	Cardiovascular diseases	[113]
PLLA	Mitomycin-C loaded hyaluronan	Burst release of 26% of drug in 2 d and then sustained release over 40 d; The release pattern can be adjusted through altering the drug concentration.	Tendon healing	[114]
PCL gelatin	PRP-derived multiple growth factors	Simultaneous delivery of multiple growth factors, such as FDGF, FGF, TGF-β1; Bust release in 5 d and following sustained release for 30 d.	Cartilage regeneration	[115]

PHBV, poly(3-hydroxybutyric acid-co-3-hydroxyvaleric acid); PS, polystyrene; PRP-derived, Platelet-rich plasma- derived; FDGF, platelet-derived growth factor; FGF, fibroblast growth factor; TGF-β1, transforming growth factor-beta.

2.2.5 Secondary carrier electrospinning

In addition to the fibrous structures as backbone, secondary carriers like micelles, liposomes, nanogels, nanoparticles and nanotubes, can be physically entrapped into the fibers to form nano-in-nano or nano-in-micro structures for multi-purpose drug delivery. In theory, multiple drug-loaded particles could be delivered simultaneously resulting in multi-drug release.

Table 5 lists the recent studies on electrospun DDS containing secondary carriers, and their highlights and applications are summarized. Technically, drug-loaded secondary carriers were dispersed into the polymer solution (with or without drugs) prior to blend electrospinning, and a co-delivery of multiple drugs was achievable according to specific requirements. The hierarchical drug delivery systems were appealing owing to the multi-barrier function, which can not only protect bioactive molecules from harsh environment and degradative conditions, but also allow sequential release of drugs under appropriate triggers.[116] In addition, prolonged drug release was feasibly achieved due to the added physical barriers or strong interactions between drugs and carriers. For instance, Chandrawati *et al.*[117] successfully embedded β-glucuronidase-loaded liposomes within PVA fibers by blend electrospinning for enzyme prodrug therapy (**Figure 6**a). They reported that enzyme-loaded liposomes remained intact within PVA fibers and the release of enzyme can be mediated *via* phase transition temperature of the liposomes for at least seven weeks. This release period is much longer than the normal active period of β-glucuronidase in biomaterials (maximum 7 days). In a study of Luo *et al.*,[34b] camptothecin was initially loaded into promicelles (PM_{CPT}) and subsequently embedded in PEG-poly(lactide) (PELA)/PEO blend fibers through blend electrospinning. Once placed in the

tumor site, PM_{CPT} were sustained released and self-assembled into folate-targeted and glutathione (GSH)-sensitive micelles, which were taken-up by the tumor cells continuously (**Figure 6**b). By adjusting the composition ratio of polymer blends, the constant release of PMs can be prolonged over 30 days, which significantly enhance the anti-tumor efficacy. Xue *et al.*[118] incorporated metronidazole (MNA)-loaded halloysite clay nanotubes (HNT) into PCL/gelatin fibers through blend electrospinning. A combination of free drugs and drug-doped HNT in the fiber resulted in a burst release in 4 days and sustained release up to 20 days, providing sufficient antibacterial effect in the GTR/GBR implant membranes.

Table 5. Representative electrospun DDS *via* secondary-carrier electrospinning and the associated highlights and applications.

Materials	Drug-loaded carrier	Highlights	Applications	Ref.
EL55	Peptide-loaded PEC nano-carriers	pH-responsive nano-in-nano system for multi-stage drug release; Nanocarriers release at pH 6 and peptides release from nanocarriers at pH 7.4.	Oral drug delivery system	[116]
PVA	β-glu-loaded liposomes	β-glu release was mediated *via* phase transition temperature of the liposomes; The active enzyme release was extended from 7 d to 7 wk.	Enzyme prodrug therapy for cardiovascular grafts	[117]
PELA PEO	Camptothecin-loaded promicelle (PM_{CPT})	Sustained release of PM_{CPT} over 30 d; Self-assembled drug-loaded micelles on the tumor site were up-taken into tumor cells *via* FA-mediation with following drug release inside of tumor cell.	Tumor chemotherapy	[34b]
PCL gelatin	Metronidazole-loaded halloysite nanotubes	Burst release and following sustained release of metronidazole up to 21 d.	Guided tissue regeneration	[118]

PLLA	DOX-loaded MSNs caped with $CaCO_3$ gates	The lower the pH, the higher amount of $CaCO_3$ was dissolved, leading higher amount of DOX release from MSNs; Sustained DOX release up to 40 d.	Cancer therapy	[55a]

EL55, Eudragit L100−55; PEC, polyelectrolyte complex; β -glu, β -glucuronidase; PM_{CPT}, camptothecin containing promicelle; MSNs, mesoporous bioactive glass nanospheres.

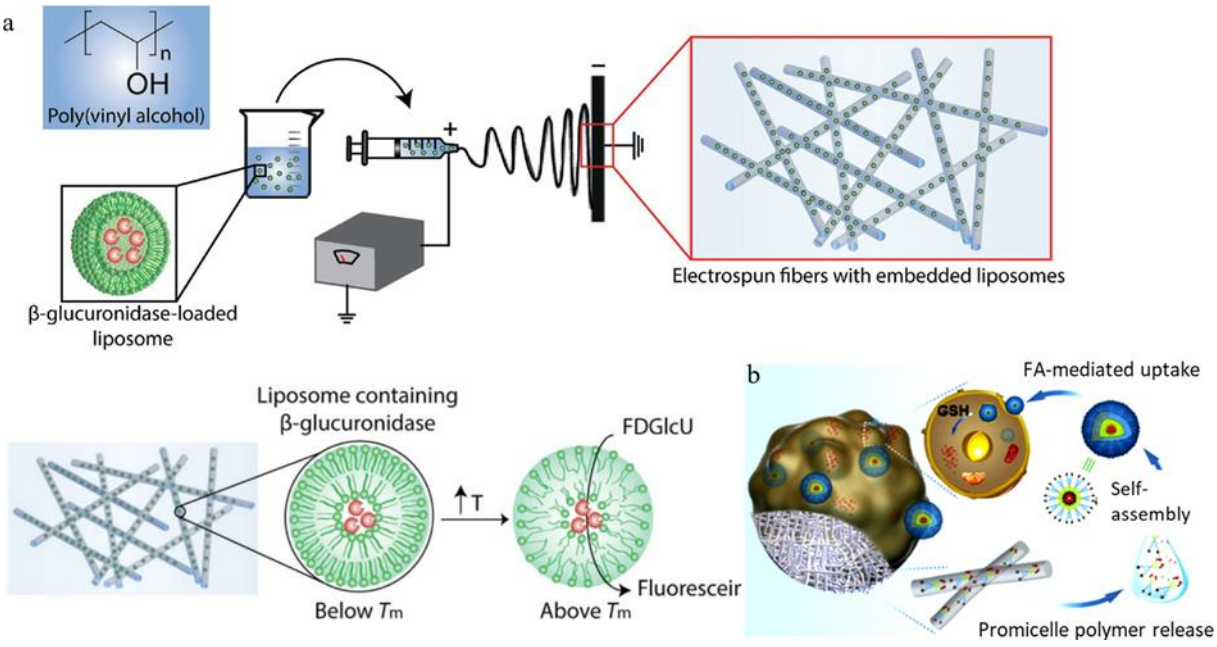

Figure 6. (a) Enzyme-loaded liposomes were encapsulated into PVA fibers through secondary carrier electrospinning and the drug release can be mediated through the thermal phase transition of liposomes. Reproduced with permission;[117] Copyright 2017, John Wiley and Sons. (b) Anticancer drug-loaded promicelles were embedded into blend polymer fibers through secondary carrier electrospinning. Reproduced with permission;[34b] Copyright 2017, Elsevier B.V.

2.2.6 Combination of multiple techniques

As an extension to secondary electrospinning, the combination of two or three drug-loading approaches have been utilized frequently, because the single DDS cannot fully fulfill the

function in the complex *in vivo* environment and cannot meet the increasing demand to deliver and precisely release the multi-drugs in a multi-stage or sequential manner. **Table 6** gives several examples that combine two or more electrospinning approaches to achieve multi-drug delivery.

Cheng *et al.*[29d] functionalized the ginsenoside-Rg3-loaded fibrous scaffolds with RGD and bFGF through pDA coating chemistry. Results indicated that surface functionalization feasibly promoted the cellular activity without impairing the original drug loading and release behavior. Man *et al.*[63] combined co-axial electrospinning with surface functionalization to deliver two biomolecules aiming for chondrogenic differentiation. The chondrogenic growth factor rhTGF-b1, which was initially entrapped in the core of PCL fibers, were gradually released up to 21 days. In addition, the BMSC-specific affinity peptide E7, which was subsequently conjugated onto the PCL fibers surface *via* covalent bonding, synchronously promoted the BMSCs adhesion and proliferation. The drug carriers were also immobilized on the fibers surface by Monteiro *et al.*[119] through covalent bonding. Thiol group was firstly inserted to bond with the amine group of chitosan fibers, and the gentamicin-loaded liposomes were then immobilized onto the modified chitosan fibers *via* maleimide reaction to achieve steady released gentamicin for antibacterial applications. The immobilization of drug-encapsulated liposomes onto the fiber surface could inhibit the drug denaturation, and avoid the toxicity brought by high dose of drug.

Li *et al.*[65] fabricated PCL-co-PEG scaffolds with dual-drug release capability in two stages. Dexamethasone (DEX) and BMP-2 encapsulated bovine serum albumin (BSA) nanoparticles were embedded into the polymer scaffolds through blend electrospinning. The burst release of

DEX was finished in the first 8 days and the BMP-2, which was protected by two barriers, were released in a sustained manner up to 35 days. This time-programmed dual-drug release manifested the highest bone repair efficiency. Song *et al.*[120] fabricated a nano-in-nano structure by encapsulating vancomycin-loaded gelatin nanospheres into the silk fibroin membranes through single-nozzle or co-axial electrospinning. The drug-loaded nanoparticles were further entrapped within the core section of electrospun fibers, enabling an extended drug release up to 14 days. Similarly, Yang *et al.*[121] successfully confined DOX-loaded FA-PCL-PEG copolymer micelles in cross-linked gelatin fibers through co-axial electrospinning. A step-wise release of initial active micelles and subsequent DOX was achieved by this micelle-in-nanofiber device. Modified tri-axial electrospinning was also combined with drug-loaded lipids to constitute a multilayer and smart drug carrier system for oral drug delivery.[16b] In a study of Yang *et al.*[16b], diclofenac sodium/phosphatidyl choline (DS/PL) lipids were entrapped in the core of ES100 fibers through tri-axial electrospinning to achieve a pH-stimuli triggered and sustained drug release. This proof-of concept research explored the influence of spinnability of outer-middle-inner solutions on the final fiber structures, and greatly enlarged the selection pool of raw materials. All types of liquid phases could be processed through this modified tri-axial electrospinning, including small molecule solutions and diluted polymer solutions, which were un-spinnable in the traditional electrospinning.

In addition to the polymer nanospheres, mesoporous bioactive glass nanoparticles (MBNs) were also regarded as superior drug carriers to prolong the drug release due to the high surface volume ratio for absorbing biomolecules. Kang *et al.*[122] incorporated fibroblast growth factor 2 (FGF2) and fibroblast growth factor 18 (FGF18)-loaded MBNs into the hollow core of PCL fibers through co-axial electrospinning. FGF2 was designed to dominantly release in the earlier period to promote the cellular angiogenesis and FGF18 was sequentially targeted for later

osteogenesis. By adjusting the single (PCL shell) or double layer (PCL shell and MBNs) of barriers, the sustained release patterns can be manipulated as desired.

The versatility of electrospun DDS also enable the production of complex and multi-functional implants possible. Liu *et al.*[62] fabricated a uniformed mixed membrane consisting of hyaluronic acid fibers and collagen fibers by simultaneously running two electrospinning apparatuses. EGF, pDFG-loaded gelatin NPs, VEGF-loaded gelatin NPs and bFGF were dispersed into collagen fibers and hyaluronic acid fibers through blend electrospinning, respectively, forming a composite scaffold with potential to deliver four growth factors in a stage-wise manner for 30 days. The earlier released bFGF and EGF were responsible for the epithelialization and vasculature sprouting and the delayed release of pDFG and VEFG were aiming for blood vessels maturation.

Table 6. Representative electrospun DDS *via* combinational-drug incorporation approaches and the associated highlights and applications.

Materials	Drugs	Highlights	Applications	Ref.
PLGA	Rg3, PEG-NH_2, RGD and bFGF	Combination of blend electrospinning and surface functionalization; Sustained release of Rg3 for 40 d; Combination of the wound healing and inhibition of hypertrophic scars formation.	Wound healing	[29d]
PCL (shell)	PVP/BSA/rhTGF-β1 (core) BMSC-E7 (surface)	Combination of co-axial electrospinning and covalent surface functionalization; Dual drug release: burst release of rhTGF-β1 in 5 d, and sustained release for 22 d; E7 on the PCL shell significantly promoted BMSC initial adhesion.	Cartilage tissue engineering	[63]
PCL-PEG copolymer	BMP-2-loaded BSA	Combination of drug-loaded BSA nanoparticles with blend electrospinning;	Bone tissue engineering	[65]

	nanoparticles and dexamethasone	Dual-drug release in a sequential manner: initial dexamethasone release in 8 d and sustained release of BMP-2 up to 35 d.		
PCL (shell) and PEO(core)	FGF2 and FGF18-loaded MBNs	Combination of drug-loaded MBNs, blend and co-axial electrospinning; Dual growth factors up to 65 d in sequential manner: fast release of FGF2 and sustained release of FGF18.	Bone tissue engineering	[122]
Cross-linked gelatin (shell)	DOX-loaded FA decorated micelles and PVA blend (core)	Combination of drug-loaded micellar system with co-axial electrospinning. Burst release of DOX in 20 h and more than 80% of DOX was released in 288 h. Delayed release of DOX was achieved by gelatin shell and micelles.	Cancer therapy	[121]
Chitosan	Gentamicin-loaded liposomes	Gentamicin-loaded liposomes were covalently immobilized onto chitosan fiber surface; Sustained release of gentamicin up to 16 h.	Wound dressing	[119]
Collagen HA	VEGF-loaded and PDGF-BB-loaded gelatin NPs; bFGF and EGF	Combination of drug-loaded gelatin NPs with blend electrospinning; Programmed, sequential release of four growth factors (burst release of bFGF and EGF; sustained release of VEGF and PDGF-BB) up to 1 month.	Chronic wound Healing	[62]
PLGA	Paclitaxel and Brefeldin A loaded polymer micelles	Dual-drug release through micelles with blend electrospinning; Burst release of paclitaxel (~ 60%) and the prolonged release of Brefeldin A (~ 20%) in the first 96 h.	Cancer therapy	[123]

Rg3, (20R)-Ginsenoside Rg3; rhTGF-β1, recombinant human transforming growth factor-b1; BMSC-E7, Bone marrow-derived stem cells specific affinity peptide E7; FGF2, fibroblast growth factor 2; FGF18, fibroblast growth factor 18; FA, folate; PDGF-BB, platelet-derived growth factor BB.

2.3 Drug release kinetics

When released from fibers, drugs go through a cascade of partitioning and diffusion processes within fibers and following dissolution in medium.[6, 124] In non-degradable fibers, the drug release rate is mainly dependent on water diffusion rate into the matrix, drug diffusion rate out

of the matrix and the drug dissolution rate in the medium, since the average drug diffusion path stays constant. However, in degradable polymer fibers, the polymer degradation rate also plays a key role, because the average diffusion path changes with time.[125] More specifically, during the fabrication of electrospun DDS, many factors relating to construct, matrix material and drugs can affect the above two-way diffusive process, and thus, influencing the drug release behavior (**Table 7**). Materials, drugs and their interactions will be particular highlighted in the following sections of this review.

Table 7. Possible factors that contribute to the drug release mechanisms [7b, 80, 124-126].

Aspect of Construct	Aspect of Material	Aspect of Drug
Geometry	Composition	Drug loading
Dimension	Molecule weight	Drug state
Porosity	Crystallinity	Drug molecule weight
Pore size	Degradation rate	Drug-solubility in medium
Fiber diameter	Swelling ability	
	Drug-polymer interactions	
	Drug distribution within fibers	

2.3.1 Influence of materials

The intrinsic nature of the drug carrier initially determines the drug release duration. When drugs were encapsulated within water-soluble polymers, such as PVA and PVP, they usually achieve full drug release within few minutes or hours.[10a, 11b] The release rate will be accelerated in electrospun fibers owing to the enhanced solubility.[10a] The hydrophilicity of natural drug carriers can increase the medium absorption, and thus, enhancing the drug diffusion, leading to rapid drug release. Cross-linking is the main strategy adopted to prolong the drug release in natural polymer fibers.[127] On the contrary, a hydrophobic polymer matrix with varying degradation rate can extend the release duration to days even months.[34a, 91-92] The exact release period also relates to the molecular weight, crystallinity and degradation rate of the

biopolymers.[128] **Table 8** gives few examples of drug release duration of electrospun DDS through blend electrospinning.

Moreover, the feasible blending of polymers provides facile approach to regulate the drug release duration aiming for diverse applications.[34a] In case of stimuli-responsive materials, DDSs usually show instant drug release upon sensing the stimuli and sustained release in absence of the stimuli.[41] Nevertheless, when the drugs were located on the surface or near surface vicinity without strong linking, the release duration may show little relevance to the materials nature.[129]

Table 8. Few examples of drug release duration of electrospun DDS through blend electrospinning.

Polymer	Molecular weight (kDa)	Release duration	Ref.
PVA	67	100% within 60 s ~240 s	[10a]
	31	100% within < 30 s	[10b]
PVP	360	100% within < 1 min	[130]
	1300	100% within ~ 120 min	[11b]
Fish gelatin	-	100% within 4 min	[12]
PCL/gelatin	70 ~ 90 (PCL)	22 d ~ 32d	[31a]
PLLA/PEG	PLLA 50, PEG 2	8 ~14 d	[34a]
PLLA/PEG	100	< 50% over 90 d	[92]
PLA	78	10% ~ 80% over 84 d	[91]
PCL	In-situ synthesis	< 15% over 56 d	[88]
Poly-urethane	In-situ synthesis	< 60% over 91 d	[81]

2.3.2 Influence of drugs and drug–polymer interactions

Drug-type (molecule weight and solubility) and drug loading ratio are two aspects that strongly influence the release kinetics. Pattama *et al.*[131] thoroughly investigated the drug release behavior of four model drugs, with varying molecule weight and water solubility, from PVA

fibers. It was observed that sodium salicylate, which had low molecule weight (160.1 g mol^{-1}) and high water solubility, reached near 100% of release within few minutes. However, only less than 40% of water insoluble indomethacin (357.8 g mol^{-1}) was released over 1400 min. The different release tendency was explained by the faster leaching out of matrix in case of low molecule weight drugs. In the early studies, Zeng *et al.*[80] studied the drug release behavior of paclitaxel, doxorubicin hydrochloride and doxorubicin base from PLLA fibers. Both PLA fibers containing paclitaxel and doxorubicin base showed constant zero-order release, which was proportional to the polymer degradation, whereas doxorubicin hydrochloride-loaded fibers showed rapid drug release, which was irrelevant to the PLA degradation. It was concluded that stable and constant drug release can be acquired when majority of the drugs were embedded inside of the fibers by selecting proper lipophilic polymer/lipophilic drug pair and hydrophilic polymer/hydrophilic drug pair.

Potrč *et al.*[129] entrapped hydrophilic ibuprofen and hydrophobic carvedilol into PCL fibers, respectively, with loading ratios ranging from 10% to 60%. The dissolution tests indicated that all systems exhibited a burst drug release following with a plateau. All fibers in PCL/ibuprofen group reached near 100% of release within 6 h; however, only 60–80% of drugs were released within 6 h in PCL/carvedilol group. In each group, higher drug loading practically delayed the drug release rate to some extent. They also pointed that the delayed release of carvedilol could be explained by the high molecular weight of carvedilol and the stronger hydrophobic–hydrophobic interactions between matrix and drugs. Similarly, in the study of Roman *et al.*[91], the sustainable release of paclitaxel from PLA fibers were notably delayed by the high drug loading ratio. Over 60% of paclitaxel was released over 84 days in PLA fibers with a drug loading ratio of 0.25%, *vs* 30% to PLA fibers with a ratio of 0.58%. However, contradictory results were showed in the studies of Xie *et al.*[24] Varying ratios of tetracycline

and chlorotetracycline were encapsulated into electrospun PDLLA fibers, respectively. Increasing the ratio of tetracycline highly accelerated the drug release, whereas increasing the ratio of chlorotetracycline significantly decreased the drug release rate. The controversial results could be due to the different polymer/drug/solvent interactions occurred.

Above studies relevant to polymer–drug interactions were all conducted in drug-laden fibers through blend electrospinning, from which the spontaneous drug distributions completely depend on the intrinsic interactions between polymers and drugs. However, through multiple modified drug incorporation techniques, drug distributions could be practically manipulated, generating programmable drug release behavior.

2.3.3 Influence of drug incorporation techniques

As thoroughly discussed in former sections, drug distributions within matrix, which directly affect the drug diffusion paths, can be feasibly manipulated through different incorporation techniques. **Figure 7** gives a summary illustration of the former discussed techniques and

Table 9 further comparatively describe the advantages, limitations and possible drug release profiles of each approaches.

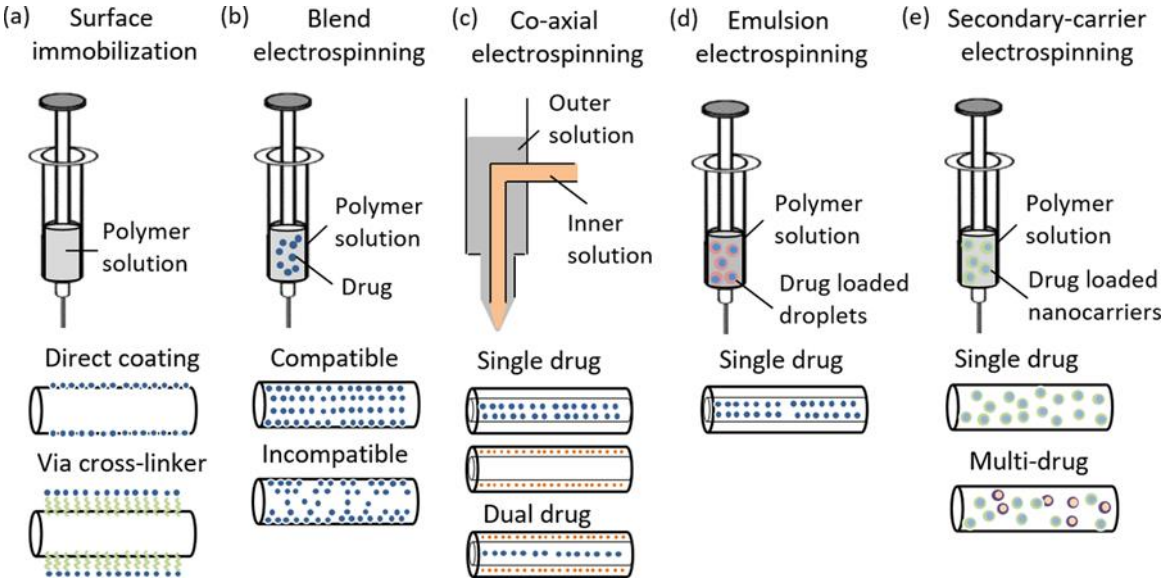

Figure 7. Schematic illustrations of different drug incorporation techniques *via* electrospinning.

Table 9. Advantages, limitations and possible drug release profiles of different drug incorporation techniques.

Techniques	Advantages	Limitations	Release Trends	Ref.
Surface Immobilization	Avoiding harmful solvents for biomolecules; Maintenance of the original physical or degradation properties of matrix;	Cross-linker necessary for long term release;	Rapid and burst release in case of weak bonding; Sustained release in case of strong covalent bonding;	[29d, 33a, 71c]
Blend Electrospinning	Simple one-step approach;	Possible denaturation of drugs in the harsh organic solvent;	Burst release in case of incompatible drug-polymer interaction;	[10a, 80, 129, 131]

		Uncontrollable drug distribution	Sustained release in case of compatible drug-polymer interaction;	
Co/tri-axial Electrospinning	Ideal for core-shell structure; Feasible entrapment of water-soluble or fragile drugs within the core of fibers; Unspinnable drug solution can be used; Achievable for dual-drug release;	Complex spinnerets configuration; Unsuitable interfacial interactions may cause failure in core-shell structure;	Rapid and burst release in case of hydrophilic and fast-degradable shell; Sustained release in case of hydrophobic and slow-degradable shell;	[94-96, 98-99]
Emulsion Electrospinning	Single one-step approach for core-shell structure;	Emulsion stability need to be well adjusted through surfactants and other emulsification parameters;	Similar trends to co-axial electrospinning;	[106b, 109, 112, 132]
Secondary-carrier and combinational Electrospinning	Ideal for multi-drug release; Feasible combination with extra stimuli-responsive carriers.	Complex system.	Achievable for multi-drug and multi-stage drug release.	[34b, 62, 116-117, 121-123]

Overall, by choosing the appropriate encapsulation approaches, various drugs can be either attached onto the surface, embedded in the surface vicinity, uniformly distributed throughout the whole fibers, or fully confined within the core section of fibers, resulting in rapid, sustained or zero-order drug release profiles. Therefore, when choosing ideal drug release platforms for specific biomedical applications, it is critical to carefully consider both the material/drug

composition and the encapsulation technique, which could synergically affect the drug release patterns and thus the treatment efficacy.

3. Applications in Biomedical Fields

As discussed above, numerous electrospun scaffolds containing diverse active ingredients can be easily produced through selecting proper materials and approaches. The resultant drug-laden architectures offer massive variations on physical topography, drug loading degree, drug release behavior, and thus, ultimately lead to therapeutic effects, which potentially meet multiple clinical needs. In the current section, the therapeutic outcomes of drug-containing electrospun DDS in some biomedical fields, with a particular focus on tissue engineering and cancer therapy, will be thoroughly discussed below.

3.1 Simple Drug Delivery Systems

Due to the high drug loading and high encapsulation efficiency, implantable drug-eluting electrospun fibers have intrinsic advantages over the conventional small-scale drug vehicles as novel drug administration methods through oral, transdermal or ocular routes.[8, 133] The following sections will summarize the recent endeavors made on these fields and highlight the superiority of electrospun drug formulations.

3.1.1 Oral drug delivery

Electrospinning technique is able to produce highly porous and fibrous membrane consisting of continuous nanofibers. The highly interconnected porous structure of electrospun fibers allow faster medium penetration, thus resulting in more rapidly dissolving or disintegration of

the hydrophilic polymers. And the nano-size dimension indicates well dispersible drug particles in polymer matrix, causing a great increase of drug solubility.[7a] These features enable the electrospun fibers good candidates for FDDDS of bitter drugs in oral cavity. Samprasit *et al.*[11b] explored the potential of electrospun PVP/cyclodextrin (CD) fibers to deliver meloxicam (MX) in oral cavity. This study demonstrated faster disintegration of electrospun PVP/CD fibers than the MX powder, commercial tablet and casting films. The optimized and taste-masked formulations were non-cytotoxic, physical stable for 6 months in storage condition and all of them disintegrated within one minute in simulated moisture environments of oral cavity (**Figure 8**a). Li *et al.*[10a] investigated the performances of drug-loaded PVA fibers as FDDDS formulation and reported that PVA/caffeine and PVA/riboflavin fibrous mats got wetted within 4.5s and started disintegration within 1.5s.

Oral formulations have also been exploited for sustained drug release *via* the sublingual route rather than FDDDS. It is an invasive administration and advantageous for the drugs that need to be continuously taken-up into the blood circulation. Sharma *et al.*[15] fabricated an anti-diabetic patch by electrospinning of insulin-loaded PVA/sodium alginate (NaAlg) composite fibers, from which the insulin was supposed to be released sublingually and absorbed through oral mucosa. The *in vivo* experiments conducted by applying the patch below the tongue of a diabetic rat. Resultant blood glucose concentration of the diabetic male Wistar rats was significantly reduced and the effect lasted for 10 h.

In addition to oromucosal delivery system, electrospun membrane can be further used as oral formulations to achieve colon-targeted release. Yang *et al.*[16b] confined lecithin diclofenac sodium (phospholipids PL-DS) within ES100 fibers through co-axial electrospinning to create a pH-sensitive drug carrier (**Figure 8**b1, 2). The outer ES100 layer could protect the central-located drug from the acid gastric fluid and only started to disintegrate in the neutral pH

environments when the drug carriers reach the colon. Subsequently, partial DS was freed when the DS-loaded lipids were converted to sub-micron sized particles and more DS was continuously released from the lipid particles (**Figure 8**b3). The *ex-vivo* permeation tests indicated highly enhanced colonic membrane permeation ability of fiber dosage compared to free drug. In another study, Jin *et al.*[44] loaded Gd(DTPA) and indomethacin within the core section of ES100 fibers through co-axial electrospinning to colon-targeted deliver the magnetic resonance contrast agent for imaging diagnosis and therapeutic agents simultaneously (**Figure 8**c).

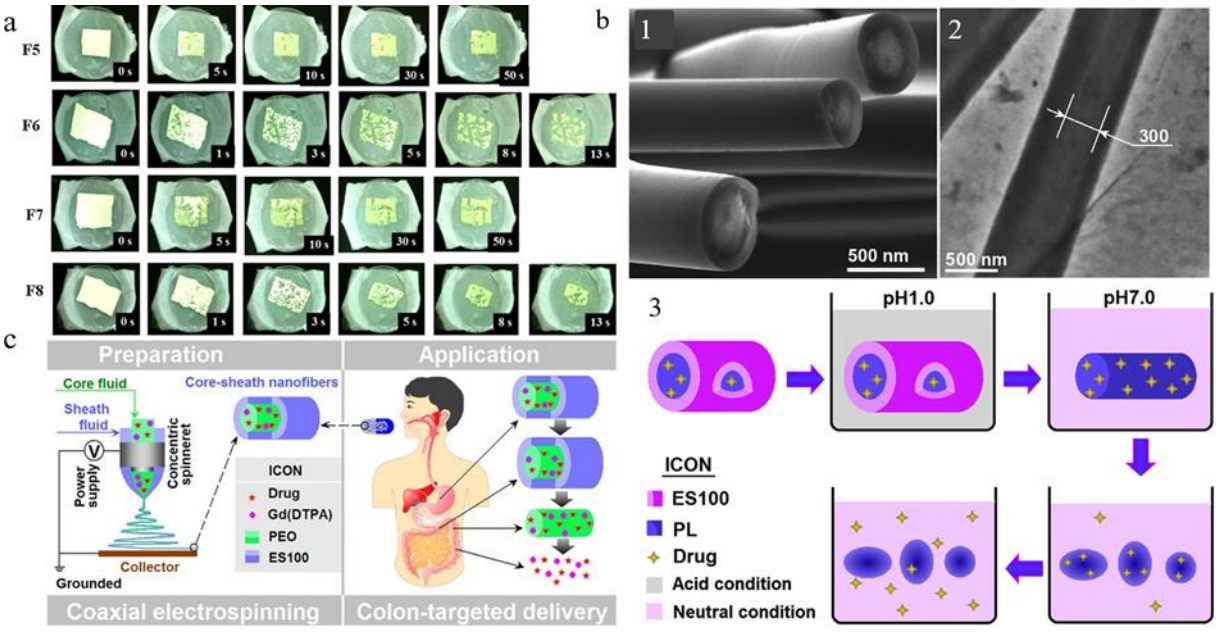

Figure 8. (a) Images of meloxicam-loaded PVP/CD fibrous mats with different compositions as FDDS in the disintegration tests. Reproduced with permission;[11b] Copyright 2015, Elsevier B.V. (b) Oral formulation of lecithin diclofenac sodium/ES100 core-shell fibers for colon-targeted drug delivery. (1) SEM and (2) TEM images of the produced core-shell fibers. (3) The proposed drug release mechanism in responsive to neutral and acid conditions. Reproduced with permission;[16b] Copyright 2016, American Chemical Society. (c) Core-shell fibers to colon-targeted deliver the magnetic resonance contrast agent for imaging diagnosis and

therapeutic agents simultaneously. Reproduced with permission;[44] Copyright 2016, Elsevier B.V.

3.1.2 Transdermal drug delivery

Transdermal drug delivery represents the strategy of drug administration through skin, which is the largest organ in human body.[134] It has several advantages over hypodermic injections, such as easy accessibility due to the high surface area of skin, less invasive operations required and avoidable hepatic first-pass metabolism.[135] The drugs can be either absorbed through skin barrier into subcutaneous tissue and systematically taken-up into the blood circle, and then the whole body, or remained locally to treat skin disorders, such as dermatitis or skin cancer, i.e. topical drug delivery.[135] As the outermost layer of skin, stratum corneum is responsible for the poor drug absorption and only small quantity of drugs can be penetrated into skin. By applying appropriate drug carriers on the skin, long term drug release can be simply achieved.[134] Conventionally, emulsions, creams, gels and transdermal patches are all ideal drug carriers for transdermal drug release.[18b] Owing to the capability of high drug loading and encapsulation efficiency of electrospinning technique, drug-loaded electrospun membranes are considered as superior options as transdermal patches.

Song *et al.*[17b] successfully embedded daidzein-loaded lipids into electrospun PLGA nanofibers as transdermal patches to address the problems associated with poor oral absorption and limited bioavailability of daidzine for treating cardiovascular and cerebrovascular disease. A skin permeation enhancer, Azone, was also blended into PLGA matrix to increase the drug diffusion rate by interacting with structured lipids of the stratum corneum. *In vitro* drug release and skin permeation studies showed ~3.8 times higher amount of fiber-released daidzein penetrated skin barrier, compared to the pure daidzein solution. Moreover, better skin retention property was

observed in case of composite fibers than daidzein-loaded lipids in the long-term period and no obvious skin irritation was observed. More studies have explored the potential of electrospun fibers from diverse polymers as transdermal patches, such as PVP,[21] PVA/chitosan,[136] PU/cellulose,[19] and PVA/Alginate.[22b]

3.1.3 Ocular drug delivery

Electrospun patch has been also investigated to deliver drugs into eyes for ocular surface repair. Most common clinical substrate for ocular surface repair is human amniotic membrane owing to its biocompatibility, anti-inflammation efficacy and angiogenesis ability.[137] However, it also has several disadvantages, such as poor mechanical strength, semitransparent appearance, difficulty of handling and the potential risk of disease transmission,[138] and therefore, alternative choices should be further explored. Compared to bulk material, electrospun patches with micro/nano- size fiber dimensions and high surface area were considered advantageous in topical application or treating the anterior segment eye diseases. Bhattarai *et al.*[139] fabricated two different dexamethasone-loaded PLA/PVA patches as ophthalmic inserts through either solvent casting or electrospinning method, and further compared the drug release behavior. Results indicated that 90% of the drug was released from the electrospun inserts over 40 h and only 24 h from the solvent-casting inserts. Compared to solvent-casting inserts, electrospun inserts showed more consistent and predictable drug release. In another study of Baskakova *et al.*[140], acyclovir, cyanocobalamin and ciprofloxacin were simultaneously incorporated into PCL fibers to fabricate fibrous matrices as intravitreal implants. Drug release using an *in vitro* eye model showed that the drug residence time (half-life) was extended to 6 days, which was much greater than the small molecule drug solutions, suggesting that the proposed matrices can be a viable option as intravitreal implant. Angkawinitwong *et al.*[98] encapsulated bevacizumab,

a VEGF neutralizing antibody, into the core area in PCL fibers through co-axial electrospinning to treat age related macular degeneration. This fibrous solid formulation highly prolonged the drug release period over two months, and therefore, reduced the administration frequency and avoided the invasive injection in the eyes.

3.2 Tissue Engineering

Tissue engineering represents a multidisciplinary field integrating the materials, chemistry and biological science. Aiming for in-situ tissue regeneration or organ restoration, cells are supposed to attach, proliferate and differentiate under the support of the 3D scaffold,s which will degrade gradually in the meanwhile.[141] Another essential link in this strategy is suitable biochemical and physicochemical factors that are molecularly affect or guide the cellular behaviors. It is well-known that electrospun scaffolds are widely applied as scaffolds for tissue regeneration owing to the excellent physical resemblance to ECM. Moreover, increasing studies focus on applications of active ingredients-loaded fibrous scaffolds in pursuit of improved therapeutic outcomes. Their achievements made on regeneration or restoration of multiple organs, such as skin, bone, cartilage, muscle, tendon, heart, nerve and blood vessels, are discussed in this section.

3.2.1 Wound healing and skin tissue regeneration

Wound healing is a dynamic and interactive process involving dermal cells (e.g., fibroblasts, endothelial cells), growth factors (e.g., EGF, FGF-2, and VEGF), cytokines, etc. Four periods consisting of hemostasis, inflammation, proliferation and remodeling/maturation are included

in this process.[142] As described above, the high porosity and surface area enable electrospun structure an optimal candidate to fulfill the mission of conventional wound dressings, such as being permeable to moisture and oxygen, protecting the wound from microbes and mechanical irritation and allowing the exudate removal.[143] Additionally, the high resemblance to ECM and feasibility for multifunctionlization make electrospun drug-loaded scaffolds prospective in treating skin trauma and disorders, especially for some chronic skin diseases which have no clinical cures yet.

Antibacterial property is the primary function required for a wound dressing material and it can be easily achieved by incorporating antibiotics,[90, 144] antibacterial peptide motif[78] and antibacterial nanoparticles,[33c] into electrospun membranes. For instance, tetracycline hydrochloride was loaded into PCL/cellulose acetate/dextran and PVA/chitosan composite membranes to facilitate wound healing, respectively.[144] The obtained membranes were proved to be biocompatible and bioactive, and effectively antibiotic against bacterial. An antimicrobial peptide motif (Cys-KR12) was immobilized onto electrospun silk fibroin nanofiber surface through EDC/NHS and thiol-maleimide click chemistry by Song *et al*.[78] In addition to the antibacterial efficacy, the immobilized Cys-KR12 further promoted the proliferation of keratinocytes and fibroblasts and the differentiation of keratinocytes, and also inhibited the inflammatory cytokine expression.

Apart from the feasible implementation in acute infections of wound sites, electrospun scaffolds are able to sustainably release therapeutic agents and simultaneously support in-situ tissue regeneration for curing chronic wound diseases, such as diabetic wound diseases.[62, 103, 145] Various drug-loaded scaffolds were designed to improve the poor angiogenesis and delayed wound closure in diabetic wounds associated with high blood glucose level, and therefore to achieve accelerated diabetic wound healing. Lai *et al*.[62] co-loaded multiple angiogenic factors

(VEGF, bFGF, PDGF and EGF) into collagen/hyaluronic acid composite scaffolds to rapidly increase the blood vessels formation and further allow fast integration with surrounding tissues. An examination on *in vivo* streptozotocin (STZ)-induced diabetic rats model confirmed increased vessel density and lumen area, elevated collagen deposition and subsequent accelerated wound closure rate. Other angiogenic agents, such as epigallocatechin-3-O-gallate and desferrioxamine, were also loaded into hyaluronic acid/PLGA and PVA/chitosan scaffolds, respectively, to dramatically increase the neovascularization and collagen deposition, and thus, promote the diabetic wound healing.[103, 146]

Ren *et al.*[145b] developed a composite scaffold consisting of both beneficial micro/nano structural cues and chemical active agents to create a synergistic microenvironment for rapid diabetic wound healing (**Figure 9**). It was observed that nanopores enhanced the protein adsorption, and thus, the cellular adhesion and proliferation, and the aligned fibers favorably regulated the endothelial cellular angiogenesis differentiation. 0%, 5%, 10% and 15% of dimethyloxalylglycine (DMOG)-loaded MSNs (PL, 5 DS-PL, 10 DS-PL and 15 DS-PL) were embedded into aligned PLLA fibers with nanopores on the surface for sustained release of both DMOG and Si ions, which both have positive effects on the angiogenesis of endothelial cells. As shown in **Figure 9**a, drug-loaded MSNs were uniformly distributed throughout the aligned PLLA fibers with interconnected nanopores and varying ratios of DMOG and Si ions can be stably released over 360 h (**Figure 9**b,c). An *in vivo* study of placing the 10% of DMOG-MSNs/PLLA fiber meshes onto wound regions in the diabetic mice proved that drug-loaded fiber meshes significantly enhanced the wound healing ratios (97%) after 15 days of treatment, compared to undressed wounds (84%) (**Figure 9**d, e, f).

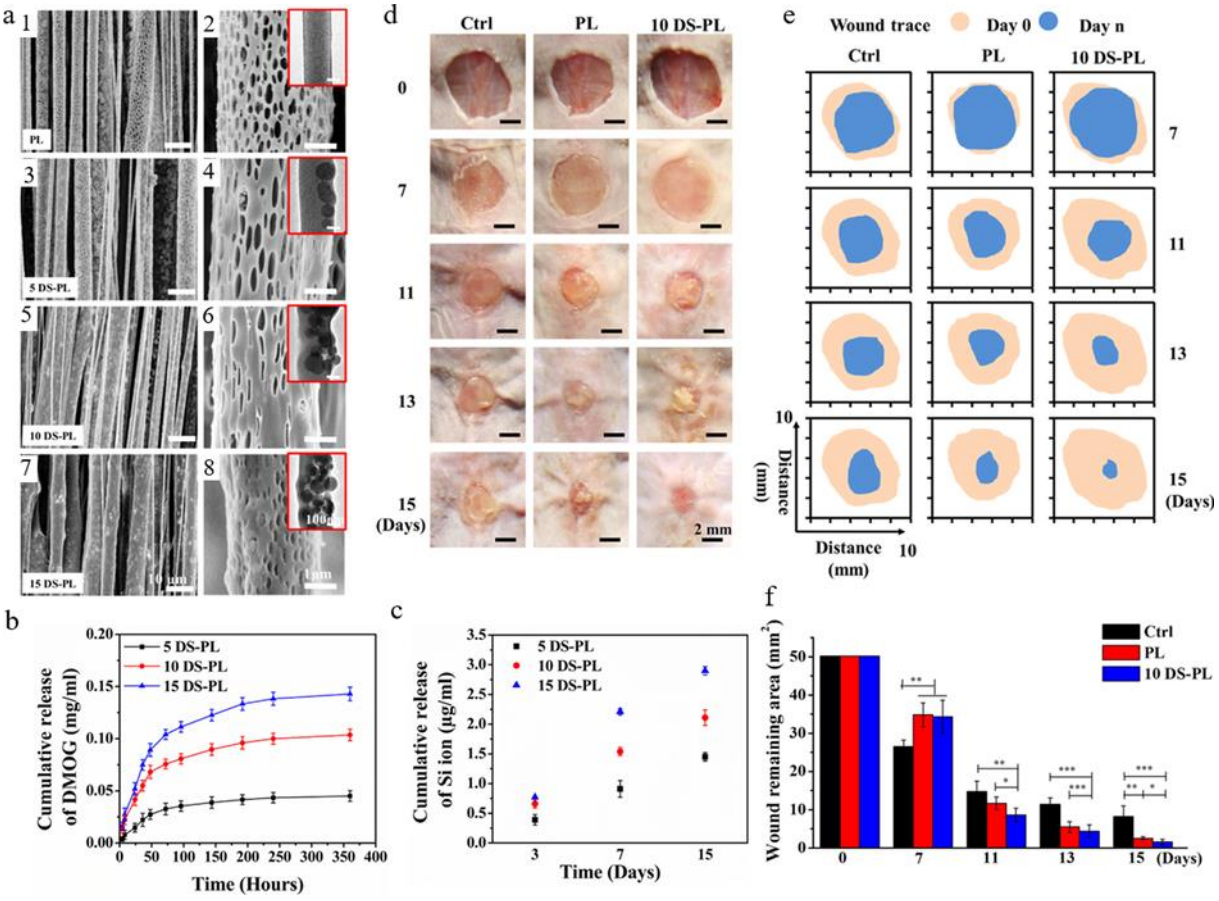

Figure 9. (a) SEM images of the aligned porous electrospun membranes with increasing drug ratios. The corresponding TEM image inserted in each SEM images. (b) DMOG and (c) Si ion release profiles. (d) Overview of the size change of the large excision wounds made in the dorsal skin of diabetic mice (control, PL and 10 DS-PL) at 0, 7, 11, 13, 15 day post-surgery. (e) Traces of wound bed closure for each treatment group *in vivo*. (f) Statistical analysis of wound area. $^{*}P < 0.05$, $^{**}P < 0.01$, $^{***}P < 0.001$. Reproduced with permission;[145b] Copyright 2018, Elsevier B.V.

Studies focusing on the other aspects of wound healing were also reported. Cheng *et al.*[29d] encapsulated a bioactive drug 20(R)-ginsenoside RG3 onto PLGA fibers through pDA coating, and then further immobilized bFGF onto fibers surfaces to inhibit the formation of hypertrophic scars during wound healing process. Dong *et al.*[147] created a handy electrospinning device to

fabricate antibacterial PCL membranes, which reduced the inflammation and promoted the wound healing *in vivo*. This convenient handy device holds great potential to meet the clinical needs in emergency medical transport, hospitals, or first aids at home.

3.2.2 Musculoskeletal tissue regeneration

Musculoskeletal tissues play a vital role to offer physical support and allow stable movement of human body and could extend to bone, skeletal muscle, and connective tissues, e.g. tendon, cartilage and ligament.[148] The disease and injury related to musculoskeletal tissues can be acute bone or muscle trauma, or chronic osteoarthritis, rheumatoid arthritis and degenerative disc disease.[148a] Large bone defects and severe injuries in muscles and connective tissues (i.e. cartilage, tendon and ligament) have low intrinsic healing capacity due to the lack of vascularization and poor blood supply.[149] Tissue engineering appeared as an innovative and promising strategy to endow the in-situ regeneration ability to these severe defect sites. The produced fibrous scaffolds are usually applied in musculoskeletal tissue regeneration in two approaches. Firstly, 3D structural scaffolds are implanted to maintain the geometrical integrity of the target tissue and provide the necessary support for cells to attach, proliferate and differentiate in the meanwhile.[150] Another method is preparing and utilizing occlusive membranes for providing space maintenance, covering the diseased area, promoting the recruitment and growth of osteogenic cells and blocking the migration of competing soft tissue cells from overlying mucosa.[77, 151]

Incorporation of small molecules or single growth factor is one of the simplest way to load therapeutics into scaffolds for better performances. For better skeletal muscle regeneration, Liu *et al*.[152] coated PCL fibers with mussel-inspired poly-norepinephrine (pNE), a catecholamine functioning as a hormone and neurotransmitter in the human brain, to obtain fiber surfaces

enriched with catechol groups that attract primary amine or thiol-based biomolecules. Their study revealed that fiber meshes with thinner fiber diameter could be more effectively functionalized by pNE, and thus had higher muscle cell proliferation and adhesion and treatment efficacy for repairing impaired musculus rectus abdominis in a rat muscle injury model. In the study of Pauly *et al*.,[153] connective tissue growth factor (CTGF) was conjugated onto longitudinally aligned PCL fiber bundles to mimic the hierarchical structures of native human anterior cruciate ligament (ACL) for ACL regeneration. CTGF was sustainably released over 2 weeks, evidenced by an ELISA assay. Elongated cells along the longitudinal axis fully covered the fiber bundles after 7 days, and significant collagen deposition specific for ligament tissue was observed on CFGF-loaded fiber bundles after 21 days of *in vitro* cell culture, which was further confirmed by the *in vivo* subcutaneous implantation tests. For repairing cartilage defects in osteochondral injuries, Liu *et al*.[115] constructed platelet-rich plasma (PRP)-loaded PCL scaffolds to obtain co-delivery of multiple therapeutic agents. Abundance of growth factors derived from PRP, such as PDGF, TGF-b and IGF, were simultaneously released from the porous scaffolds over 30 days. Highly enhanced gene expression of collagen-II, aggrecan and SOX9 suggested beneficial chondrogenesis of BMSCs when cultured on PRP containing scaffolds. The *in vivo* healing efficacy was evaluated by implanting the scaffolds in a New Zealand rabbit model with full-thickness cartilage and subchondral bone defect. The cartilage defect was nearly filled with regenerated tissues with glossy and normal articular surface 12 weeks after the surgery, while there was still a gap to be filled in the pure PCL scaffolds group. Tendon tissues mainly constituting of parallel collagen fibrils work as an intermediate connector between the bone and muscle to achieve stress transfer and joint stability.[154] Although aligned fibers have been reported to promote tenogenesis, it is not enough for teno-differentiation of stem cells.[155] Zhang *et al*.[92] encapsulated small molecule Trichostatin A

(TSA), an histone deacetylases inhibitor, into aligned PLLA nanofibers to commit teno-differentiation of stem cells for tendon tissue regeneration. Comparative *in vitro* tendon stem/progenitor cell culture studies on random fibers and pure polymer fibers, displayed highly elevated tendon-associated genes expression and collagen accumulation in groups with both aligned topography and TSA entrapment, which could be further verified by the enhanced neotendon formation in an *in vivo* Achilles tendon repair model. Adhesion formation associated with fibroblast adhesion and proliferation is the major clinical complication in tendon healing after tendon surgery, and it could severely affect the joint movement. To eliminate the risk of adhesion formation, Zhao *et al.*[114] prepared core-shell hyaluronan/PLLA fibrous scaffolds with mitomycin-C (MMC) embedded in the core area of fibers, since MMC was reported to prevent the adhesion formation without impairing the tendon healing process (**Figure 10**a). The obtained fibrous membrane was designed to act as a physical barrier to mediate apoptotic gene expression and inhibit collagen expression in adhesion tissues. *In vitro* drug release study showed sustained release of MMC up to 40 days (**Figure 10**b), which efficiently inhibited the survival, adhesion and proliferation of fibroblasts. The healing efficacy were evaluated in both animal models of rabbit flexor digitorum profundus (FDP) tendon and rat Achilles tendon (**Figure 10**c, d). Severe adhesions were observed in the untreated control group in both models, and groups treated with PLLA-only membranes generated small bundles of fibrous tissues, connecting the tendon with surrounding tissues. Very little adhesion was observed in the repaired tendon and the peritendinous tissue when treated with MMC-loaded PLLA membranes in both models. This gross observation was further confirmed by the following histological analysis (**Figure 10**c2, d2). Consequently, the adhesion scores and grades for the histological tendon adhesions of the drug-loaded groups were both significantly lower than the control and PLLA-alone group (**Figure 10**e, f). This dramatically inhibition of adhesion formation was

further explained by the identification of the up-regulation of apoptotic protein Bax expression and down-regulation of proteins Bcl2, collage I, collagen III and α-SMA during the healing process with minimum adhesion formations. Overall, the proposed scaffolds were considered to be highly prospective as anti-adhesion materials in tendon tissue regeneration.

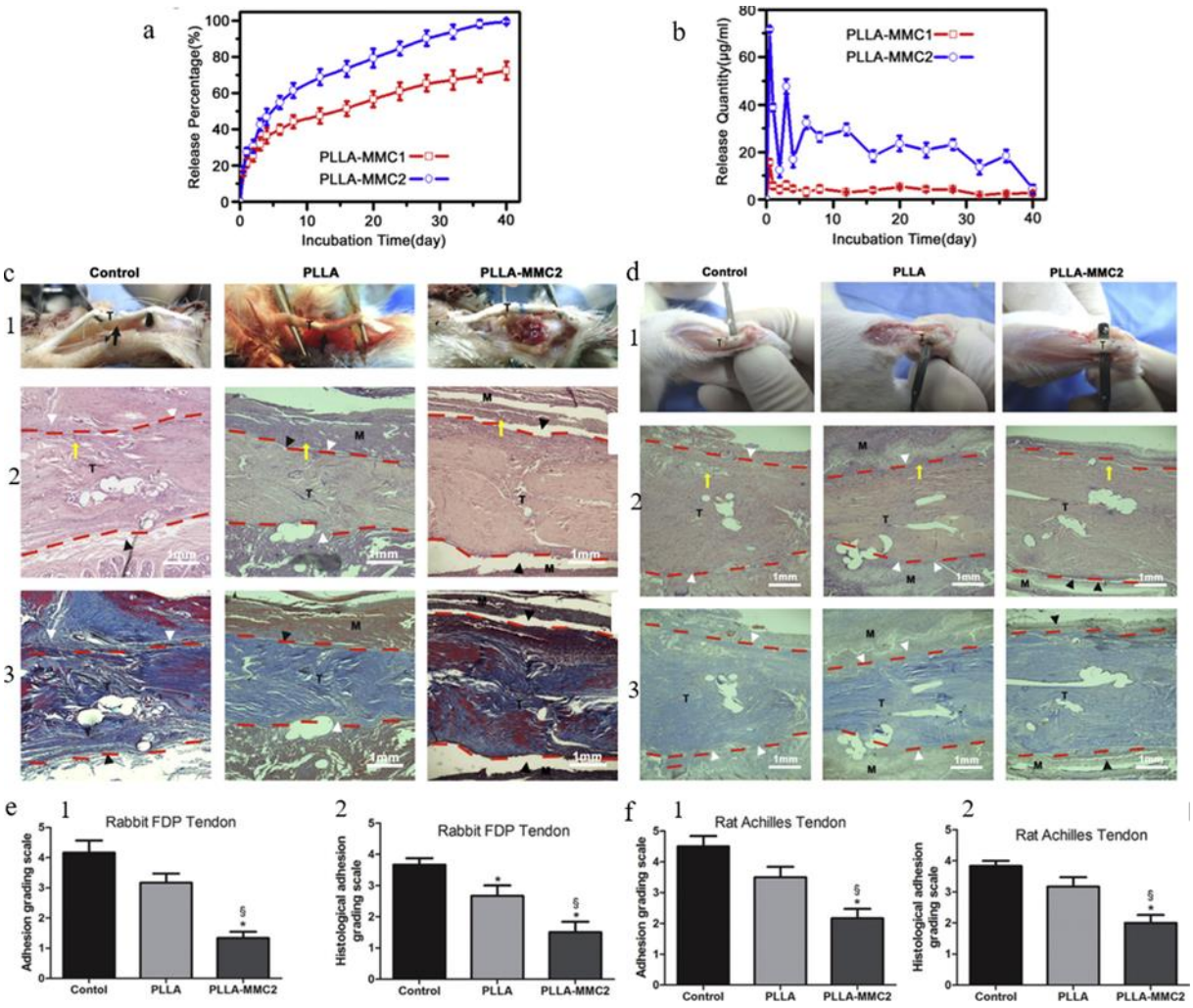

Figure 10. (a) Cumulative release and (b) daily release of MMC from electrospun PLLA-MMC fibers (1 and 4% of MMC in MMC1 and MMC2). (c1 and d1) Gross evaluation of the rabbit FDP tendon and rat Achilles tendon model in control, PLLA and PLLA-MMC2 groups. HE (c2 and c3) and Masson (d2 and d3) staining of control, PLLA and PLLA-MMC2 groups. T, tendon; M, membrane. 21 days after surgery, tendon repair and peritendinous adhesions were assessed by macroscopic evaluation of tendon adhesions (e1 and f1), and histological adhesion

grade (e2 and f2). *P < 0.05 compared with control group; §P < 0.05 compared with PLLA group. Reproduced with permission;[114] Copyright 2015, Elsevier B.V.

Biomaterials-associated bone tissue engineering refers to the construction of an artificial implant which can accelerate bone vascularization and mineralization, therefore resulting the reconstruction of injured or diseased bones.[77, 118, 151] Kang *et al.*[122] proposed a novel therapeutic design which embedded and delivered two growth actors simultaneously in core-shell fibers in combination of mesoporous bioactive glass nanospheres (MBNs), which acted as drug carriers and meanwhile enhanced the apatite-forming ability and mechanical properties of the scaffolds. FGF18-loaded MBNs and FGF 2 were co-encapsulated into the core section of PCL/PEO fibers to achieve an earlier release of FGF2 for cell proliferation and angiogenesis and later release of FGF18 for osteogenesis. Both growth factors were sustainably released over 65 days owing to the protective PCL shell. *In vitro* rat mesenchymal stem cells study presented significantly increased cell proliferation, ALP activity and expression of bone-related genes (Col I, ALP and OPN) and cellular mineralization on the composite fibrous scaffolds. When implanted in rat calvarium defects for 6 weeks, FGF2/FGF18 loading substantially increased the hard tissue ingrowth regions, which was evidenced by the highly increased bone volume and bone surface density from micro-CT images. In the study of Weng *et al.*[156], ultralight 3D fibrous aerogels composed of electrospun PLGA/collagen/gelatin fibers and Sr–Cu co-doped bioactive glass fibers were constructed by combining electrospinning and freeze-drying methods for cranial bone defect healing (**Figure 11**a). Heptaglutamate E7 domain specific BMP-2 peptides were further conjugated onto the optimized scaffolds for osteoinductive feature. *In vitro* release study suggested that 90% of the peptide was released within the first week followed by sustained release up to 4 weeks (**Figure 11**b). The sustainably released E7-BMP-

2 peptide and bioactive ions (Ca^{2+}, Si^{4+}, Sr^{2+} and Cu^{2+}) from bioglass fibers can work synergically to enhance bone healing and defect closure as the *in vivo* results showed an almost 3-times higher (20 mm^3 *v.s.* 7 mm^3) regenerated bone volume in comparison to non-peptide group after treatment for 8 weeks (**Figure 11**c). Moreover, μ-CT images were used to quantitatively confirm that the high- density bone mineral covered more than half of the cranial defect after 8 weeks in E7-BMP-2-loaded group.

Electrospun scaffolds displayed favorable advantages in musculoskeletal tissue regenerations that required intensive vascularization and possible specific configuration, such as alignment. Co-loading of multiple therapeutic agents could efficiently enhance the treatment efficacy and avoid the side effects maximally. Specifically for bone tissue regeneration, vascularization and further mineralization could be both achieved by co-loading of angiogenic factors and bioactive agents that induced biomineralization. Moreover, large volume scaffolds that closely mimic the native tissue and organs could be feasibly created by combining electrospinning and other fabrication techniques. Nevertheless, the produced scaffolds still have limited applications in high load-bearing bones and long-term degradation profiles were still missing in most of the studies.

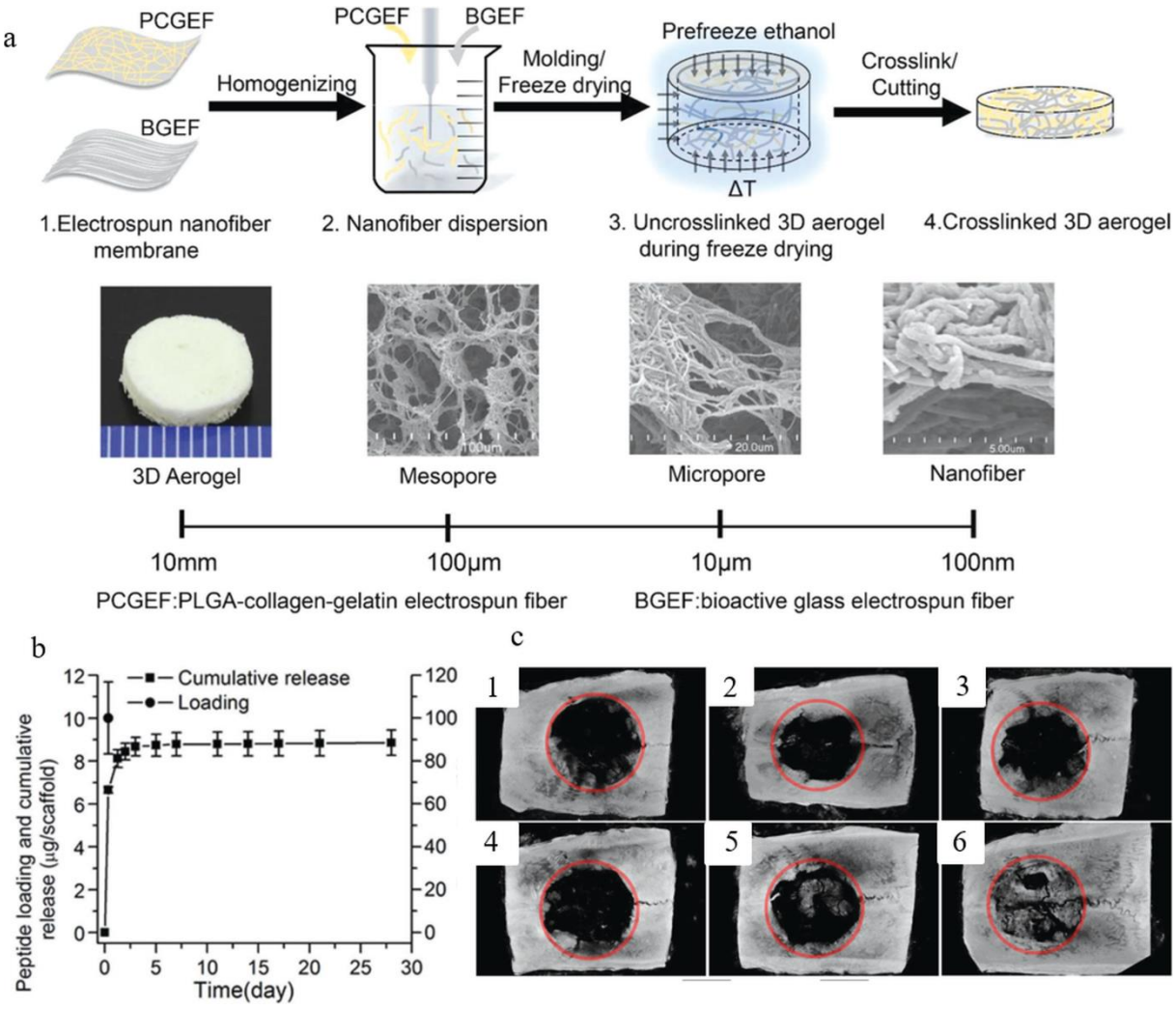

Figure 11. (a) Schematic illustration on the formation of the 3D hybrid nanofiber aerogel and its structure at different length scales. (b) Loading of E7-BMP-2-FITC peptide on 3D aerogels and their cumulative release. (c) Representative planar radiographs of cranial bone defects at 4 and 8 weeks after implantation: (c1/c4) No treatment (4w/8w). (c2/c5) 3D aerogel group (4w/8w). (c3/c6) Peptide-loaded aerogels group (4w/8w). Reproduced with permission;[156] Copyright 2018, John Wiley and Sons.

3.2.3 Cardiac tissue engineering

Cardiovascular diseases such as myocardial infarction (MI) or progressing heart failure have become the major cause of morbidity and mortality world widely.[157] Developing therapies that

induce regeneration or prevent degeneration of myocardial tissue after MI is highly clinically relevant since cardiac tissues have limited regenerative capacity and the possibility to self-renew and restore is rare.[158] The strategies of cardiac tissue regeneration have come up in two related directions: *in vitro* engineering and maturation of cardiac tissues followed by implantation, and development of methods for controllable drugs/siRNA/protein delivery into the heart.[159] Related to electrospun cardiac patches, earlier reports have emphasized on the mimicking of structural, mechanical and conductive properties of native cardiac tissues, aiming to facilitate the *in vitro* adhesion and maturation of cardiovascular cells.[160] Currently, combinational implementations of the two aspects, i.e., tissue regeneration and drug delivery, emerged as prospective approaches to achieve full recovery of the dysfunctional myocardium. It is well known that many growth factors and cytokines, such as VEGF and bFGF, are highly implicated in cardiomyocytes proliferation and survival and the maintenance of cardiac function.[161] However, their clinical uses were severely restricted by the fast degradation/elimination from the biological environment. Drug-loaded electrospun cardiac patches were thus expected to achieve sustained release in local area and further help restore the myocardium function. Lakshmanan *et al*.[87] embedded two angiogenesis growth factors (VEGF and bFGF) into a blend polymeric scaffold to promote vascularization for functional cardiac regeneration. The encapsulated VEGF and bFGF were sustainably released over 300 h and efficiently rescued cells from hypoxic stress for both *in vitro* chemical hypoxia model and *in vivo* ischemic model. In an acute *in vivo* rabbit acute myocardial infarction (AMI) model, the dual-growth factor releasing patches accelerated neovascularization and functional recovery of the ischemic heart. In another study, VEGF was confined within PCL/gelatin fibers through co-axial electrospinning, resulting a sustained release over 21 days.[162]

Gene therapy was combined with electrospun patches as well to explore the potential to remodel dysfunctional heart tissues after MI. Gu *et al.* [68] incorporated recombinant adeno-associated virus (AAV) vectors into PEUU and PEEUU fibers by both blend and co-axial electrospinning methods (**Figure 12**a). AAV encoding green fluorescent protein (GFP) from co-axial fibers can be stably released over 2 months (**Figure 12**b). After implantation in the rat left ventricular lesions after MI, the fibrous cardiac patches exhibited extensive cellular infiltration and the AAV-GFP-loaded patches showed higher gene expression compared to the AAV-alone injection without support and patches without AAV (**Figure 12**c). In addition, both α-SMA and cardiac troponin T positive cells could be successfully transduced by the cardiac patch containing AAV, proving improved cardiac function and remodeling.

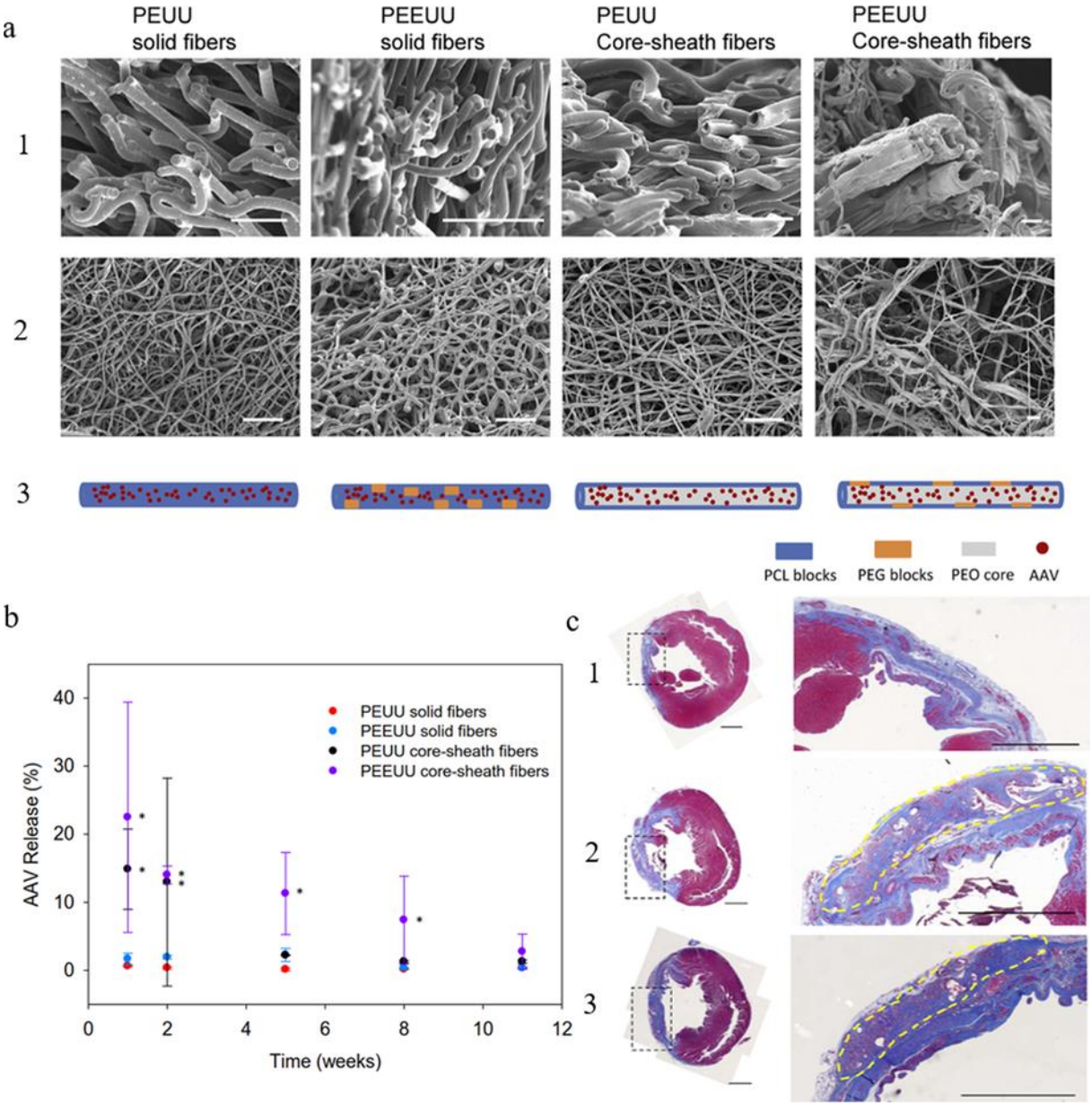

Figure 12. (a) SEM images and schematic illustrations on AAV encapsulation strategies of different scaffolds. (1) Cross section, scale bar, 10 μm; (2) surface, scale bar, 20 μm. (b) Release profiles of AAV DNA from scaffolds. *P < 0.05 compared with PEUU solid fibers. (c) Representative composite views of cross-sections of infarcted rat hearts harvested at 12 weeks, and stained by Masson's trichrome for (1) direct injection of AAV9-cmv-GFP, (2) PEEUU group, and (3) PEEUU/AAV9-cmv-GFP group. Yellow dashed lines trace the implanted

material areas. Scale bars, 2 mm. Reproduced with permission;[68] Copyright 2017, Elsevier B.V.

Another key aspect of mimicking the native myocardium is to mimic the conductive properties, which are responsive for coordinated propagation of electrical signals to produce synchronous contractions that pump blood forward.[163] Conductive materials, such as carbon nanotubes (CNTs) and polyaniline (PANI), were incorporated as the "therapeutic agents" in these cases to form the conductive network in the scaffolds.[160d, 164] Liu *et al.*[164] loaded up to 6% of CNTs into highly aligned PEG-PLLA copolymer (PELA) fibers through both blend and co-axial electrospinning. *In vitro* cardiomyocytes culture indicated that scaffolds containing higher ratios of CNTs could favorably maintain the cell viabilities, induce the cell elongation, accelerate the production of sarcomeric α-actinin and troponin I, and enhance the synchronous beating of cardiomyocytes. By comparing the blend and core-shell fibers, they concluded that core-shell fibers with 5% of CNTs could beneficially support the cardiomyocyte proliferation with a generation of organized contractile proteins and a pulsation frequency close to that of the atrium without external electric stimulation. Similarly, Wang *et al.*[160d] blended up to 3 wt% of PANI into PLA fibers to construct fibrous nano sheets with improved electrical conductivity and enhanced cardiomyocytes maturation and spontaneous beating for cardiac tissue regeneration and cardiomyocytes-based 3D bioactuators.

A recent study firstly reported the electrospinning of decellularized porcine cardiac ECM to fabricate well-defined cardiac scaffolds, which preserved the unique collagenous composition, microstructure, mechanical performances, bioactivity, and biocompatibility of cardiac ECM.[165] However, other functions such as electrical conductivity have not been explored yet. Future research and developments could still concentrate on minimizing the differences

between synthetic scaffolds and native ECM by integrating multiple functions into the well-defined cardiac scaffolds for better resemblance.

3.2.4 Nerve tissue regeneration

The application of electrospun scaffolds extends to both peripheral nerve injury,[76, 88, 101, 166] and central nervous system injury,[28a, 167] which consists of traumatic brain injury [168] and spinal cord injury.[33b, 91, 169] Those neurodegenerative diseases and traumatic nerve injuries vastly deteriorate the life quality and proper treatment methods are yet missing. As the nerves have limited capacity to spontaneously regenerate after traumatic injury, innovative strategies are being perused to promote the functional repair. The standard treatment can be summarized as "support and therapeutic", which is the combination of localized delivery of therapeutic molecules along with specialized architectures to support axonal growth and conformal repair.[170] Earlier studies have already demonstrated that micro- and nano-scale fibrous substrates could enhance neurite outgrowth,[171] neuronal maturation,[172] and neuronal differentiation.[173] And aligned fibers could guide the neuron cells to elongate along the major axis and form orientated cellular morphology.[166a, 174] Furthermore, drug-loaded electrospun scaffolds can function as both the drug carriers and the protective dressings for nerve systems, and then beneficially facilitate the neural tissue repair.

Suzuki *et al.*[88] studied the capacity of electrospun PCL membrane to continuously deliver methylcobalamin to the peripheral nerve injury site for nerve regeneration. Evidenced by the *in vitro* drug release and *in vivo* rat sciatic nerve crush injury model, sustained release of methylcobalamin over 8 weeks sufficiently promoted the recovery of the motor and sensory function, the recovery of nerve conduction velocity, and the promotion of myelination. Naseri-Nosar *et al.*[175] produced a fibrillated cellulose acetate (shell)/PLA (core) scaffolds and then

coated with citalopram-loaded gelatin nanoparticles. The citalopram-releasing scaffolds were further implanted in a rat sciatic nerve defect model to evaluate the potential for neural regeneration. The sciatic functional index (SFI) value corresponding to the drug releasing scaffolds was −34.23 ± 4.15 at 60th days, whereas −55.03 ± 3.16 for blank scaffolds, implying the significantly promoted treatment progress through immobilization of drug-loaded nanoparticles.

In addition to the small molecular drugs, biomacromolecules such as growth factors and peptides were also proved beneficial to the adhesion, expansion and maturation of neural cells. Li *et al.*[33b] embedded stromal-cell-derived factor-1α (SDF1α) in radially aligned collagen/PCL fibermats to provide directional cues, i.e., alignment topography and biological gradients, for recruitment of neural stem cells from the central canal region to the lesion site to repair spinal cord injury. A collagen-binding domain (CBD) was conjugated onto SDF1α for stronger binding to collagen, resulting in gradient and sustained release of SDF1α over 7 days. The gradient distribution of chemokine SDF1α and the radical aligned topography both contributed to the elongation of cells along the radical direction and highly accelerated cell migration from periphery towards center area. The produced materials were proved to be solid matrices for neuronal cell migration, differentiation and axonal outgrowth as well as bridges to guide axons extension to establish functional connections. Zhang *et al.*[101] loaded nerve growth factor (NGF) into conductive composite scaffolds through co-axial electrospinning, and further studied and assessed the synergistic effects of electrical stimulation and NGF on the neuron growth. It was found that the aligned structure, electrical stimulation and NGF release all stimulated PC12 cell differentiation and contributed to the enhanced neurite outgrowth of PC12 cells.

Aiming for bridging the defected nerve with a gap larger than 10 mm, Zhu *et al.* [76] produced a tubular PCL nerve conduit composed of electrospun microfibers. Peptide self-assembled RGD and YIGSR layers were non-covalently bonded to the obtained PCL fibers and were expected to improve the biocompatibility of hydrophobic PCL fibers (**Figure 13**a, b). *In vitro* cell culture demonstrated that RGD and YIGSR synergistically enhanced the cellular proliferation and neurite outgrowth. Sciatic nerve defects were surgically created on adult male Sprague-Dawley rats and then sutured with surface-modified PCL conduits to evaluate the *in vivo* axonal regeneration (**Figure 13**c). The morphometric analysis of the harvested nerves after 12 weeks displayed that the PCL conduits with RGD/YIGSR coating exhibited equivalent and comparable healing effect to auto grafts regarding the total area of regenerated axons, the total number of myelinated axons, and the diameter of myelinated axons. By comparing with the RGD-only and YIGSR-only group, they concluded that the co-existence of RGD and YIGSR synergistically promoted axonal regeneration and contributed to greater neurologic functional recovery.

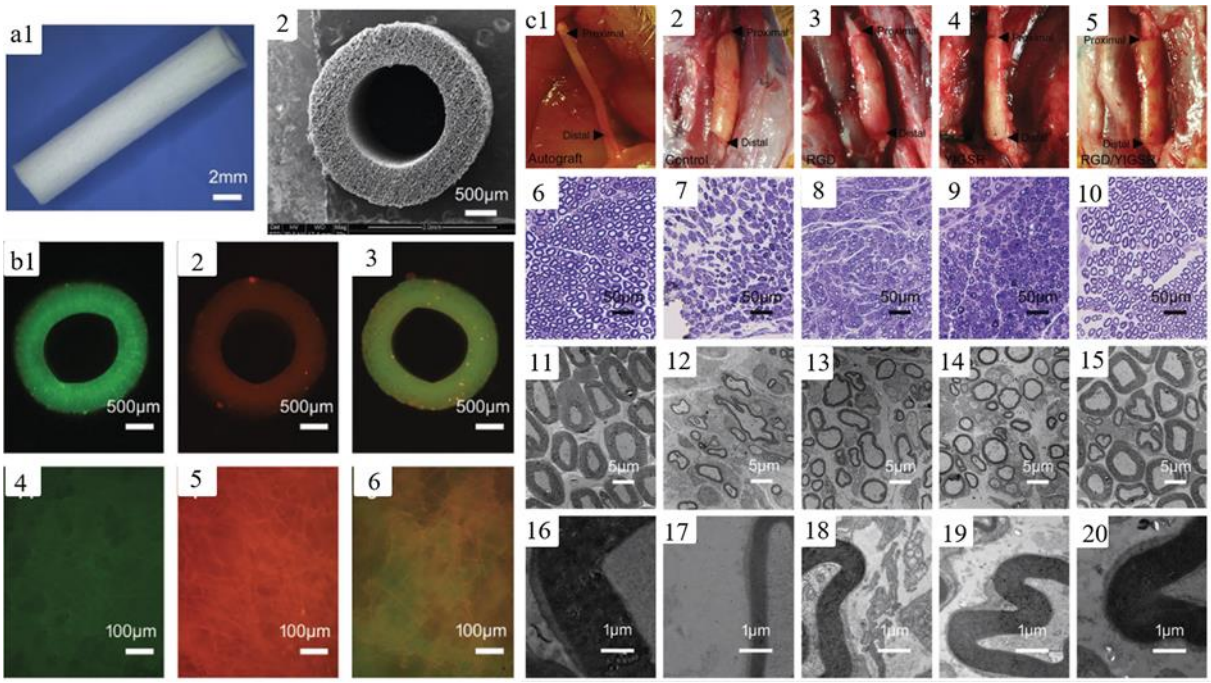

Figure 13. (a) Structure characterization of PCL and peptide modified PCL tubular grafts: (1) Optical image and (2) SEM images for the cross-section. Fluorescence microscopy image of cross-section of tubular scaffold and film scaffold for (b1, 4) FITC-labeled PCL-RGD; (b2, 5) rhodamine-labeled PCL-YIGSR; (b3, 6) both FITC-labeled RGD and rhodamine-labeled YIGSR together. (c) The gross view of the regenerated nerve, toluidine blue staining of regenerated axons, TEM of regenerated axon, and myelin sheath at middle portion in all groups at 12 weeks after surgery: (c1, 6, 11, 16) autograft group, (c2, 7, 12, 17) control group, (c3, 8, 13, 18) RGD group, (c4, 9, 14, 19) YIGSR group, and (c5, 10, 15, 20) RGD/YIGSR group. Reproduced with permission;[76] Copyright 2017, John Wiley and Sons.

Besides traditional drugs and biomolecules, novel materials such as graphene oxide were employed in nerve tissue engineering as well.[176] Directional guidance, inherent regulation *via* biomolecules and synergy effects from multiple factors are the main themes of the current research in nerve tissue engineering. However, matched biodegradation profiles of scaffolds were mostly missing though intensive studies have focused on the grafts fabrication and *in vitro* and *in vivo assays*.

3.2.5 Blood vessel regeneration

Cardiovascular diseases, such as coronary artery and peripheral vascular diseases still remain as the prevalent cause of death due to the continued growing of aged population world widely.[31b, 33a, 72] Artificial vascular grafts to replace diseased or narrowed vessels have been recognized as the clinical focus owing to the limited donation of autologous vessels. Although commercial products such as Dacron and Teflon have been successfully applied as large diameter (> 6 mm) vascular grafts with high blood flow, acute thrombus formation and intimal

hyperplasia could be initiated in case of small diameter vascular grafts (SDVGs) (< 6 mm), by the surface thrombogenicity and low compliance of Dacron and Teflon.[177] The development of SDVGs is still clinically necessary. In recent years, electrospun fibrous scaffolds were intensively investigated to fabricate SDVGs due to its feasibility for generating a tubular and porous structure by collecting on a rotating mandrel. Moreover, the electrospun scaffolds can be easily functionalized to meet the clinical requirements for SDVGs, for instance, to prevent thrombosis, to inhibit hyperplasia (over-proliferation of smooth muscle cells) and to promote rapid endothelialization for vascular regeneration.[33a, 81]

Punnakitikashem *et al.*[81] produced multifunctional tubular BPU scaffolds containing dipyridamole to achieve full generation of small diameter vessels since dipyridamole was reported to not only inhibit the thrombosis formation and over-proliferation of smooth muscle cells, but also promote and stimulate the proliferation of vascular endothelial cells. The sustained release of dipyridamole extended to 91 days, which effectively increased the human blood clotting time, reduced the human platelet deposition, inhibited the human aortic smooth muscle cell proliferation and finally improved the proliferation of human aortic endothelial cells. Surface modification, such as heparin immobilization, represents another crucial strategy to functionalize the tubular fibrous scaffolds for SDVGs regeneration. [33a, 72, 178] In the study of Yao *et al.*[33a], heparin was immobilized onto PLC/chitosan electrospun fibers through ionic bonding, resulting in stable release over 37 days to improve the hemocompatibility. When implanted in rat abdominal aorta for 1 month, the scaffolds showed well anti-thrombogenic effect and enhanced in-situ endothelialization. Qiu *et al.*[72] immobilized heparin onto polycarbonate-urethane (PCU) fibrous scaffolds with plasma-treated fiber surface (**Figure 14**a). It was found that plasma treatment could more effectively introduce amine groups for subsequent heparin conjugation, in comparison to other methods, such as aminolysis or physical

adsorption. The patency of heparin-conjugated PCU grafts was testified by implanting in the left common carotid artery of Sprague-Dawley rats. As shown in **Figure 14**b, more visible microvessels can be observed around the heparin-coated grafts harvested after both 2 and 4 weeks *in vivo*, indicating enhanced vascularization. More SMA+ cells migrated through the outer layer of PCU-heparin grafts, suggesting promoted cell infiltration (**Figure 14**c). The patency, early stage of endothelialization and graft integration were dramatically improved by heparin conjugation.

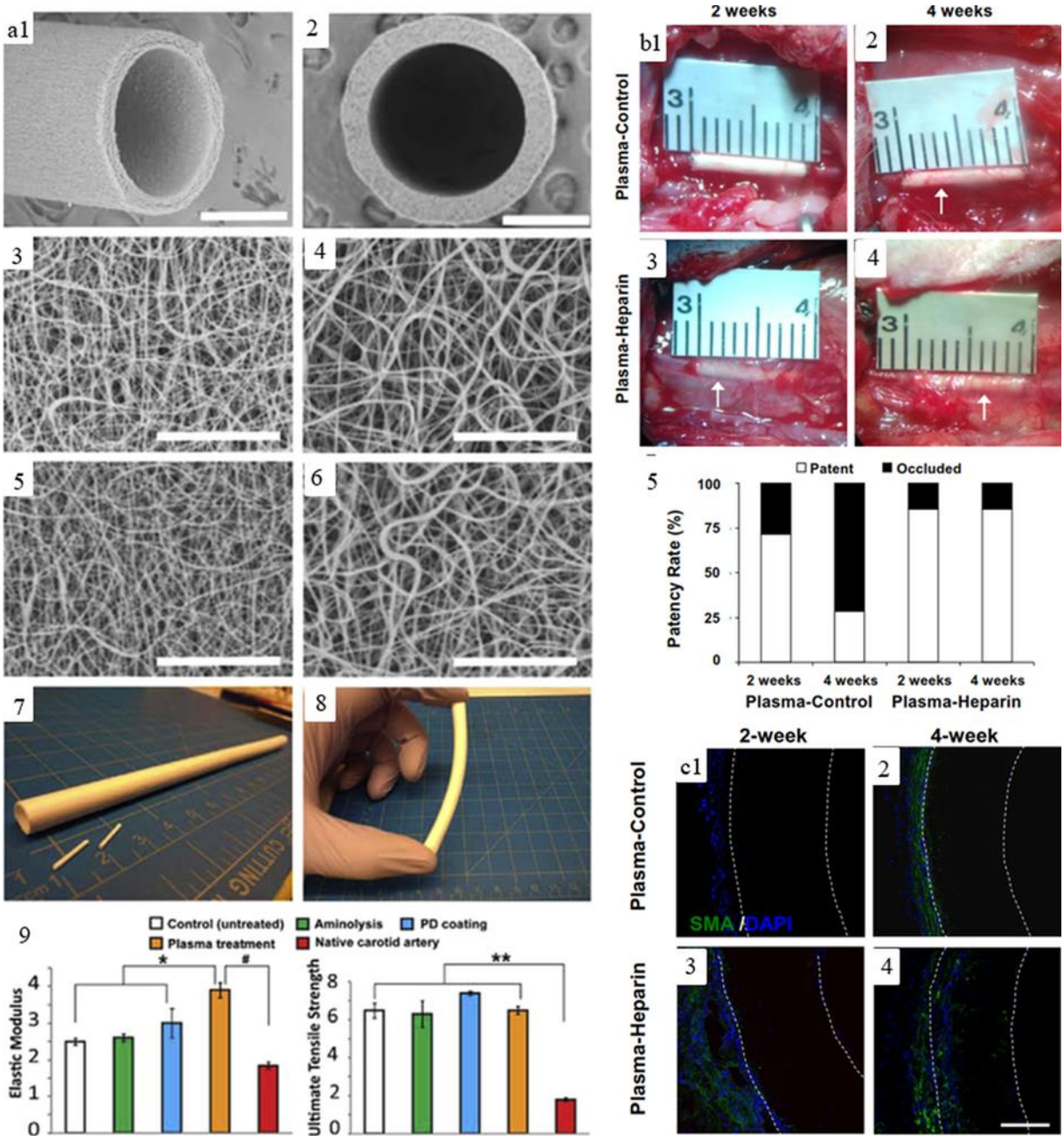

Figure 14. (a) Structural and mechanical characterizations of PCU vascular graft. SEM images of (1) side and (2) top view of an PCU graft. SEM images before and after the plasma treatment in the (3, 5) inner (luminal) and (4, 6) outer surface of the graft. (7) PCU grafts of various inner diameters (1 mm and 6 mm). (8) Bending of a 6 mm-diameter PCU graft. (9) Mechanical characterizations among control (untreated), aminolyzed, polydopamine (PD)-coated, plasma-treated grafts and native common carotid arteries (n = 5). Scale bar = 500 μm in 1, 2; scale bar

= 30 μm in 3, 4, 5, 6. (b) Representative images of graft explantation of control group and plasma-treated group after 2 weeks (1, 3) and 4 weeks (2, 4) and patency of the grafts were compared in (5). (c) Cross-section immunostaining of PCU plasma-control and plasma-heparin grafts after 2 and 4 weeks *in vivo*. Immunostaining for SMA (green), cell nuclei (DAPI, blue). Scale bar = 100 μm. Reproduced with permission;[72] Copyright 2017, Elsevier B.V.

Electrospun scaffolds-based gene therapy was also developed to remedy cardiovascular disease in the study of Zhou *et al*.[66] A bilayer tubular scaffold, consisting of PCL/gelatin fibers as the outer layer and miRNA-126 complexes-loaded PELCL fibers as the inner layer, was produced through dual-power electrospinning and emulsion electrospinning, respectively. The other layer was designed to physically maintain the configuration, and the gene-loaded inner layer was expected to regulate the cellular behaviors of vascular endothelial cells. Attributed to the multi-barriers in the bilayer scaffolds, miRNA-126 was sustainably released over 56 days. The stably released miRNA-126 was proved to highly promote the proliferation of human umbilical vein endothelial cells and down-regulate the expression of SPRED-1, which could diminish the transmission of intracellular angiogenic signals generated by VEGFs and FGFs. *In vivo* examination indicated extensive cell infiltration and highly enhanced ratio of endothelialization after implantation of the gene-loaded samples, in comparison to the pure polymer samples. The well-preserved miRNA activity and well-maintained patency of bilayer vascular graft suggested its prospective application in vascular tissue reconstruction.

Instead of fabricating a graft for in-situ tissue regeneration, Liu *et al.*[177] engineered a blood vessel graft in *ex vivo* conditions by co-cultivating vascular endothelial and smooth muscle cells onto layered electrospun membrane with plasmid DNA encoding bFGF and VEGF integrated, which could be further implanted *in vivo* to replace the damaged blood vessels.

Electrospun fibrous membrane can also found its application in vascular surgery. To prevent vasospasm and repair vascular tissue after vascular surgery, Zhu *et al.*[34a] produced papaverine-loaded PLLA/PEG scaffolds with adjustable drug releasing rate and degradation period. The *in vivo* healing efficiency was certified by warping around the incision sites in the vascular anastomosis of the rabbit neck. After 2 weeks, vessels implanted with drug-loaded PLLA/PEG membranes had no shrinkage in diameter, untraceable hyperplasia and minimized inflammation, compared to PLLA-alone group. Normal vessel morphology with regularly arranged vessel walls were observed on drug-loaded group, indicating great antispasmodic effect and potential to inhibit vasospasm and repair vascular damage.

3.3 Cancer Therapy

Cancer is a leading cause of mortality worldwide. The heterogeneity and adaptive resistance of cancer are the major challenges that are difficult to surmount through traditional chemotherapy. The fast-growing nano-medicine technology, which endowed passive or active targeting capacity to cancer cells, can significantly improve the pharmacokinetic profiles of drugs and further enhance the drug accumulation in tumor, offering new strategies to treat cancer. Electrospinning has emerged as a highly competitive technology in cancer research, in view of the tunable surface morphology for modulating drug pharmacokinetics and the robust loading capacity for combining various therapeutics.[59b] A variety of anticancer agents ranging from small molecular drugs to aptamer and RNA can be incorporated into electrospun fibers by simultaneous encapsulation and surface modification, and then undergo a diffusion-controlled or degradation-controlled release profiles depending on the materials and fabricating approaches.[3b, 179] The traditional approaches for drug loading are summarized in **Table 10**.

By the virtue of the high surface-to-volume ratio of nanofibers, enhanced local topographic interactions between the substrates and components (e.g., microvilli and filopodia) on cellular surface can also be achieved.[180] Thus, electrospun scaffolds modified with specific biomarker molecules own great potential for capturing the circulating tumor cells (CTCs) and cancer detection.[181] Furthermore, compared with other nanostructures, the similarity of the prepared fibers to the collagen fibrils in the ECM can offer better scaffold- and matrix-based 2D or 3D models to enhance the cell–cell and cell–matrix interactions than other nanostructures, which endow the electrospun scaffolds with distinguish advantage in cancer treatment by regulating the cancer cell behaviors.[182] This resemblance can be further improved by modifying the fibers with ECM proteins or peptides.[59b, 183] For example, Rabolt *et al.*[183] found that covalently conjugating perlecan domain IV (PlnDIV) peptide onto the electrospun PCL/gelatin composite scaffolds significantly enhanced the adherence and infiltration of metastatic prostate cancer cells towards the electrospun substrates. In this section, we will introduce the recent developments of electrospun scaffolds in the application of cancer research mainly on the cancer therapy and CTCs detection and capture.

Table 10. Recent studies on electrospun scaffolds-based approaches for anticancer drugs and gene delivery.

Anticancer reagents	Polymer matrix	Cancer cell lines	Highlights	Ref.
Camptothecin	PCL	C2C12 cell, *in vitro*	Sustained release > 6 d; ~ 25% more decrease in cell proliferation than free drugs after 72 h;	[184]
	PLA	HepG2 cell, *in vitro* and *in vivo*	20-fold higher cytotoxicity than free drugs after 72 h; More necrosis and apoptosis;	[185]

Paclitaxel	PLGA	C6 glioma cells	Sustained release > 80 d; ~ 44% smaller tumors in comparison to free drug control on day 24;	[186]
	chitosan/ HA	DU145 prostate cancer cell	Reduced cell adhesion and proliferation;	[187]
Cisplatin	PCL/PGC-C18	Lewis Lung carcinoma cell	Superhydrophobic; Sustained release in a linear profile > 90 d; significant increase in median recurrence-free survival to > 23 d;	[59a]
Doxorubicin	PEG-PLA	murine mammary carcinoma EMT6 cell, *in vivo*	limited injury to neighboring tissue and systemic adverse reactions within 42 d;	[188]
	PEG-PLA	SMMC7721 cell, *in vitro* and hepatocarcinoma H22 cell, *in vivo*	Sustained release for 12 d ; ~ 40% decrease in cell proliferation compared with free drugs after 10 d;	[189]
paclitaxel and doxorubicin	PEG-PLA	C6 Glioma cells	Synergistic inhibition effects on tumor cell;	[190]
Plasmid DNA encoding for Cdk2 shRNA	PCL	MCF-7 breast cancer cell	~40% increase in cell inhibition compared with control scaffold; Sustained release > 21 d;	[191]
Paclitaxel and MMP-2 RNAi	PLGA	U87MG-luc2 cell	Significant synergistic anticancer effect;	[192]

PCL: poly(ε-caprolactone); PLA: poly(L-lactic acid)-poly(ethylene glycol); HA: hyaluronic acid; PGC-C18: poly(glycerol monostearate-cocaprolactone); PEG: poly(ethylene glycol); shRNA: short hairpin RNA.

3.3.1 Scaffolds-based drug delivery systems for cancer therapy

As previously mentioned, various anticancer reagents obtained sustained release profile and prolonged activities by encapsulating within electrospun substrates. The fabricated drug-loaded scaffolds can be implanted or injected into the tumor bed after tumor localization.[193] For instance, Ramachandran *et al.*[193a] demonstrated that implanting the Temozolomide-loaded PLGA-PLA-PCL fibrous scaffolds into the rat with orthotopic glioma caused long-term (> 4 months) survival of 85.7% of the animals. Wei *et al.*[193b] injected hydroxycamptothecin-loaded

PLA-PEG scaffolds to treat H22-tumor bearing mice and studied the effect of the fiber lengths on the biodistribution of fibers in the tumor. They found that longer fiber lengths led to a higher tumor accumulation and retention, but less diffusion.

However, two major limitations restricted the clinical application of electrospinning for cancer treatment. Firstly, most of the drug release behaviors relied on the passive diffusion, lacking the controllability for necessary drug concentrate to kill cancer cells.[40] Therefore, introducing stimuli-responsive blocks to endow the electrospun scaffolds with on-demand release capacity is a basic requirement in recent studies.[40, 194] The other concerns related to the insufficient cancer cellular uptake of the therapeutics. Due to the susceptibility to multidrug resistance for most of the cancer cells and the inherent properties of some therapeutics (such as the negative charges of oligonucleotides) that is unfavorable for cancer cell internalization, direct drug delivery in a "fiber-to-cell" manner is insufficient for effective cancer treatment.[195]

Incorporation of functional nanoparticles into the electrospun scaffolds is a promising strategy to solve the aforementioned problems, in view of the well-studied stimuli-responsive capacities to physical stimuli and the additional surface for targeting molecules conjugation.[194] Kim *et al.*[196] encapsulated magnetic nanoparticles into DOX-loaded thermo-sensitive polymer N-isopropylacrylamide (PNIPAAm) fibers *via* electrospinning to develop a magnetic hyperthermia-controlled drug release system (**Figure 15**a). The self-generated heat under the alternating magnetic field led to the "on-off" drug release from the fibers. Attributed to the synergistic effect of hyperthermia and chemotherapy, 70% of human melanoma cells died within 5 min. Ghavaminejad *et al.*[197] then employed catecholic polymer nanofibers to carry and bind the IONPs and bortezomib drugs for synergistic effects from hyperthermia and pH-triggered chemotherapy, which reduced the cytotoxicity to healthy tissues/cells.

Moreover, the formed hierarchical nano-in-nano architectures owned improved biocompatibility and cargo release tunability.[198] Qiu *et al.*[199] incorporated the DOX-loaded MSNs into PLLA nanofibers *via* electrospinning, and the obtained PLLA/DOX@MSNs nanofibrous scaffolds showed improved thermal stability than PLLA nanofiber and better anti-proliferation efficacy to Hela cells than the MSNs-free counterparts. An implantable DOX-loaded micelle-in-nanofiber device was developed *via* co-axial electrospinning to treat 4T1 murine breast tumor in nude mice (**Figure 15b**).[121] The folate-conjugated PCL-PEG micelles with DOX were loaded within PVA core region and further shielded by cross-linked gelatin shell. During the degradation of the nanofiber matrix, the micelles were sustainably released from the matrix and accumulated into tumor tissues by interstitial transport and enhanced permeation and retention (EPR) effect, then finally internalized by tumor cells *via* folate receptor-mediated endocytosis. By using this nanodevice, both the side effects of anticancer drugs and the administration frequency can be greatly reduced, while the therapeutic efficacy was maintained.

In addition to the conventional nano- or micro- particles, adenoviral (Ad) can also be used to construct nanocomplexes by electrospinning.[200] Park *et al.*[200a] demonstrated that Ad can be ionically cross-linked with chitosan-PEG-folate polymer *via* electrospinning. The formed Ad/chitosan-PEG-folate nanocomplexes maintained the biological activity as naked Ad. Moreover, for the folate receptor-expressing KB cells, the transduction efficiency of the Ad-based nanocomplexes was higher than the receptor-negative U343 cells. Besides that, this nanocomplexes also showed reduced immune reaction against Ad.

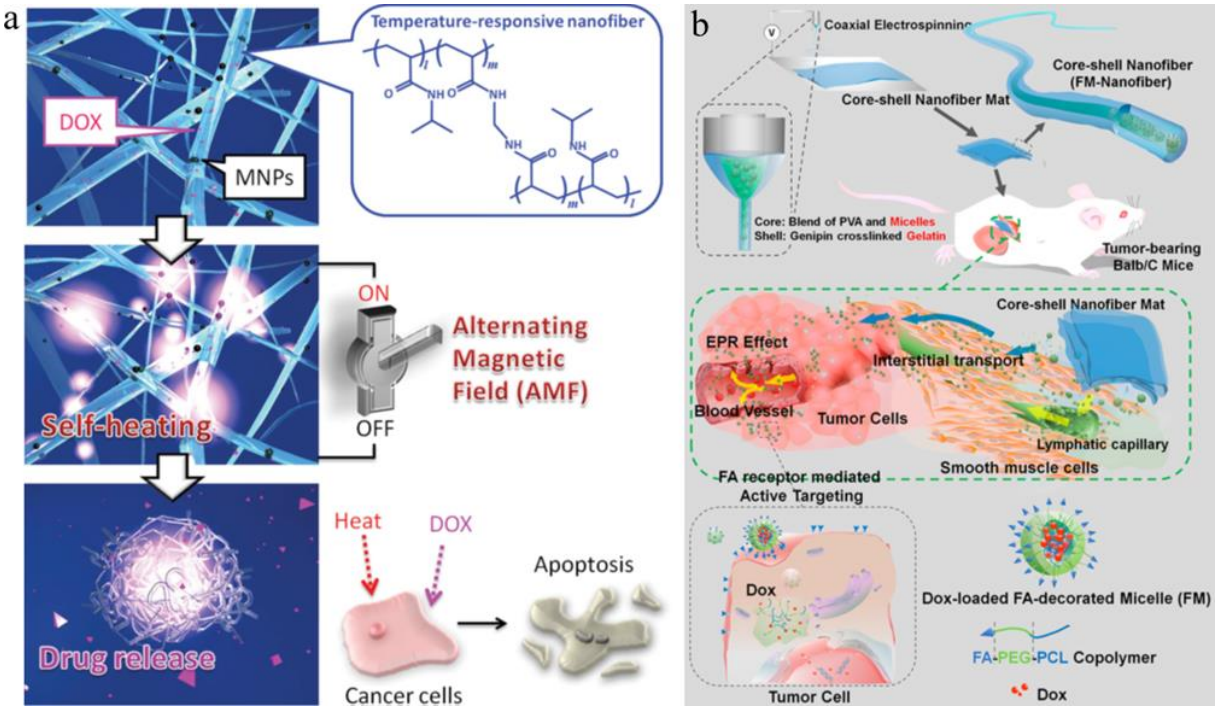

Figure 15. (a) The magnetic nanoparticles incorporated temperature-responsive poly(NIPAAm-co-HMAAm) nanofibers for DOX release. Reproduced with permission;[196] Copyright 2013, John Wiley and Sons. (b) Schematic illustrations on the fabrication of the DOX-loaded micelle-in-nanofiber device and the delivery process of these folate-modified DOX-loaded micelles by EPR effect and finally to tumor cells. Reproduced with permission;[121] Copyright 2015, American Chemical Society.

3.3.2 Biosensors for detection and capture of circulating tumor cell (CTCs)

The detection and capture of cancer cells, especially the CTCs from the patient blood rely on the specific and sensitive recognition of the overexpressed markers on the surface of cancer cells.[201] However, the low abundance and heterogeneity of the cancer cells in blood environment prevent reliable analyses.[202] Owing to the tunable morphologies of electrospun fibers that can enhance the local topographic interactions with cancer cells, specific biomarkers modification on fibers-based substrate can amplify the bioassay signals and the antigen-

antibody binding with improved accuracy and sensitivity.[59b, 203] Various proteins on cancer cell surface have been adopted as biomarkers for cancer cell recognition, such as EGFR2 or ErbB2 and carcinoma antigen-125.[36, 181b, 181d] For instance, Ali *et al.*[36] fabricated electrospun mesoporous ZnO nanofibers with femtomolar sensitivity for breast cancer diagnostics. After oxygen plasma treatment, the carbon-doped ZnO fibers were available for the conjugation of the antibody of ErbB2 (anti-ErbB2), and they showed high immunoelectrode to ErbB2 with an association constant of 404.8 kM^{-1} s^{-1}.

The overexpression of tumor matrix proteins, such as matrix metalloproteinases 9 (MMP-9), can also be used as the biomarker for cancer cell detection. Han *et al.*[204] prepared a hydrogel-framed polystyrene/poly(styrene-*alt*-maleic anhydride) by electrospinning, and immobilized the fiber with fluorescein isocyanate (FITC)-labeled MMP-9 specific peptides. This enzymatic cleavage-based detection strategy can achieve a detection limit of 10 pM with a response time of 30 min.

The CTCs usually circulated in the blood stream during the tumor metastatic process, which can be regarded as "liquid biopsies" of the primary tumors and the specific mechanism for cancer metastasis.[201, 205] Zhang *et al.*[181d] fabricated horizontally packed ultra-long calcinated TiO_2 nanofibers (TiNFs) through electrospun titanium n-butoxide (TBT)/PVP fibers (**Figure 16**a). Compared with the vertically oriented silicon nanopillars, the horizontally oriented architecture of TiNFs can better mimic the ECM condition, thus leading to further improved cell–substrate interactions. Then the streptavidin was immobilized onto the TiNFs for the follow-up conjugation of the biotinylated epithelial cell adhesion molecule antibody (anti-EpCAM). Based on the enhanced local topographic interactions and the anti-EpCAM/EpCAM biological recognition, this TiNFs showed considerable capture efficiency to the CTCs in both artificial CTC blood samples and whole blood samples from colorectal and gastric cancer

patients. To avoid the impurities caused by non-specific captured cells, Hou *et al.*[206] used a transparent PLGA-nanofiber-embedded nanovelcro chip to replace the non-transparent silicon substrate (**Figure 16**b). Then anti-CD146 antibody was used as melanoma-specific capture agent to conjugate onto the fiber. The nanovelcro chip can efficiently capture the metastatic cells from the blood samples of stage-IV melanoma patients. A Leica LMD7000 microscope equipped with a 355 nm laser microdissection setup was used to cut the PLGA nanofibers for single cell isolation. The obtained cell sample subsequently underwent the whole-genome amplification and specific PCR amplification for the final Sanger g DNA sequencing. This laser microdissection-based single-CMC detection strategy offered an opportunity to investigate the gene-related variations for cancer diagnose.

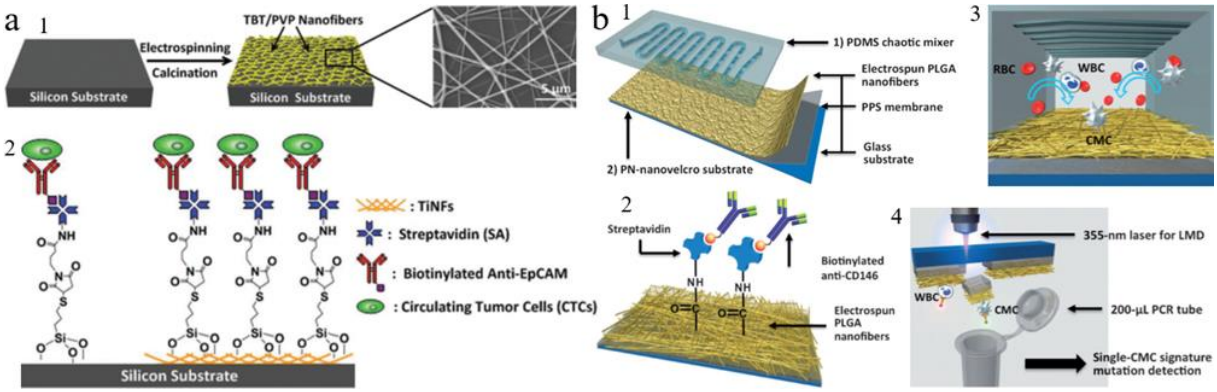

Figure 16. (a) Schematic illustrations of epithelial-cell adhesion-molecule antibody (anti-EpCAM) modified TiO_2 electrospun nanofibers for cancer cell capture. Reproduced with permission;[181d] Copyright 2012, John Wiley and Sons. (b) Schematic illustrations of anti-CD146 antibody-grafted PLGA nanofiber-embedded nanovelcro chip for capturing circulating tumor cells. (b1) Fabrication of the nanovelcro substrate. (b2) Chemical conjugation of streptavidin for anchoring of biotinylated anti-CD146. (b3) Schematic illustrations of the mechanism of the nanovelcro CMC chip. (b4) Scheme of the laser microdissection-based single-CMC isolation. Reproduced with permission;[206] Copyright 2013, John Wiley and Sons.

In summary, electrospun fibrous scaffolds have evolved from a drug reservoir for sustained drug release to a powerful and combinational therapy platform with high compatibility that can bridge chemotherapy, thermotherapy and post-surgery tumor treatment. Moreover, new therapeutic strategies, such as the tumor guide device, have shown great value for clinical translation. However, most of the studies are still restricted on the preclinical level, and the systemic investigation and evaluation on the immunogenicity, metabolic cycle and safety of the scaffolds are still limited. Besides that, the studies of physical parameters-related patient compliance, such as the effects of length, tensile strength, structure and morphology on the retention and distribution in the tumor, still require tremendous data support.

4. Conclusions and Future Perspectives

4.1 Conclusions and remarks

Electrospun drug delivery vehicles have emerged as one of the essential applications of electrospinning in the biomedical field. The high diversity in source materials, drug loading techniques and the resultant morphological, physiochemical and biological performances of the obtained drug-loaded systems all contributed to the widespread implementations. By choosing appropriate polymer matrix, the drugs can be released in seconds, minutes, hours, days or months according to diverse requirements in oral/transdermal drug release, tissue regeneration or anti-recurrence of tumors. Moreover, by varying the drug loading approaches, loaded drugs can be released in rapid, sustained, biphasic or zero-order fashion to meet the timely-varied demands during the difference phases of a healing or regeneration process of *in vivo* environments. By adding another or more drug delivery vehicles either in particulate formulations or another fibrous formulation into the main platform, multifunctional drug carriers with time-programed or sequential release of multiple drugs can be created to suit

complex *in vivo* conditions. Additionally, pH, temperature, light, electrical or magnetic field responsive polymers were employed to further endow the drug carrier systems with controlled or multi-staged release features upon exposure to the corresponding stimuli.

Compared to the traditional drug formulations, electrospun fibrous formulations could greatly enhance the solubility of water-insoluble drugs due to the highly increased solid dispersion induced by high surface-to-volume ratio of electrospun fibers, resulting in faster drug dissolving in oral cavity or higher diffusion rate through skin. As an implantable drug-eluting device, apart from being the template to support and accommodate the cell proliferation and differentiation, electrospun scaffolds can effectively prevent the infection or promisingly enhance the cellular metabolism activities through releasing of growth factors or other biomolecules as well. For anti-cancer treatment, the possibility to load multiple therapeutics enables the combinational therapeutic strategy simultaneously, such as hyperthermic-chemotherapy and photothermal-chemotherapy. The electrospun inorganic fibers loaded with biomarkers also represented a new strategy to fabricate immunosensor with hypersensitivity for disease diagnosis.

Overall, electrospun architectures undoubtedly have become multifunctional platforms carrying active ingredients to promisingly address the existing medical challenges.

4.2 Future perspectives

Nevertheless, there is still a great gap between the lab validation to clinical trials and then the actual commercialization. Currently, no electrospun products have been approved by FDA and only few clinical trials have been documented to further testify the function of the designed drug delivery platforms.[207] In a double-blind, randomized and placebo-controlled clinical trial of Pathon, a NO releasing PU patch, no sufficient efficacy was observed compared to standard

treatment.[208] Apparently, although *in vivo* studies have already been conducted to verify the curing efficacy under the complex *in vivo* environments, the huge difference on size and metabolism systems between human and small animals used *in vivo* study could cause unexpected results during the clinical trials.[209] Furthermore, both economic burdens and limitations in production rate hindered the large-scale clinical trials in human.[210] Enormous efforts are still demanding in this aspect.

Another limitation for actual commercialization is the low yield of the laboratory electrospinning apparatus. Although high throughput electrospinning systems, such as needleless electrospinning and multi-needle electrospinning are already capable of scaling up the fiber production, the study of drug-loading systems from those equipment were rarely reported.[211] Several issues restrict the scaling-up and further applications in biomedical fields. For instance, the massive organic solvent evaporation during the high-throughput production could cause severe environmental risk and the solvent residue may compromise the therapeutic effect.[210] Additionally, quality control and high reproducibility is also challenging in high-throughput electrospinning due to the massive charge accumulation during the long-time process.[211] The scale-up process may generate drug delivery systems with distinct drug release profiles and physiochemical performances due to the mutual influence among the multi-electrodes, and this long-term charges accumulation. Although some companies have started to work on these problems by designing new spinneret configurations, there is still a long way to go for commercialization of biomedical products.

As a multi-disciplinary subject associated with materials science, pharmaceutical engineering and life science, more dialogues among scientists in diverse disciplines should be opened-up and thus, promote and speed-up the mutual cooperation to further solve the missing puzzles

existing in this chain of design – fabrication – laboratory verification – clinical trials – commercialization.

Acknowledgements

Y.D. acknowledges the Orion Research Foundation for financial support. H.A.S. acknowledges financial support from the University of Helsinki Research Funds, the Sigrid Jusélius Foundation (decision no. 4704580), the Helsinki Institute of Life Science, and the European Research Council under the European Union's Seventh Framework Programme (FP/2007–2013, grant no. 310892).

Received: ((will be filled in by the editorial staff))

Revised: ((will be filled in by the editorial staff))

Published online: ((will be filled in by the editorial staff))

References

[1] A. Formhals, *US Patent, 1975504* **1934**.

[2] a) N. Bhardwaj, S. C. Kundu, *Biotechnol. Adv.* **2010**, 28, 325; b) D. H. Reneker, A. L. Yarin, *Polymer* **2008**, 49, 2387; c) A. Greiner, J. H. Wendorff, *Angew. Chem. Int. Ed.* **2007**, 46, 5670.

[3] a) T. J. Sill, H. A. von Recum, *Biomaterials* **2008**, 29, 1989; b) X. Hu, S. Liu, G. Zhou, Y. Huang, Z. Xie, X. Jing, *J. Control. Release* **2014**, 185, 12; c) C. Shixuan, B. S. Kumar, B. S. K., L. Xiaoran, X. Jingwei, *Adv. Healthc. Mater.* **2018**, 7, 1701024.

[4] a) D. H. Reneker, A. L. Yarin, H. Fong, S. Koombhongse, *J. Appl. Phys.* **2000**, 87, 4531; b) D. Li, Y. Xia, *Adv. Mater.* **2004**, 16, 1151.

[5] C. B. J. Manuel, V. G. L. Jesús, S. M. Aracely, in *Electrospinning - Material, Techniques, and Biomedical Applications*, DOI: 10.5772/65939 (Eds: S. Haider, A. Haider), InTech, Rijeka **2016**, p. Ch. 07.

[6] S.-F. Chou, D. Carson, K. A. Woodrow, *J. Control. Release* **2015**, 220, 584.

[7] a) G. R. Williams, N. P. Chatterton, T. Nazir, D.-G. Yu, L.-M. Zhu, C. J. Branford-White, *Ther. Deliv.* **2012**, 3, 515; b) N. Goonoo, A. Bhaw-Luximon, D. Jhurry, *J. Biomed. Nanotechnol.* **2014**, 10, 2173.

[8] F. Ignatious, L. Sun, C.-P. Lee, J. Baldoni, *Pharm. Res.* **2010**, 27, 576.

[9] N. Angelova, D. Hunkeler, *Trends Biotechnol.* **1999**, 17, 409.

[10] a) X. Li, M. A. Kanjwal, L. Lin, I. S. Chronakis, *Colloids Surf. B Biointerfaces* **2013**, 103, 182; b) Z. K. Nagy, K. Nyúl, I. Wagner, K. Molnár, G. Marosi, *Express Polym. Lett.* **2010**, 4, 763; c) C. Dott, C. Tyagi, L. K. Tomar, Y. E. Choonara, P. Kumar, L. C. du Toit, V. Pillay, *J. Nanomater.* **2013**, 2013, 19.

[11] a) D.-G. Yu, X.-X. Shen, C. Branford-White, K. White, L.-M. Zhu, S. A. Bligh, *Nanotechnology* **2009**, 20, 055104; b) W. Samprasit, P. Akkaramongkolporn, T. Ngawhirunpat, T. Rojanarata, R. Kaomongkolgit, P. Opanasopit, *Int. J. Pharm.* **2015**, 487, 213.

[12] H. W. Kwak, H. Woo, I.-C. Kim, K. H. Lee, *RSC Adv.* **2017**, 7, 40411.

[13] D. C. Aduba, J. A. Hammer, Q. Yuan, W. Andrew Yeudall, G. L. Bowlin, H. Yang, *Acta Biomater.* **2013**, 9, 6576.

[14] M. Palo, K. Kogermann, I. Laidmäe, A. Meos, M. Preis, J. Heinämäki, N. Sandler, *Mol. Pharm.* **2017**, 14, 808.

[15] A. Sharma, A. Gupta, G. Rath, A. Goyal, R. Mathur, S. Dhakate, *J. Mater. Chem. B* **2013**, 1, 3410.

[16] a) X. Wang, D.-G. Yu, X.-Y. Li, S. A. Bligh, G. R. Williams, *Int. J. Pharm.* **2015**, 490, 384; b) C. Yang, D. G. Yu, D. Pan, X. K. Liu, X. Wang, S. W. A. Bligh, G. R. Williams, *Acta Biomater.* **2016**, 35, 77.

[17] a) L. Naves, C. Dhand, L. Almeida, L. Rajamani, S. Ramakrishna, G. Soares, *Prog. Biomater.* **2017**, 6, 1; b) J. Song, X. Fan, Q. Shen, *Int. J. Pharm.* **2016**, 501, 245.

[18] a) Y. Liu, A. Nguyen, A. Allen, J. Zoldan, Y. Huang, J. Y. Chen, *Mater. Sci. Eng. C* **2017**, 74, 485; b) C. Valenta, B. G. Auner, *Eur. J. Pharm. Biopharm.* **2004**, 58, 279.

[19] A. Gencturk, E. Kahraman, S. Güngör, G. Özhan, Y. Özsoy, A. S. Sarac, *Artif. Cells Nanomed. Biotechnol.* **2017**, 45, 655.

[20] A. C. Mendes, C. Gorzelanny, N. Halter, S. W. Schneider, I. S. Chronakis, *Int. J. Pharm.* **2016**, 510, 48.

[21] M. Rasekh, C. Karavasili, Y. L. Soong, N. Bouropoulos, M. Morris, D. Armitage, X. Li, D. G. Fatouros, Z. Ahmad, *Int. J. Pharm.* **2014**, 473, 95.

[22] a) T. Ngawhirunpat, P. Opanasopit, T. Rojanarata, P. Akkaramongkolporn, U. Ruktanonchai, P. Supaphol, *Pharm. Dev. Technol.* **2009**, 14, 73; b) K. Kataria, A. Gupta, G. Rath, R. Mathur, S. Dhakate, *Int. J. Pharm.* **2014**, 469, 102.

[23] K. Madhaiyan, R. Sridhar, S. Sundarrajan, J. R. Venugopal, S. Ramakrishna, *Int. J. Pharm.* **2013**, 444, 70.

[24] Z. Xie, G. Buschle‐Diller, *J. Appl. Polym. Sci.* **2010**, 115, 1.

[25] Q. Zhang, Y. Li, Z. Y. Lin, K. K. Y. Wong, M. Lin, L. Yildirimer, X. Zhao, *Drug Discov. Today* **2017**, 22, 1351.

[26] K. J. Rambhia, P. X. Ma, *J. Control. Release* **2015**, 219, 119.

[27] M. Sokolsky-Papkov, K. Agashi, A. Olaye, K. Shakesheff, A. J. Domb, *Adv. Drug Deliv. Rev.* **2007**, 59, 187.

[28] a) J. M. Zuidema, M. C. Hyzinski-García, K. Van Vlasselaer, N. W. Zaccor, G. E. Plopper, A. A. Mongin, R. J. Gilbert, *Biomaterials* **2014**, 35, 1439; b) H. J. Cho, S. K. Madhurakkat Perikamana, J. H. Lee, J. Lee, K. M. Lee, C. S. Shin, H. Shin, *ACS Appl. Mater. Interfaces* **2014**, 6, 11225; c) T. Xu, H. Yang, D. Yang, Z. Z. Yu, *ACS Appl. Mater. Interfaces* **2017**, 9, 21094.

[29] a) A. F. De Faria, F. Perreault, E. Shaulsky, L. H. Arias Chavez, M. Elimelech, *ACS Appl. Mater. Interfaces* **2015**, 7, 12751; b) J. Yu, A. R. Lee, W. H. Lin, C. W. Lin, Y. K. Wu, W. B. Tsai, *Tissue Eng. Part A* **2014**, 20, 1896; c) Y. J. Lee, J.-H. Lee, H.-J. Cho, H. K. Kim, T. R. Yoon, H. Shin, *Biomaterials* **2013**, 34, 5059; d) L. Cheng, X. Sun, X. Zhao, L. Wang, J. Yu, G. Pan, B. Li, H. Yang, Y. Zhang, W. Cui, *Biomaterials* **2016**, 83, 169.

[30] a) J. Hu, M. P. Prabhakaran, L. Tian, X. Ding, S. Ramakrishna, *RSC Adv.* **2015**, 5, 100256; b) A. V. Bagdadi, M. Safari, P. Dubey, P. Basnett, P. Sofokleous, E. Humphrey, I. Locke, M. Edirisinghe, C. Terracciano, A. R. Boccaccini, J. C. Knowles, S. E. Harding, I. Roy, *J. Tissue Eng. Regen. Med.* **2018**, 12, e495.

[31] a) J. Xue, M. He, H. Liu, Y. Niu, A. Crawford, P. D. Coates, D. Chen, R. Shi, L. Zhang, *Biomaterials* **2014**, 35, 9395; b) P. Campagnolo, A. J. Gormley, L. W. Chow, A. G. Guex, P. A. Parmar, J. L. Puetzer, J. A. M. Steele, A. Breant, P. Madeddu, M. M. Stevens, *Adv. Healthc. Mater.* **2016**, 5, 3046; c) M. B. Taskin, R. Xu, H. Gregersen, J. V. Nygaard, F. Besenbacher, M. Chen, *ACS Appl. Mater. Interfaces* **2016**, 8, 15864.

[32] a) Y. Ding, J. A. Roether, A. R. Boccaccini, D. W. Schubert, *Eur. Polym. J.* **2014**, 55, 222; b) Y. Ding, W. Li, T. Müller, D. W. Schubert, A. R. Boccaccini, Q. Yao, J. A. Roether, *ACS Appl. Mater. Interfaces* **2016**, 8, 17098.

[33] a) Y. Yao, J. Wang, Y. Cui, R. Xu, Z. Wang, J. Zhang, K. Wang, Y. Li, Q. Zhao, D. Kong, *Acta Biomater.* **2014**, 10, 2739; b) X. Li, M. Li, J. Sun, Y. Zhuang, J. Shi, D. Guan, Y.

Chen, J. Dai, *Small* **2016**, 12, 5009; c) X. Yang, J. Yang, L. Wang, B. Ran, Y. Jia, L. Zhang, G. Yang, H. Shao, X. Jiang, *ACS Nano* **2017**, 11, 5737.

[34] a) W. Zhu, S. Liu, J. Zhao, S. Liu, S. Jiang, B. Li, H. Yang, C. Fan, W. Cui, *Acta Biomater.* **2014**, 10, 3018; b) X. Luo, M. Chen, Z. Chen, S. Xie, N. He, T. Wang, X. Li, *Acta Biomater.* **2017**, DOI: 10.1016/j.actbio.2017.12.003; c) P. Dubey, P. Gopinath, *J. Mater. Chem. B* **2016**, 4, 726.

[35] M. Ahmad, C. Pan, Z. Luo, J. Zhu, *J. Phys. Chem. C* **2010**, 114, 9308.

[36] M. A. Ali, K. Mondal, C. Singh, B. Dhar Malhotra, A. Sharma, *Nanoscale* **2015**, 7, 7234.

[37] J. S. Jang, S. J. Choi, S. J. Kim, M. Hakim, I. D. Kim, *Adv. Funct. Mater.* **2016**, 26, 4740.

[38] K. Mondal, A. Sharma, *RSC Adv.* **2016**, 6, 94595.

[39] Y. Ding, W. Li, A. Correia, Y. Yang, K. Zheng, D. Liu, D. W. Schubert, A. R. Boccaccini, H. A. Santos, J. A. Roether, *ACS Appl. Mater. Interfaces* **2018**, DOI: 10.1021/acsami.8b02656.

[40] C. Huang, S. J. Soenen, J. Rejman, B. Lucas, K. Braeckmans, J. Demeester, S. C. De Smedt, *Chem. Soc. Rev.* **2011**, 40, 2417.

[41] M. Chen, Y. F. Li, F. Besenbacher, *Adv. Healthc. Mater.* **2014**, 3, 1721.

[42] S. Thakral, N. K. Thakral, D. K. Majumdar, *Expert Opinion on Drug Delivery* **2013**, 10, 131.

[43] D. Han, A. J. Steckl, *ACS Appl. Mater. Interfaces* **2017**, 9, 42653.

[44] M. Jin, D.-G. Yu, C. F. G. C. Geraldes, G. R. Williams, S. W. A. Bligh, *Mol. Pharm.* **2016**, 13, 2457.

[45] S. Demirci, A. Celebioglu, Z. Aytac, T. Uyar, *Polym. Chem.* **2014**, 5, 2050.

[46] Y. Guan, Y. Zhang, *Soft Matter* **2011**, 7, 6375.

[47] L. Li, G. Yang, G. Zhou, Y. Wang, X. Zheng, S. Zhou, *Adv. Healthc. Mater.* **2015**, 4, 1658.

[48] J. Hu, H.-Y. Li, G. R. Williams, H.-H. Yang, L. Tao, L.-M. Zhu, *J. Pharm. Sci.* **2016**, 105, 1104.

[49] T. Tran, M. Hernandez, D. Patel, J. Wu, *Advances in Materials Science and Engineering* **2015**, 2015, 6.

[50] H. Yuan, B. Li, K. Liang, X. Lou, Y. Zhang, *Biomed. Mater.* **2014**, 9, 055001.

[51] Y. F. Li, P. Slemming‐Adamsen, J. Wang, J. Song, X. Wang, Y. Yu, M. Dong, C. Chen, F. Besenbacher, M. Chen, *J. Tissue Eng. Regen. Med.* **2017**, 11, 2411.

[52] B. Song, C. Wu, J. Chang, *Regen. Biomater.* **2015**, 2, 229.

[53] D. Han, X. Yu, Q. Chai, N. Ayres, A. J. Steckl, *ACS Appl. Mater. Interfaces* **2017**, 9, 11858.

[54] B. Wang, H. Zheng, M.-W. Chang, Z. Ahmad, J.-S. Li, *Colloids Surf. B Biointerfaces* **2016**, 145, 757.

[55] a) X. Zhao, Z. Yuan, L. Yildirimer, J. Zhao, Z. Y. Lin, Z. Cao, G. Pan, W. Cui, *Small* **2015**, 11, 4284; b) A. R. K. Sasikala, A. R. Unnithan, Y. H. Yun, C. H. Park, C. S. Kim, *Acta Biomater.* **2016**, 31, 122.

[56] H. K. Patra, Y. Sharma, M. M. Islam, M. J. Jafari, N. A. Murugan, H. Kobayashi, A. P. F. Turner, A. Tiwari, *Nanoscale* **2016**, 8, 17213.

[57] Y. Gao, Y. Bach Truong, Y. Zhu, I. Louis Kyratzis, *J. Appl. Polym. Sci.* **2014**, 131, n/a.

[58] a) A. GhavamiNejad, A. Rajan Unnithan, A. Ramachandra Kurup Sasikala, M. Samarikhalaj, R. G. Thomas, Y. Y. Jeong, S. Nasseri, P. Murugesan, D. Wu, C. Hee Park, C. S. Kim, *ACS Appl. Mater. Interfaces* **2015**, 7, 12176; b) A. Nasajpour, S. Ansari, C. Rinoldi, A. S. Rad, T. Aghaloo, S. R. Shin, Y. K. Mishra, R. Adelung, W. Swieszkowski, N. Annabi, A. Khademhosseini, A. Moshaverinia, A. Tamayol, *Adv. Funct. Mater.* **2018**,

28, 1703437; c) C. H. Woo, Y. C. Choi, J. S. Choi, H. Y. Lee, Y. W. Cho, *Journal of Biomaterials Science, Polymer Edition* **2015**, 26, 841.

[59] a) J. A. Kaplan, R. Liu, J. D. Freedman, R. Padera, J. Schwartz, Y. L. Colson, M. W. Grinstaff, *Biomaterials* **2016**, 76, 273; b) S. Chen, S. K. Boda, S. K. Batra, X. Li, J. Xie, *Adv Healthc. Mater.* **2018**, 7, e1701024.

[60] Z. Zhang, S. Liu, H. Xiong, X. Jing, Z. Xie, X. Chen, Y. Huang, *Acta Biomater.* **2015**, 26, 115.

[61] W. Ji, Y. Sun, F. Yang, J. J. J. P. van den Beucken, M. Fan, Z. Chen, J. A. Jansen, *Pharm. Res.* **2011**, 28, 1259.

[62] H. J. Lai, C. H. Kuan, H. C. Wu, J. C. Tsai, T. M. Chen, D. J. Hsieh, T. W. Wang, *Acta Biomater.* **2014**, 10, 4156.

[63] Z. Man, L. Yin, Z. Shao, X. Zhang, X. Hu, J. Zhu, L. Dai, H. Huang, L. Yuan, C. Zhou, H. Chen, Y. Ao, *Biomaterials* **2014**, 35, 5250.

[64] J. Hu, L. Tian, M. Prabhakaran, X. Ding, S. Ramakrishna, *Polymers* **2016**, 8, 54.

[65] L. Li, G. Zhou, Y. Wang, G. Yang, S. Ding, S. Zhou, *Biomaterials* **2015**, 37, 218.

[66] F. Zhou, X. Jia, Y. Yang, Q. Yang, C. Gao, S. Hu, Y. Zhao, Y. Fan, X. Yuan, *Acta Biomater.* **2016**, 43, 303.

[67] E. N. James, A. M. Delany, L. S. Nair, *Acta Biomater.* **2014**, 10, 3571.

[68] X. Gu, Y. Matsumura, Y. Tang, S. Roy, R. Hoff, B. Wang, W. R. Wagner, *Biomaterials* **2017**, 133, 132.

[69] a) A. Townsend-Nicholson, S. N. Jayasinghe, *Biomacromolecules* **2006**, 7, 3364; b) S. N. Jayasinghe, S. Irvine, J. R. McEwan, *Nanomedicine* **2007**, 2, 555; c) S. L. Sampson, L. Saraiva, K. Gustafsson, S. N. Jayasinghe, B. D. Robertson, *Small* **2014**, 10, 78.

[70] B. Wang, Y. Wang, T. Yin, Q. Yu, *Chem. Eng. Commun.* **2010**, 197, 1315.

[71] a) L. Wistlich, J. Kums, A. Rossi, K. H. Heffels, H. Wajant, J. Groll, *Adv. Funct. Mater.* **2017**, DOI: 10.1002/adfm.201702903; b) Z.-G. Wang, L.-S. Wan, Z.-M. Liu, X.-J. Huang, Z.-K. Xu, *J. Mol. Catal. B: Enzym.* **2009**, 56, 189; c) N. Sachot, M. A. Mateos-Timoneda, J. A. Planell, A. H. Velders, M. Lewandowska, E. Engel, O. Castaño, *Nanoscale* **2015**, 7, 15349.

[72] X. Qiu, B. L. P. Lee, X. Ning, N. Murthy, N. Dong, S. Li, *Acta Biomater.* **2017**, 51, 138.

[73] J. Lee, S. K. M. Perikamana, T. Ahmad, M. S. Lee, H. S. Yang, D. G. Kim, K. Kim, B. Kwon, H. Shin, *Tissue Eng. Part A* **2017**, 23, 323.

[74] R. R. R. Janairo, Y. Zhu, T. Chen, S. Li, *Tissue Eng. Part A* **2014**, 20, 285.

[75] C. Jia, B. Luo, H. Wang, Y. Bian, X. Li, S. Li, H. Wang, *Adv. Mater.* **2017**, DOI: 10.1002/adma.201701154.

[76] L. Zhu, K. Wang, T. Ma, L. Huang, B. Xia, S. Zhu, Y. Yang, Z. Liu, X. Quan, K. Luo, D. Kong, J. Huang, Z. Luo, *Adv. Healthc. Mater.* **2017**, 6.

[77] A. Mathew, C. Vaquette, S. Hashimi, I. Rathnayake, F. Huygens, D. W. Hutmacher, S. Ivanovski, *Adv. Healthc. Mater.* **2017**, 6.

[78] D. W. Song, S. H. Kim, H. H. Kim, K. H. Lee, C. S. Ki, Y. H. Park, *Acta Biomater.* **2016**, 39, 146.

[79] E.-R. Kenawy, G. L. Bowlin, K. Mansfield, J. Layman, D. G. Simpson, E. H. Sanders, G. E. Wnek, *J. Control. Release* **2002**, 81, 57.

[80] J. Zeng, L. Yang, Q. Liang, X. Zhang, H. Guan, X. Xu, X. Chen, X. Jing, *J. Control. Release* **2005**, 105, 43.

[81] P. Punnakitikashem, D. Truong, J. U. Menon, K. T. Nguyen, Y. Hong, *Acta Biomater.* **2014**, 10, 4618.

[82] A. Y. A. Kaassis, N. Young, N. Sano, H. A. Merchant, D.-G. Yu, N. P. Chatterton, G. R. Williams, *J. Mater. Chem. B* **2014**, 2, 1400.

[83] G. Pan, S. Liu, X. Zhao, J. Zhao, C. Fan, W. Cui, *Biomaterials* **2015**, 53, 202.

[84] A. J. Meinel, O. Germershaus, T. Luhmann, H. P. Merkle, L. Meinel, *Eur. J. Pharm. Biopharm.* **2012**, 81, 1.

[85] Q. Shi, J. Hou, C. Zhao, Z. Xin, J. Jin, C. Li, S. C. Wong, J. Yin, *Nanoscale* **2016**, 8, 2022.

[86] Z. Zhang, S. Liu, Y. Qi, D. Zhou, Z. Xie, X. Jing, X. Chen, Y. Huang, *J. Control. Release* **2016**, 235, 125.

[87] R. Lakshmanan, P. Kumaraswamy, U. M. Krishnan, S. Sethuraman, *Biomaterials* **2016**, 97, 176.

[88] K. Suzuki, H. Tanaka, M. Ebara, K. Uto, H. Matsuoka, S. Nishimoto, K. Okada, T. Murase, H. Yoshikawa, *Acta Biomater.* **2017**, 53, 250.

[89] J. F. C. Viana, J. Carrijo, C. G. Freitas, A. Paul, J. Alcaraz, C. C. Lacorte, L. Migliolo, C. A. Andrade, R. Falcão, N. C. Santos, S. Gonçalves, A. J. Otero-González, A. Khademhosseini, S. C. Dias, O. L. Franco, *Nanoscale* **2015**, 7, 6238.

[90] C. Dhand, M. Venkatesh, V. A. Barathi, S. Harini, S. Bairagi, E. Goh Tze Leng, N. Muruganandham, K. Z. W. Low, M. H. U. T. Fazil, X. J. Loh, D. K. Srinivasan, S. P. Liu, R. W. Beuerman, N. K. Verma, S. Ramakrishna, R. Lakshminarayanan, *Biomaterials* **2017**, 138, 153.

[91] J. A. Roman, I. Reucroft, R. A. Martin, A. Hurtado, H. Q. Mao, *Adv. Healthc. Mater.* **2016**, 5, 2628.

[92] C. Zhang, X. Wang, E. Zhang, L. Yang, H. Yuan, W. Tu, H. Zhang, Z. Yin, W. Shen, X. Chen, Y. Zhang, H. Ouyang, *Acta Biomater.* **2018**, 66, 141.

[93] Z. Sun, E. Zussman, A. L. Yarin, J. H. Wendorff, A. Greiner, *Adv. Mater.* **2003**, 15, 1929.

[94] R. Sedghi, A. Shaabani, *Polymer* **2016**, 101, 151.

[95] H. Jiang, L. Wang, K. Zhu, *J. Control. Release* **2014**, 193, 296.

[96] L. E. Sperling, K. P. Reis, P. Pranke, J. H. Wendorff, *Drug Discov. Today* **2016**, 21, 1243.

[97] K. T. Shalumon, G. J. Lai, C. H. Chen, J. P. Chen, *ACS Appl. Mater. Interfaces* **2015**, 7, 21170.

[98] U. Angkawinitwong, S. Awwad, P. T. Khaw, S. Brocchini, G. R. Williams, *Acta Biomater.* **2017**, 64, 126.

[99] D. G. Yu, X. Y. Li, X. Wang, J. H. Yang, S. W. A. Bligh, G. R. Williams, *ACS Appl. Mater. Interfaces* **2015**, 7, 18891.

[100] G. Z. Yang, J. J. Li, D. G. Yu, M. F. He, J. H. Yang, G. R. Williams, *Acta Biomater.* **2017**, 53, 233.

[101] J. Zhang, K. Qiu, B. Sun, J. Fang, K. Zhang, H. Ei-Hamshary, S. S. Al-Deyab, X. Mo, *J. Mater. Chem. B* **2014**, 2, 7945.

[102] D. Han, S. Sherman, S. Filocamo, A. J. Steckl, *Acta Biomater.* **2017**, 53, 242.

[103] Y. C. Shin, D. M. Shin, E. J. Lee, J. H. Lee, J. E. Kim, S. H. Song, D. Y. Hwang, J. J. Lee, B. Kim, D. Lim, S. H. Hyon, Y. J. Lim, D. W. Han, *Adv. Healthc. Mater.* **2016**, 5, 3035.

[104] C. H. Chen, S. H. Chen, K. T. Shalumon, J. P. Chen, *Acta Biomater.* **2015**, 26, 225.

[105] E. H. Sanders, R. Kloefkorn, G. L. Bowlin, D. G. Simpson, G. E. Wnek, *Macromolecules* **2003**, 36, 3803.

[106] a) J. Hu, M. P. Prabhakaran, X. Ding, S. Ramakrishna, *Journal of Biomaterials Science, Polymer Edition* **2015**, 26, 57; b) Z. Wang, Y. Qian, L. Li, L. Pan, L. W. Njunge, L. Dong, L. Yang, *J. Biomater. Appl.* **2016**, 30, 686.

[107] a) T. Briggs, T. L. Arinzeh, *J. Biomed. Mater. Res. A* **2014**, 102, 674; b) N. Nikmaram, S. Roohinejad, S. Hashemi, M. Koubaa, F. J. Barba, A. Abbaspourrad, R. Greiner, *RSC Adv.* **2017**, 7, 28951.

[108] G. Yazgan, A. M. Popa, R. M. Rossi, K. Maniura-Weber, J. Puigmartí-Luis, D. Crespy, G. Fortunato, *Polymer* **2015**, 66, 268.

[109] A. O. Basar, S. Castro, S. Torres-Giner, J. M. Lagaron, H. Turkoglu Sasmazel, *Mater. Sci. Eng. C* **2017**, 81, 459.

[110] N. Cai, C. Han, X. Luo, G. Chen, Q. Dai, F. Yu, *Macromol. Mater. Eng* **2017**, 302, 1600364.

[111] W. Li, Y. Ding, R. Rai, J. A. Roether, D. W. Schubert, A. R. Boccaccini, *Mater. Sci. Eng. C* **2014**, 41, 320.

[112] X. Xu, X. Zhuang, X. Chen, X. Wang, L. Yang, X. Jing, *Macromol. Rapid Commun.* **2006**, 27, 1637.

[113] H. J. Chung, J. T. Kim, H. J. Kim, H. W. Kyung, P. Katila, J. H. Lee, T. H. Yang, Y. I. Yang, S. J. Lee, *J. Control. Release* **2015**, 205, 218.

[114] X. Zhao, S. Jiang, S. Liu, S. Chen, Z. Y. W. Lin, G. Pan, F. He, F. Li, C. Fan, W. Cui, *Biomaterials* **2015**, 61, 61.

[115] J. Liu, H. Nie, Z. Xu, F. Guo, S. Guo, J. Yin, Y. Wang, C. Zhang, *J. Mater. Chem. B* **2015**, 3, 581.

[116] C. W. He, M. Parowatkin, V. Mailänder, M. Flechtner-Mors, U. Ziener, K. Landfester, D. Crespy, *ACS Appl. Mater. Interfaces* **2017**, 9, 3885.

[117] R. Chandrawati, M. T. J. Olesen, T. C. C. Marini, G. Bisra, A. G. Guex, M. G. de Oliveira, A. N. Zelikin, M. M. Stevens, *Adv. Healthc. Mater.* **2017**, 6.

[118] J. Xue, Y. Niu, M. Gong, R. Shi, D. Chen, L. Zhang, Y. Lvov, *ACS Nano* **2015**, 9, 1600.

[119] N. Monteiro, M. Martins, A. Martins, N. A. Fonseca, J. N. Moreira, R. L. Reis, N. M. Neves, *Acta Biomater.* **2015**, 18, 196.

[120] J. Song, A. Klymov, J. Shao, Y. Zhang, W. Ji, E. Kolwijck, J. A. Jansen, S. C. G. Leeuwenburgh, F. Yang, *Adv. Healthc. Mater.* **2017**, 6.

[121] G. Yang, J. Wang, Y. Wang, L. Li, X. Guo, S. Zhou, *ACS Nano* **2015**, 9, 1161.

[122] M. S. Kang, J. H. Kim, R. K. Singh, J. H. Jang, H. W. Kim, *Acta Biomater.* **2015**, 16, 103.

[123] W. Liu, J. Wei, Y. Wei, Y. Chen, *J. Biomed. Nanotechnol.* **2015**, 11, 428.

[124] I. Sebe, P. Szabó, B. Kállai-Szabó, R. Zelkó, *Int. J. Pharm.* **2015**, 494, 516.

[125] H. R. Munj, J. J. Lannutti, D. L. Tomasko, *J. Biomater. Appl.* **2017**, 31, 933.

[126] a) M. V. Natu, H. C. de Sousa, M. H. Gil, *Int. J. Pharm.* **2010**, 397, 50; b) M. Sadri, A. Mohammadi, H. Hosseini, *Nanomedicine Research Journal* **2016**, 1, 112.

[127] a) S. Nagarajan, L. Soussan, M. Bechelany, C. Teyssier, V. Cavailles, C. Pochat-Bohatier, P. Miele, N. Kalkura, J.-M. Janot, S. Balme, *J. Mater. Chem. B* **2016**, 4, 1134; b) A. Laha, C. S. Sharma, S. Majumdar, *Mater. Sci. Eng. C* **2017**, 76, 782.

[128] A. Bohr, Y. Wang, N. Harmankaya, J. J. Water, S. Baldursdottír, K. Almdal, M. Beck-Broichsitter, *Eur. J. Pharm. Biopharm.* **2017**, 115, 140.

[129] T. Potrč, S. Baumgartner, R. Roškar, O. Planinšek, Z. Lavrič, J. Kristl, P. Kocbek, *European Journal of Pharmaceutical Sciences* **2015**, 75, 101.

[130] Y.-N. Jiang, H.-Y. Mo, D.-G. Yu, *Int. J. Pharm.* **2012**, 438, 232.

[131] T. Pattama, R. Uracha, S. Pitt, *Nanotechnology* **2006**, 17, 2317.

[132] F. Spano, A. Quarta, C. Martelli, L. Ottobrini, R. M. Rossi, G. Gigli, L. Blasi, *Nanoscale* **2016**, 8, 9293.

[133] a) A. Akhgari, Z. Shakib, S. Sanati, *Nanomedicine Journal* **2017**, 4, 197; b) M. Rahmani, S. Arbabi Bidgoli, S. M. Rezayat, *Nanomedicine Journal* **2017**, 4, 61.

[134] R. Goyal, L. K. Macri, H. M. Kaplan, J. Kohn, *J. Control. Release* **2016**, 240, 77.

[135] M. R. Prausnitz, R. Langer, *Nat. Biotechnol.* **2008**, 26, 1261.

[136] a) Z. Cui, Z. Zheng, L. Lin, J. Si, Q. Wang, X. Peng, W. Chen, *Adv. Polym. Tech.* **2017**, 0; b) R. Najafi-Taher, M. A. Derakhshan, R. Faridi-Majidi, A. Amani, *RSC Adv.* **2015**, 5, 50462.

[137] R. J. Tsai, L. M. Li, J. K. Chen, *N. Engl. J. Med.* **2000**, 343, 86.

[138] A. Baradaran-Rafii, E. Biazar, S. Heidari-Keshel, *Int. J. Polym. Mate.* **2015**, 64, 879.

[139] R. S. Bhattarai, A. Das, R. M. Alzhrani, D. Kang, S. B. Bhaduri, S. H. S. Boddu, *Mater. Sci. Eng. C* **2017**, 77, 895.

[140] A. Baskakova, S. Awwad, J. Q. Jiménez, H. Gill, O. Novikov, P. T. Khaw, S. Brocchini, E. Zhilyakova, G. R. Williams, *Int. J. Pharm.* **2016**, 502, 208.

[141] L. G. Griffith, G. Naughton, *Science* **2002**, 295, 1009.

[142] J. Janis, C. Attinger, *Plast. Reconstr. Surg.* **2006**, 117, 12S.

[143] M. Norouzi, S. M. Boroujeni, N. Omidvarkordshouli, M. Soleimani, *Adv. Healthc. Mater.* **2015**, 4, 1114.

[144] a) N. Liao, A. R. Unnithan, M. K. Joshi, A. P. Tiwari, S. T. Hong, C.-H. Park, C. S. Kim, *Colloids Surf. A Physicochem. Eng. Asp.* **2015**, 469, 194; b) A. C. Alavarse, F. W. de Oliveira Silva, J. T. Colque, V. M. da Silva, T. Prieto, E. C. Venancio, J.-J. Bonvent, *Mater. Sci. Eng. C* **2017**, 77, 271.

[145] a) F. Lv, J. Wang, P. Xu, Y. Han, H. Ma, H. Xu, S. Chen, J. Chang, Q. Ke, M. Liu, Z. Yi, C. Wu, *Acta Biomater.* **2017**, 60, 128; b) X. Ren, Y. Han, J. Wang, Y. Jiang, Z. Yi, H. Xu, Q. Ke, *Acta Biomater.* **2018**.

[146] H. Chen, P. Jia, H. Kang, H. Zhang, Y. Liu, P. Yang, Y. Yan, G. Zuo, L. Guo, M. Jiang, J. Qi, Y. Liu, W. Cui, H. A. Santos, L. Deng, *Adv. Healthc. Mater.* **2016**, 5, 907.

[147] R. H. Dong, Y. X. Jia, C. C. Qin, L. Zhan, X. Yan, L. Cui, Y. Zhou, X. Jiang, Y. Z. Long, *Nanoscale* **2016**, 8, 3482.

[148] a) B. D. Smith, D. A. Grande, *Nat. Rev. Rheumatol.* **2015**, 11, 213; b) J. L. Madrigal, R. Stilhano, E. A. Silva, *Tissue Eng. Part B Rev.* **2017**, 23, 347.

[149] a) B. J. Kwee, D. J. Mooney, *Curr. Opin. Biotechnol.* **2017**, 47, 16; b) Q. Chen, J. Jing, H. Qi, I. Ahmed, H. Yang, X. Liu, T. L. Lu, A. R. Boccaccini, *ACS Appl. Mater. Interfaces* **2018**, 10, 11529.

[150] Y. Yu, S. Hua, M. Yang, Z. Fu, S. Teng, K. Niu, Q. Zhao, C. Yi, *RSC Adv.* **2016**, 6.

[151] B. Zhang, T. M. Filion, A. B. Kutikov, J. Song, *Adv. Funct. Mater.* **2017**, 27.

[152] Y. Liu, G. Zhou, Z. Liu, M. Guo, X. Jiang, M. B. Taskin, Z. Zhang, J. Liu, J. Tang, R. Bai, F. Besenbacher, M. Chen, C. Chen, *Sci. Rep.* **2017**, 7, 8197.

[153] P. H. M., S. B. N., O. Dinorath, M. H. O., K. D. J., P. K. C., D. N. J., H. D. T. Lynn, *Tissue Eng. Part A* **2017**, 23, 823.

[154] T. S. Edward, S. N. Navraj, T. Saket, K. Wasim, J. C. Andrew, *Curr. Stem Cell Res. Ther.* **2018**, 13, 1.

[155] a) M. Younesi, A. Islam, V. Kishore, J. M. Anderson, O. Akkus, *Adv. Funct. Mater.* **2014**, 24, 5762; b) C. Zhang, H. Yuan, H. Liu, X. Chen, P. Lu, T. Zhu, L. Yang, Z. Yin, B. C. Heng, Y. Zhang, H. Ouyang, *Biomaterials* **2015**, 53, 716.

[156] L. Weng, S. K. Boda, H. Wang, M. J. Teusink, F. D. Shuler, J. Xie, *Adv. Healthc. Mater.* **2018**.

[157] J. R. McCarthy, *Current cardiovascular imaging reports* **2010**, 3, 42.

[158] G. Zhao, X. Zhang, T. J. Lu, F. Xu, *Adv. Funct. Mater.* **2015**, 25, 5726.

[159] H. Parsa, K. Ronaldson, G. Vunjaknovakovic, *Adv. Drug Deliv. Rev.* **2015**, 96, 195.

[160] a) M. Tallawi, D. C. Zebrowski, R. Rai, J. A. Roether, D. W. Schubert, M. El Fray, F. B. Engel, K. E. Aifantis, A. R. Boccaccini, *Tissue Eng. Part C Methods* **2015**, 21, 585; b) D. Kai, M. P. Prabhakaran, G. Jin, S. Ramakrishna, *J. Biomed. Mater. Res. A* **2011**, 99A, 376; c) M. Li, Y. Guo, Y. Wei, A. G. MacDiarmid, P. I. Lelkes, *Biomaterials* **2006**, 27, 2705; d) L. Wang, Y. Wu, T. Hu, B. Guo, P. X. Ma, *Acta Biomater.* **2017**, 59, 68.

[161] a) S. Pascualgil, T. Simónyarza, E. Garbayo, F. Prósper, M. J. Blancoprieto, *Int. J. Pharm.* **2017**, 523, 531; b) S. Pascual-Gil, E. Garbayo, P. Díaz-Herráez, F. Prosper, M. J. Blanco-Prieto, *J. Control. Release* **2015**, 203, 23.

[162] D. Kai, M. P. Prabhakaran, G. Jin, L. Tian, S. Ramakrishna, *J. Tissue Eng. Regen. Med.* **2015**.

[163] Y. Liu, G. Xu, J. Wei, Q. Wu, X. Li, *Materials Science & Engineering C Materials for Biological Applications* **2017**, 81, 500.

[164] Y. Liu, J. Lu, G. Xu, J. Wei, Z. Zhang, X. Li, *Mater. Sci. Eng. C* **2016**, 69, 865.

[165] B. Schoen, R. Avrahami, L. Baruch, Y. Efraim, I. Goldfracht, O. Elul, T. Davidov, L. Gepstein, E. Zussman, M. Machluf, *Adv. Funct. Mater.* **2017**, 27.

[166] a) C. Huang, Y. Ouyang, H. Niu, N. He, Q. Ke, X. Jin, D. Li, J. Fang, W. Liu, C. Fan, T. Lin, *ACS Appl. Mater. Interfaces* **2015**, 7, 7189; b) J. Xue, J. Yang, D. M. O'Connor, C. Zhu, D. Huo, N. M. Boulis, Y. Xia, *ACS Appl. Mater. Interfaces* **2017**, 9, 12299.

[167] S. Baiguera, C. Del Gaudio, E. Lucatelli, E. Kuevda, M. Boieri, B. Mazzanti, A. Bianco, P. Macchiarini, *Biomaterials* **2014**, 35, 1205.

[168] Z. Álvarez, O. Castaño, A. A. Castells, M. A. Mateos-Timoneda, J. A. Planell, E. Engel, S. Alcántara, *Biomaterials* **2014**, 35, 4769.

[169] A. Raspa, A. Marchini, R. Pugliese, M. Mauri, M. Maleki, R. Vasita, F. Gelain, *Nanoscale* **2016**, 8, 253.

[170] P. Kumar, Y. E. Choonara, G. Modi, D. Naidoo, V. Pillay, *Curr. Pharm. Des.* **2015**, 21, 1517.

[171] D. R. Nisbet, S. Pattanawong, N. E. Ritchie, W. Shen, D. I. Finkelstein, M. K. Horne, J. S. Forsythe, *J. Neural. Eng.* **2007**, 4, 35.

[172] C. C. Gertz, M. K. Leach, L. K. Birrell, D. C. Martin, E. L. Feldman, J. M. Corey, *Dev. Neurobiol.* **2010**, 70, 589.

[173] V. Mahairaki, S. H. Lim, G. T. Christopherson, L. Xu, I. Nasonkin, C. Yu, H. Q. Mao, V. E. Koliatsos, *Tissue Eng. Part A* **2011**, 17, 855.

[174] A. Hurtado, J. M. Cregg, H. B. Wang, D. F. Wendell, M. Oudega, R. J. Gilbert, J. W. McDonald, *Biomaterials* **2011**, 32, 6068.

[175] M. Naseri-Nosar, M. Salehi, ShahriarHojjati-Emami, *Int. J. Biol. Macromol.* **2017**, 103.

[176] K. Zhang, H. Zheng, S. Liang, C. Gao, *Acta Biomater.* **2016**, 37, 131.

[177] Y. Liu, J. Lu, H. Li, J. Wei, X. Li, *Acta Biomater.* **2015**, 11, 114.

[178] W. Gong, D. Lei, S. Li, P. Huang, Q. Qi, Y. Sun, Y. Zhang, Z. Wang, Z. You, X. Ye, Q. Zhao, *Biomaterials* **2016**, 76, 359.

[179] a) M. Zamani, M. P. Prabhakaran, S. Ramakrishna, *Int. J. Nanomedicine* **2013**, 8, 2997; b) S. Lee, G. Jin, J.-H. Jang, *Journal of Biological Engineering* **2014**, 8, 30.

[180] W. F. Liu, C. S. Chen, *Adv. Drug Deliv. Rev.* **2007**, 59, 1319.

[181] a) Z. Zha, L. Jiang, Z. Dai, X. Wu, *Appl. Phys. Lett.* **2012**, 101, 193701; b) K. B. Paul, V. Singh, S. R. K. Vanjari, S. G. Singh, *Biosens. Bioelectron.* **2017**, 88, 144; c) M. A. Ali, C. Singh, K. Mondal, S. Srivastava, A. Sharma, B. D. Malhotra, *ACS Appl. Mater. Interfaces* **2016**, 8, 7646; d) N. Zhang, Y. Deng, Q. Tai, B. Cheng, L. Zhao, Q. Shen, R.

He, L. Hong, W. Liu, S. Guo, K. Liu, H. R. Tseng, B. Xiong, X. Z. Zhao, *Adv. Mater.* **2012**, 24, 2756.

[182] X. Xu, M. C. Farach-Carson, X. Jia, *Biotechnol. Adv.* **2014**, 32, 1256.

[183] O. Hartman, C. Zhang, E. L. Adams, M. C. Farach-Carson, N. J. Petrelli, B. D. Chase, J. F. Rabolt, *Biomaterials* **2010**, 31, 5700.

[184] T. Amna, N. A. M. Barakat, M. S. Hassan, M.-S. Khil, H. Y. Kim, *Colloids Surf. A Physicochem. Eng. Asp.* **2013**, 431, 1.

[185] X. Luo, C. Xie, H. Wang, C. Liu, S. Yan, X. Li, *Int. J. Pharm.* **2012**, 425, 19.

[186] S. H. Ranganath, C.-H. Wang, *Biomaterials* **2008**, 29, 2996.

[187] G. Ma, Y. Liu, C. Peng, D. Fang, B. He, J. Nie, *Carbohydr. Polym.* **2011**, 86, 505.

[188] S. Liu, G. Zhou, D. Liu, Z. Xie, Y. Huang, X. Wang, W. Wu, X. Jing, *J. Mater. Chem. B* **2013**, 1, 101.

[189] T. Lu, X. Jing, X. Song, X. Wang, *J. Appl. Polym. Sci.* **2012**, 123, 209.

[190] X. Xu, X. Chen, Z. Wang, X. Jing, *Eur. J. Pharm. Biopharm.* **2009**, 72, 18.

[191] C. Achille, S. Sundaresh, B. Chu, M. Hadjiargyrou, *PLoS ONE* **2012**, 7, e52356.

[192] C. Lei, Y. Cui, L. Zheng, P. Kah-Hoe Chow, C.-H. Wang, *Biomaterials* **2013**, 34, 7483.

[193] a) R. Ramachandran, V. R. Junnuthula, G. S. Gowd, A. Ashokan, J. Thomas, R. Peethambaran, A. Thomas, A. K. K. Unni, D. Panikar, S. V. Nair, M. Koyakutty, *Sci. Rep.* **2017**, 7, 43271; b) J. Wei, X. Luo, M. Chen, J. Lu, X. Li, *Acta Biomater.* **2015**, 23, 189.

[194] S. Mura, J. Nicolas, P. Couvreur, *Nat. Mater.* **2013**, 12, 991.

[195] a) M. M. Gottesman, T. Fojo, S. E. Bates, *Nat. Rev. Cancer* **2002**, 2, 48; b) J. C. Kaczmarek, P. S. Kowalski, D. G. Anderson, *Genom. Med.* **2017**, 9, 60.

[196] Y. J. Kim, M. Ebara, T. Aoyagi, *Adv. Funct. Mater.* **2013**, 23, 5753.

[197] A. Ghavaminejad, A. R. K. Sasikala, A. R. Unnithan, R. G. Thomas, Y. Y. Jeong, M. Vatankhah-Varnoosfaderani, F. J. Stadler, C. H. Park, C. S. Kim, *Adv. Funct. Mater.* **2015**, 25, 2867.

[198] a) B. Song, C. Wu, J. Chang, *Acta Biomater.* **2012**, 8, 1901; b) F. Zheng, S. Wang, S. Wen, M. Shen, M. Zhu, X. Shi, *Biomaterials* **2013**, 34, 1402.

[199] K. Qiu, C. He, W. Feng, W. Wang, X. Zhou, Z. Yin, L. Chen, H. Wang, X. Mo, *J. Mater. Chem. B* **2013**, 1, 4601.

[200] a) Y. Park, E. Kang, O.-J. Kwon, T. Hwang, H. Park, J. M. Lee, J. H. Kim, C.-O. Yun, *J. Control. Release* **2010**, 148, 75; b) I. C. Liao, S. Chen, J. B. Liu, K. W. Leong, *J. Control. Release* **2009**, 139, 48.

[201] S. Maheswaran , L. V. Sequist , S. Nagrath , L. Ulkus , B. Brannigan , C. V. Collura , E. Inserra , S. Diederichs , A. J. Iafrate , D. W. Bell , S. Digumarthy , A. Muzikansky , D. Irimia , J. Settleman , R. G. Tompkins , T. J. Lynch , M. Toner , D. A. Haber *N. Engl. J. Med.* **2008**, 359, 366.

[202] D. A. Smirnov, D. R. Zweitzig, B. W. Foulk, M. C. Miller, G. V. Doyle, K. J. Pienta, N. J. Meropol, L. M. Weiner, S. J. Cohen, J. G. Moreno, M. C. Connelly, L. W. M. M. Terstappen, S. M. O'Hara, *Cancer Res.* **2005**, 65, 4993.

[203] J.-J. Xu, W.-W. Zhao, S. Song, C. Fan, H.-Y. Chen, *Chem. Soc. Rev.* **2014**, 43, 1601.

[204] S. W. Han, W.-G. Koh, *Anal. Chem.* **2016**, 88, 6247.

[205] V. Plaks, C. D. Koopman, Z. Werb, *Science* **2013**, 341, 1186.

[206] S. Hou, L. Zhao, Q. Shen, J. Yu, C. Ng, X. Kong, D. Wu, M. Song, X. Shi, X. Xu, W.-H. OuYang, R. He, X.-Z. Zhao, T. Lee, F. C. Brunicardi, M. A. Garcia, A. Ribas, R. S. Lo, H.-R. Tseng, *Angew. Chem. Int. Ed.* **2013**, 52, 3379.

[207] R. J. Stoddard, A. L. Steger, A. K. Blakney, K. A. Woodrow, *Ther. Deliv.* **2016**, 7, 387.

[208] P. López-Jaramillo, M. Y. Rincón, R. G. García, S. Y. Silva, E. Smith, P. Kampeerapappun, C. García, D. J. Smith, M. López, I. D. Vélez, *The American Journal of Tropical Medicine and Hygiene* **2010**, 83, 97.

[209] S. Soodabeh, M. Azadeh, A. Mohammad, *Current Drug Discovery Technologies* **2015**, 12, 218.

[210] P. Luana, C. Andrea, T. Cagri, P. Dario, *Macromol. Mater. Eng* **2013**, 298, 504.

[211] Y. Miao, D. Rui‐Hua, Y. Xu, Y. Gui‐Feng, Y. Ming‐Hao, N. Xin, L. Yun‐Ze, *Macromol. Mater. Eng* **2017**, 302, 1700002.

The table of contents description

Drug-loaded electrospun architectures are gaining increasing attention in various biomedical applications. By carefully choosing materials/drugs and drug loading techniques, electrospun structures with adjustable topography, tunable porosity, high surface area, and controllable drug release behaviors can be manufactured for biomedical applications, such as simple drug delivery systems, tissue engineering and cancer therapy. The recent progresses are thoroughly overviewed in this review.

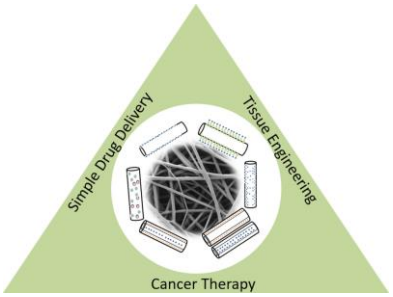

Biography

Dr. Yaping Ding is a postdoctoral researcher in Prof. Santos' group at the Faculty of Pharmacy, University of Helsinki. She received her Bachelor's (2008) and Master's (2011) degrees in materials science and engineering from Xi'an Jiaotong University. She then studied polymers and biomaterials under the supervision of Prof. Dirk W. Schubert and Prof. Aldo R. Boccaccini at University of Erlangen-Nuremberg and obtained her Ph.D. degree in 2015. Her research interests are related to drug delivery, biomaterials, and tissue engineering.

Dr. Dongfei Liu earned his Ph.D. in Pharmacy from the University of Helsinki in 2014, under the supervision of Prof. Santos. From 2016 to 2018, he visited Prof. David A. Weitz's group at Harvard University. Currently, he is a principal investigator at the Faculty of Pharmacy and is selected as a HiLIFE Fellow, University of Helsinki. He is well-versed in a variety of fields, such as drug encapsulation, controlled release, microfluidics, biomaterials, and regenerative medicine among others. He is interested in how to engineer biomaterials with ultrahigh mass fraction of therapeutics for controlled drug delivery; he also focuses on the biomedical applications of the fabricated drug delivery systems, such as spinal cord injury therapy, analgesia, and antipsychotic medication.

Prof. Hélder A. Santos obtained his Doctor of Science in Technology (Chem. Eng.) in 2007 from the Helsinki University of Technology, Finland. Currently, he is also the Head of the Division of Pharmaceutical Chemistry and Technology, the Head of the Preclinical Drug Formulation and Analysis Group, and the Head of the Nanomedicines and Biomedical Engineering Group, all at the Faculty of Pharmacy, University of Helsinki, Finland. Prof. Santos is also a HiLIFE Fellow, University of Helsinki. His scientific expertise lies in the development of nanoparticles/nanomedicines for biomedical and healthcare applications, particularly porous silicon nanomaterials for simultaneous controlled drug delivery, diagnostic and treatment of cancer, diabetes, and cardiovascular diseases.

Click here to access/download
Supporting Information
copyrights permission.7z

Click here to access/download

Supporting Information

Revised 20180915 clear.docx

Figure 1

Figure 2

Figure 3

Figure 4

Figure 5

Figure 6

Figure 7

Figure 8

Figure 9

Figure 10


Click here to access/download
Production Data
Figure 10.tif

Figure 11


Click here to access/download
Production Data
Figure 11.tif

Figure 12


Click here to access/download
Production Data
Figure 12.tif

Figure 13


Click here to access/download
Production Data
Figure 13.tif

Figure 14

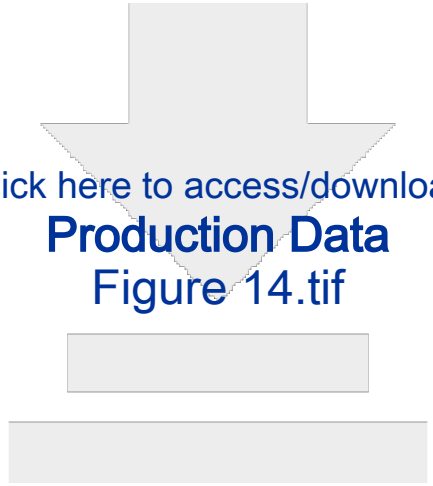
Click here to access/download
Production Data
Figure 14.tif

Figure 15


Click here to access/download
Production Data
Figure 15.tif

Figure 16


Click here to access/download
Production Data
Figure 16.tif

Graphical Abstract

Click here to access/download

Production Data

Graphic Abstract AFM Ding.tif